Improving monoclonal antibody quality and efficacy: Studies on a camelid heavy-chain monoclonal antibody

by

Neha Mishra

A Thesis submitted to the Faculty of Graduate Studies of
The University of Manitoba
in partial fulfilment of the requirements for the degree of

Doctor of Philosophy

Department of Microbiology
University of Manitoba
Winnipeg, Canada

Acknowledgements

I would like to thank my PhD supervisor, Dr. Michael Butler, for all his support, patience and guidance throughout my PhD and beyond. I would also like to extend my heartfelt thanks to Dr. Deborah Court, my co-supervisor, who has supported me through difficult situations and my committee members Dr. Teresa de Kievit and Dr. Jörg Stetefeld.

A very big thank you to Dr. Maureen Spearman, who has been and continues to be my mentor and friend. I will forever be grateful for your support. I would also like to thank Vincent Jung for his technical support, camaraderie and his company during coffee breaks. A special thank you to Dr. Lynda Donald and Dr. Helene Perreault for their contribution and support in publishing some of the work described in the thesis. Thank you to Dr. Christine Zhang at University of Manitoba Flow Cytometry Facility for her help in running the flow cytometry experiments described in the thesis.

Thank you to all the members of Butler lab – Venkata Tayi, Ben Dionne, Sarah Chan, Katrin Braasch, Natalie Krahn, Carina Villacres and Viridiana Urena. A very special thanks to Grishma for her friendship, it would not have been the same experience living in Winnipeg without you.

I am grateful to Krishna, my husband, without whose support and encouragement, this PhD would not have been possible. Thanks for being there for me, always. Thank you to my parents Nandita and Ajit and my brother, Rohan, for all their love, support and undeniable faith that I will complete this epic adventure.

The work presented in this thesis was supported by a Natural Science and Engineering Research Council grant, MabNet. Additional funding from Faculty of Science and GETS (Graduate Enhancement of Tri-Council Stipends) is much appreciated.

Dedication

To my parents, Nandita and Ajit

“We can do anything we want to do if we stick to it long enough.” – Helen Keller

Table of Contents

Abstract

Glycosylation is a critical quality attribute of biotherapeutics as it contributes to their quality and efficacy. The work described in this thesis aims to investigate these aspects of an EG2-hFc chimeric (camelid heavy chain Fab-human Fc) single domain monoclonal antibody by increasing the antibody-dependent cell cytotoxicity response. Two methods of generating non-fucosylated antibodies are compared. The first method involves the fucosyltransferase inhibitor, 2 fluoro peracetylated fucose (2FF) with Chinese Hamster Ovary (CHO) cells producing EG2-hFc and the second uses the prokaryotic RMD gene, which was transfected into CHO EG2-hFc cells. Both methods successfully generated reduced fucosylation, but neither produced completely non-fucosylated antibodies. The fucosylation levels of the RMD transfected CHO EG2-hFc cells could be reversed with increasing concentrations of fucose added to the cells. To analyse the fucosylation pattern of EG2-hFc samples, electrospray ionization mass spectrometry (ESI-MS) was applied. It was observed that the addition of fucose was inhibited by 2FF in a concentration-dependent manner.

An attempt was made to develop a non-radioactive ADCC assay using engineered NK-92 effector cells. The optimization assays performed as expected, with the cytotoxicity% increasing with the increasing concentrations of antibody, but experimental assays using EG2 samples did not result in the same cytotoxicity%. Therefore, this LDH-based ADCC assay requires further optimization before it can be a standard for measuring the ADCC of an antibody.

To investigate the effect of bioprocess parameters such as redox potential on glycosylation of CHO EG2-hFc, a study was designed to detect the internal redox potential, which may be one factor influencing the intracellular machinery in the ER and Golgi where

glycan processing occurs. Redox sensitive green fluorescent proteins were targeted to the organelles of CHO EG2-hFc cells. Flow cytometry data provided a proof-of-concept that the roGFP probes can be utilized to determine the redox status.

Together, these results advance the understanding of fucosylation for ADCC and provided the basis for the development of tools to analyse ADCC and redox state of cells producing a potential therapeutic.

List of abbreviations

2-AB	2- aminobenzamide
ADCC	Antibody dependent cell cytotoxicity
ADCP	Antibody dependent cell phagocytosis
ATP	Adenosine triphosphate
BC	Background control
BHK	Baby hamster kidney
CD	Chemically defined
CDC	Complement dependent cytotoxicity
CFTR	Cystic fibrosis transmembrane conductance regulator
C_H	Constant domain heavy chain
CHO	Chinese hamster ovary
C_L	Constant domain light chain
CRISPR	clustered regularly interspaced short palindromic repeats
CRP	Culture redox potential
DMEM	Dulbecco's Modified Eagle Medium
DMJ	Deoxymannojirimycin
DMSO	Dimethyl sulfoxide
DNA	Deoxyribonucleic acid
DO	Dissolved oxygen
DPBS	Dulbecco's phosphate-buffered saline
DPS	4 - 4´dipyridyl disulfide
DTT	Dithiothreitol
EDTA	Ethylenediaminetetraacetic acid
EGFP	Enhanced green fluorescent protein

EGFR	Epidermal growth factor receptor
ER	Endoplasmic reticulum
ESI	Electrospray ionization
FACS	Fluorescence-activated cell sorting
FBS	Fetal bovine serum
FUT	Fucosyltransferase
GDP	Guanosine diphosphate
GFP	Green fluorescence protein
GI	Galactosylation index
GSH	Glutathione
GSSG	Glutathione disulphide
GU	Glucose unit
HEK	Human embryonic kidney
HEPES	4-(2-hydroxyethyl)-1-piperazineethanesulfonic acid
HILIC	hydrophilic interaction liquid chromatography
HM	High mannose
HPLC	High-performance liquid chromatography
KDEL	(Lys-Asp-Glu-Leu) endoplasmic reticulum protein retention receptor 1
LDH	Lactate dehydrogenase
MAb	Monoclonal antibody
MCS	Multiple cloning site
MR	Maximal release
MS	Mass spectrometry
MWCO	Molecular weight cut off
NAD	Nicotinamide adenine dinucleotide

NADH	Nicotinamide adenine dinucleotide hydrogen
NK	Natural killer
NMR	Nuclear magnetic resonance
NS0	Murine myeloma cells
NSCLC	Non-small-cell lung carcinoma
OST	oligosaccharyltransferase
PBMC	peripheral blood mononuclear cell
PBS	Phosphate buffered saline
PBST	Phosphate buffered saline with tween
PCR	Polymerase chain reaction
PDI	Protein disulphide isomerase
PNGase-F	N-glycosidase F
PQA	Product quality attribute
RMD	GDP-6-deoxy-D-lyxo-4-hexulose reductase
RNA	Ribonucleic acid
RPMI	Roswell Park Memorial Institute media
SR	Spontaneous release
TNFR	Tumor necrosis factor receptor
TOF	Time of flight
TRF	Time resolved fluorescence
VEGFA	Vascular Endothelial Growth Factor A
V_H	Variable domain heavy chain
V_L	Variable domain light chain

List of figures

List of tables

1

Introduction and Background

1.1 Introduction

Biopharmaceuticals, which include monoclonal antibodies (MAbs), growth factors, and hormones, have been generated for various diseases and have been a major contribution towards improving people's lives. Production of these biopharmaceuticals in mammalian cells requires certain critical quality attributes for compliance, which includes safety and efficacy as well as quality of the protein (Jungbauer and Graumann, 2012). Safety of the protein refers to the capability of the therapeutic to avoid generating an immunogenic response, whereas efficacy relates to eliciting an immune response against a pathogen, as well as dosage requirements. Product quality can be affected by the bioprocess parameters used in production, such as expression systems, nutrient composition within the media used for the expression systems, as well as production conditions such as temperature, pH etc. (Butler, 2005). The common theme tying these factors together is glycosylation. This thesis discusses efficacy as well as heterogeneity affecting product quality by studies conducted on two such aspects: efficacy affected by manipulation of N-linked glycosylation in a novel camelid-human chimeric antibody format and product quality affected by redox potential, which is a bioprocess parameter, in the same antibody.

The introduction is divided into subsections that introduce topics relevant to each project and are discussed in the same order as the chapters. However, some of the topics also overlap between chapters and will be referred to accordingly.

1.1.1 Monoclonal Antibody Therapeutics

Monoclonal antibody (MAb) production has developed extensively over the years from 1975, from using hybridoma cell lines (Köhler and Milstein, 1975) to currently using different mammalian cell lines with improved expression, titre and antibody engineering that imparts enhanced efficacy and specificity. The first therapeutic MAb was an immunosuppressant, Orthoclone OKT3, that was approved in 1986 for human use in organ transplant patients (Ecker et al., 2015). Use of MAbs, especially as therapeutics, has increased with projected sales of $125 billion worldwide by 2020 (Ecker et al., 2015). As of 2017, there are more than 58 MAbs available on the market for use as therapeutics for diseases (Chung, 2017). In the past year, all 10 approved MAbs were IgGs, out of which 6 were IgG1s (Kaplon and Reichert, 2018). MAbs are highly specific, stable and have long half-lives (Spiegelberg and Fishkin, 1972), because of which they are increasingly being used as cancer therapeutics. Vascular endothelial growth factor A (VEGFA)-targeting Bevacizumab, human epidermal growth factor receptor 2 (HER2)- specific Trastuzumab, CD-20-specific Rituximab and epidermal growth factor receptor (EGFR)- targeting Cetuximab are some of the cancer therapeutics available in the market (Leavy, 2010).

Early on, one of the main challenges in production of MAbs was low product titres, which was overcome with advances in cell line development, increase in production capabilities and cell specific productivity (F. Li et al., 2010). Now, the ever-increasing demand to develop and manufacture MAbs has led to biopharmaceutical companies investing heavily into research and development programs focusing on product quality and consistency. MAbs, being glycoproteins, undergo post-translational modifications such as glycosylation that may affect

product quality and their use as therapeutics, thus leading to the main focus of research discussed in this thesis.

1.1.2 Antibody Structure and Function

Antibodies or immunoglobulins (Igs) are responsible for stimulating the innate immune system to elicit an immune response to specific antigens. In the human blood serum, varying concentrations of different types of antibodies are produced. Categorized into five types, (IgG, IgA, IgM, IgD, IgE), the most abundant of these proteins in serum is IgG (13.5 mg/mL). IgGs are further categorized into IgG1, IgG2, IgG3 and IgG4 (in decreasing order of their concentration in human blood serum). The number of inter-chain disulphide bonds differs amongst IgGs. The 'Y' shaped molecules are comprised of two identical heavy chains with V_H (variable), C_H1, C_H2 and C_H3 (constant) domains and two identical light chains comprised of V_L and C_L domains. Connecting the heavy chain domains is the proline rich hinge region, which renders flexibility to the molecule, thus contributing to the antigen binding capability of Igs. The presence of cysteine residues in the hinge region facilitates heavy chain dimerization (Y.-K. Lee et al., 1999; Spearman et al., 2011). IgGs trigger effector functions in response to antigens, which include neutralization of pathogen, Complement-dependent cytotoxicity (CDC), opsonization and antibody-dependent cell cytotoxicity (ADCC) (Owen and Stranford, 2013). IgG also has the most potent effector functions (S. Raju, 2003) and consequently, has been used for the development of therapeutic antibodies for various diseases.

The core structure of an antibody is primarily formed by two heavy chains and two light chains, which are joined via disulphide linkages. This basic structure consists of the antigen binding Fab region and the crystallisable fragment, the Fc portion Figure 1-1. The oligomeric structure of antibodies varies depending on the class of molecules, which in turn affects their

size. IgM forms a pentameric structure by multiple linkages whereas secretory IgA forms a dimeric structure (Y.-K. Lee et al., 1999; Schroeder and Cavacini, 2010; Spearman et al., 2011). In IgG1 Figure 1-4, two disulphide bonds are present. The heavy chains are 50 kDa in weight whereas light chains are 25 kDa - the total size of an antibody thus adding up to ~150 kDa.

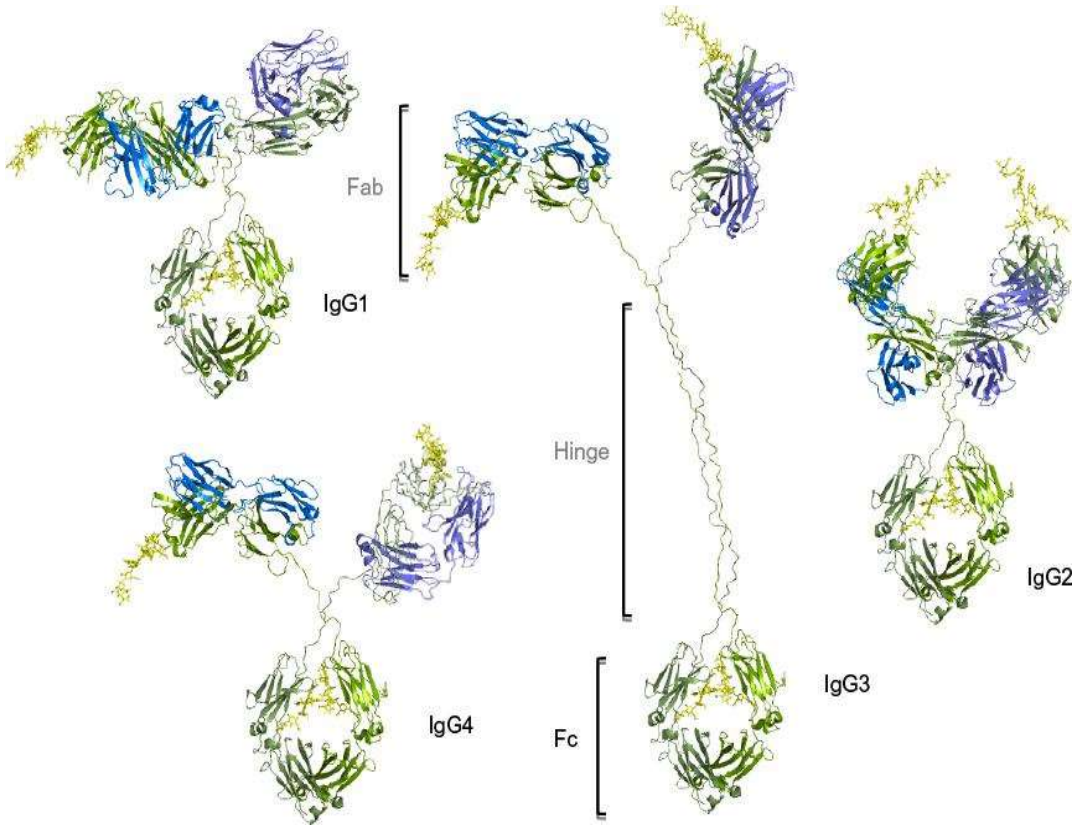

Figure* 1-1*: Structures of IgGs: This figure shows the four different subtypes of IgGs present in human blood serum. (Image taken with permission from (Hayes et al., 2016))

1.1.3 Glycosylation

With the growing demand for monoclonal antibodies as therapeutics comes the challenge to successfully produce these on a large scale without affecting the product quality whilst maintaining or increasing its efficacy. Post-translational modifications occur within the cellular environments and include protein folding, oxidation, glycosylation, and deamidation (Hmiel et

al., 2014). A major factor affecting product quality is glycosylation, which is required to be consistent throughout the production process. Glycosylation is an enzymatic, post-translational modification on secretory proteins that adds oligosaccharides to specific amino acid sites, thus making them glycoproteins. There are many forms of glycosylation, but the two most common types of glycosylation are N-linked glycosylation and O-linked glycosylation. N-linked glycans are attached to the amide nitrogen of an asparagine residue whereas O-linked glycans are attached to the oxygen of a serine or threonine residue (Bryan and Kong, 2018). Approximately 70% of proteins are glycoproteins with N-linked glycans (Butler and Spearman, 2014). N-linked glycosylation has also been shown to affect structural stability, pharmacokinetics, pharmacodynamics and immunogenicity. Moreover, with an increasing demand for biosimilars, control of glycosylation patterns is more so required (S. Wang et al., 2015). Mammalian N-linked glycosylation occurs in the endoplasmic reticulum (ER) and Golgi and results in the formation of three groups of glycans (high mannose, complex and hybrid; Figure 1-2). It involves a complex process of : 1) sequential formation of precursor glycans on a lipid carrier dolichol phosphate precursor (Glc3Man9GlcNAc2-P-P-dol) through the action of an array of glycosyltransferases; 2) transfer of the high mannose/glucose glycan to the asparagine of Asn-X-Ser/Thr of specific sequons of nascent secretory/membrane proteins in the ER lumen by oligosaccharyltransferase (OST) (Aebi, 2013; Stanley, 2011; Taniguchi and Kizuka, 2015); 3) trimming and processing of the high mannose/glucose glycans in the Golgi to introduce further heterogeneity into the glycan structures resulting in glycan profiles specific to the protein structure Figure 1-3 (Aebi, 2013; Stanley, 2011; Taniguchi and Kizuka, 2015).

The impact of variation in N-glycosylation on therapeutics is significant, with changes affecting protein folding, stability, pharmacokinetics, immunogenicity, etc. (Walsh, 2009).

This determines their efficacy and ability to induce cell-mediated responses such as Antibody-Dependent Cell Cytotoxicity (ADCC) and Complement Dependent Cytotoxicity (CDC), which are important for cancer therapeutics, as well as Antibody-Dependent Cellular Phagocytosis (ADCP) (Tay et al., 2019)which is important in viral responses. The Fc fragment of an antibody is N-glycosylated with the glycan attached to Asn 297 (Asn-X-Ser/Thr, where X is any amino acid except proline). In some forms of Igs, the Fab region is also either N- or O- glycosylated, albeit to a lesser degree in IgG (about 20%), whereas IgA, IgD, IgE and IgM are glycosylated on both Fab and Fc regions (Jefferis, 2005). IgG1s are most useful for their ability to induce the ADCC/CDC responses, making them excellent candidates for cancer therapeutics (Jefferis, 2009a). Site-specific variability of N-glycosylation (macroheterogeneity) or variability in glycan structures (microheterogeneity) affects antibody bioactivity, including its effector functions and serum half-life (Butler, 2005; Butler and Reichl, 2017; Butler and Spearman, 2014).

A number of bioprocess parameters contribute to variation in glycosylation profiles: expression/production systems, dissolved oxygen (DO) concentration, pH, culture reduction potential (CRP), ammonia levels and nutrient depletion. Some of these factors have been studied extensively (Gawlitzek et al., 2000; Kunkel et al., 1998; Muthing et al., 2003; Yang and Butler, 2002a; 2000). A study conducted to investigate the effect of different expression systems used IgGs produced from 13 different species including a human cell line (T. S. Raju et al., 2000) It was observed that the IgGs had variations in core fucosylation, terminal galactosylation and sialylation due to expression in different cell lines and therefore, host cell lines need to be chosen with careful consideration towards potential immunogenic reactions. It has been shown that when DO is decreased to 10% in cell culture from 50-100%, the amount of non-glycosylated MAbs increased. One possible explanation for this phenomenon is that the

variation in DO led to a change in redox status and thus affected the glycosylation profile (Kunkel et al., 1998).

An increase in ammonia concentration in cell cultures is known to affect cell growth and glycosylation, specifically sialylation, by decreasing the activity of sialyltransferases (Gawlitzek et al., 2000; Yang and Butler, 2002b; 2000). pH variation is known to decrease the activity of glycosylating enzymes thus leading to differences in glycosylation profiles (Muthing et al., 2003). It has been suggested that intracellular pH levels in ER and Golgi and the negative effects of increased ammonia levels are inter-related. A recent publication has re-emphasized the impact of ammonia concentration on glycosylation by studying its effect on N-glycosylation-related gene expression in an Fc-fusion protein (Ha et al., 2015). An increase in ammonia concentration led to a corresponding up regulation of thirteen glycosylation related genes out of the fifty-two studied, as observed after a five-day culture period. In particular, an increase in sialidases (neu-1 and neu-3) expression was observed, thereby decreasing the sialic acid content. This also points to the importance of combining cellular, genetic and biochemical data to further understand and unravel complex mechanisms of glycosylation and its effect on MAb production.

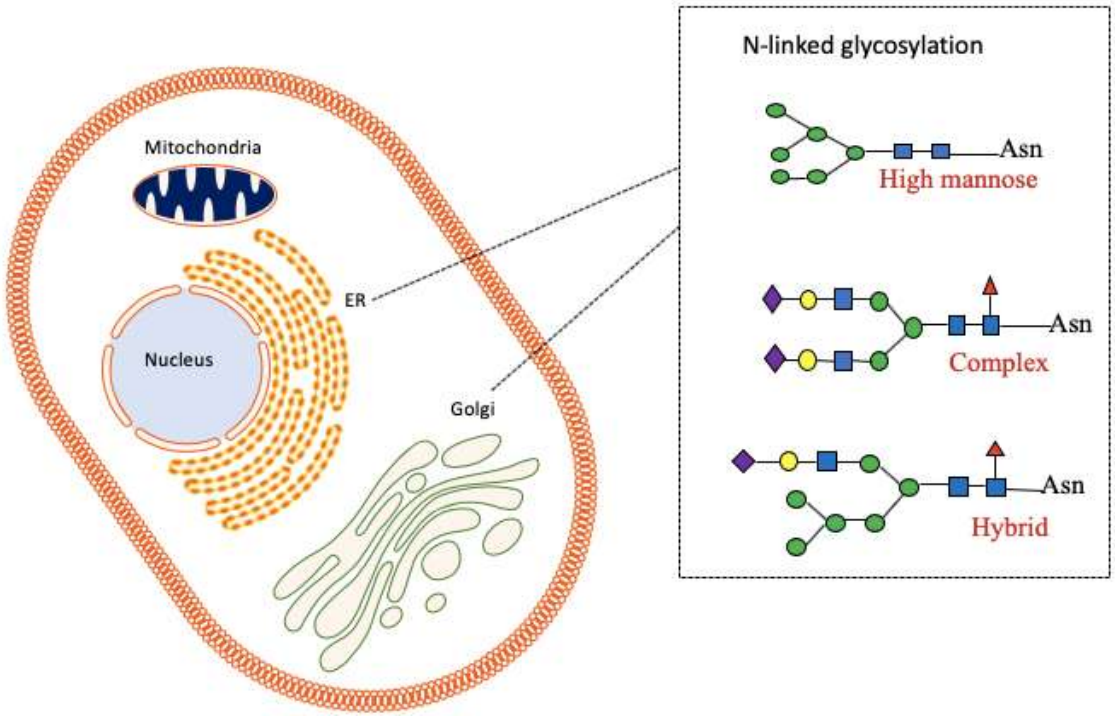

Figure 1-2: N-linked glycosylation occurs in ER and Golgi: Three main types of N-glycosylation are observed in mammalian cells- 1) High Mannose 2) Complex 3) Hybrid

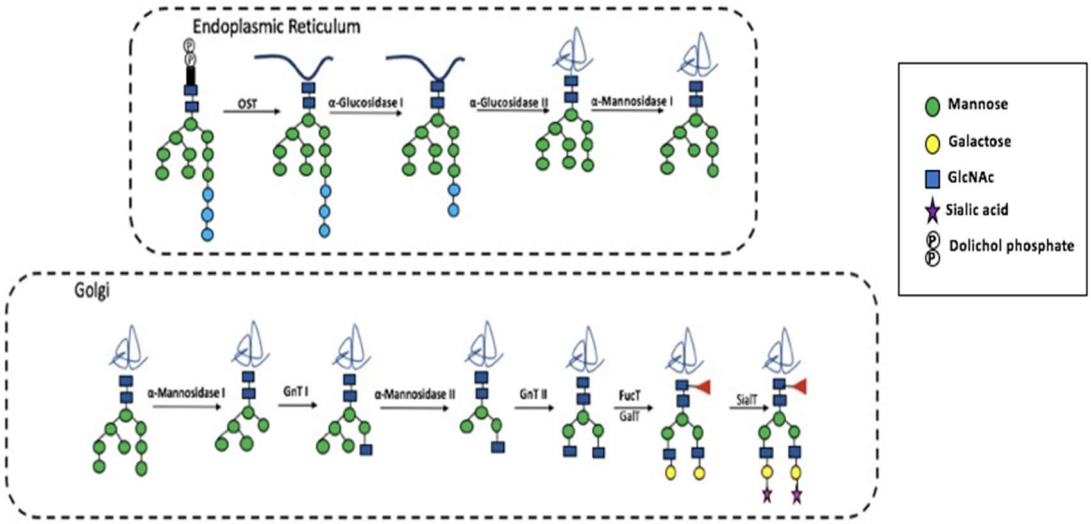

Figure 1-3: N-Linked glycosylation pathway in mammalian cells: The pathway starts in ER with the Glc3Man9GlcNAc2-P-P-dol being formed, which is transferred onto the specific Asn-X-Ser/Thr sequon of the nascent protein by oligosaccharyltransferase (OST). The pathway ends with the addition of fucose to the core structure and terminal capping of the glycan structure with sialic acids residues in Golgi. (adapted from (Aebi, 2013))

1.1.4 Novel Antibody Formats - EG2: the MabNet antibody

A large molecule size such as an IgG1 (150 kDa) for a cancer therapeutic results in inefficient tissue penetration. Moreover, larger doses of antibodies are required to be injected for adequate efficacy, leading to increased production costs (Chames et al., 2009). This has led to an exploration of antibody engineering as an option to increase specificity, reduce molecule size, increase tumor penetration and decrease production costs (Bell et al., 2010). Novel antibody formats have been designed to fulfill this purpose. Some of these formats include antibody-binding fragment (Fab) only antibodies, single chain fragment variable (scFv) and single domain antibodies (sdAb). Bispecific antibodies have also been generated, which are capable of recognising two different epitopes, that might be of the same or different antigens.

They have been categorised into orthodox (IgG-like) and heterodox (non-IgG like) and are designed using some of the novel formats mentioned above as the base structure ((Cuesta et al., 2010)).

With the goal of engineering an antibody with increased tissue penetration, low dosage requirements and decreased production costs, the EG2-hFc chimeric (camelid heavy chain Fab-human Fc) single domain monoclonal antibody was designed at BRI-NRC, Montreal by Dr. Yves Durocher's group (Bell et al., 2010). This MAb is designed such that it is devoid of the light chains because of its derivation from a camelid IgG, which is a single domain heavy chain Fab, about 12-15 kDa in size. Thus, its total size is reduced to ~80 kDa (without considering glycosylation) compared to ~150 kDa seen in full-length antibodies (Figure 1-4). EG2-hFc targets the epidermal growth factor recetor EGFR, which is over-expressed in a number of cancers, most commonly in non-small cell lung cancer (NSCLC) (da Cunha Santos et al., 2011). EG2-hFc is stably expressed in the CHO-DXB11 cell line (Bell et al., 2010; Jianbing Zhang et al., 2009).

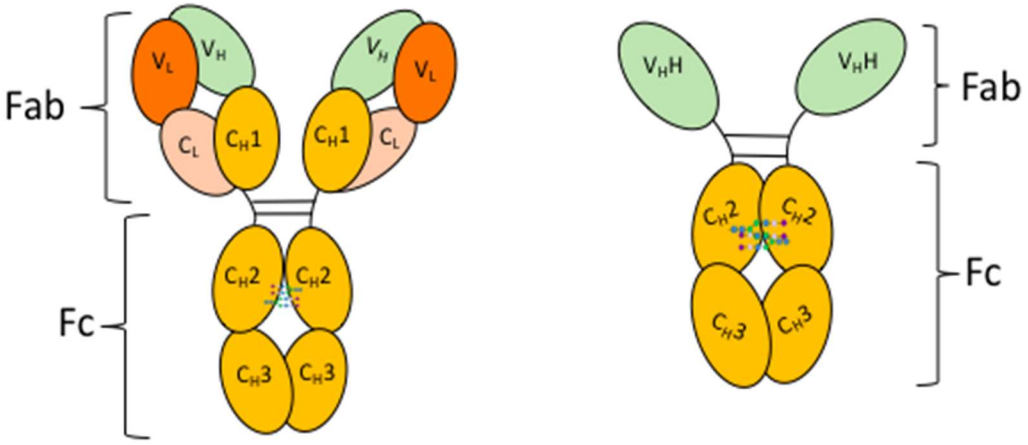

Figure 0-4: Comparison between IgG1 and EG2-hFc antibodies: EG2-hFc is a camelid Fab-based antibody and is devoid of light chains. (Bell et al., 2010) figure adapted from (D'Eall et al., 2019)

Table 1-1: Commonly used Mammalian Expression Systems: The table lists different mammalian systems commonly used for recombinant protein production (Lalonde and Durocher, 2017)

Hamster	Mouse	Human
CHO	NS0	HEK 293
BHK	Sp2/0	Per.C6

1.1.5 Mammalian Expression Systems: CHO cells and Glycosylation

The previous challenges dealing with product titres have been improved to a great extent with the availability of media development, improvement in bioprocess parameters and genetic engineering techniques (Wurm, 2004). Various mammalian expression systems have been used for recombinant protein production and some of the commonly used ones have been listed in Table 1-1. Production of recombinant proteins, including MAbs, in CHO cells has been a standard within the industry since the approval of t-PA (trade name-Activase®, Genentech, USA) in 1987 and 70% of recombinant proteins are now produced in CHO cells (Kim et al., 2011). CHO cells were first isolated by Dr. Theodore Puck in 1957 (Puck, 1958) and have since been well characterized and used frequently. Due to their ease of adaptability to suspension culture and serum free media, they are more convenient to use than adherent cells and can be grown in high density cultures, thus becoming the "workhorses of biopharmaceutical industry" (Jayapal et al., 2007). CHO cells are also less susceptible to human viruses, which has been attributed to lack of expressed viral entry receptor genes in the genome. Most importantly in the context of the work presented in this thesis, CHO cells

produce highly fucosylated MAbs, especially on the glycan core structure. Fucose on the core structure has been well-researched and known to decrease affinity between the FcγRIIa receptor and the antibody (Shields et al., 2002; Shinkawa et al., 2003), decreasing the efficacy of the MAb. The α-1,6 fucosyltransferase enzyme, which is encoded by fucosyltransferase 8 (FUT8) has been the subject of many studies wherein knockout of the FUT8 gene has resulted in afucosylated antibodies (Malphettes et al., 2010a). The gene responsible for expression of a bisecting GlcNAc on the core structure, which also has been reported to reduce fucosylation, is quiescent in CHO (Lewis et al., 2013). Researchers have also overexpressed the GnTIII gene which encodes the beta 1,4-N-acetylglucosaminyltransferase III enzyme and introduces bisecting GlcNAc (N-acetylglucosamine) in CHO cells to produce non-fucosylated products with considerable success (Davies et al., 2001; Sburlati et al., 1998; Umaña et al., 1999). CHO cells produce human-like glycan profiles, which eliminates the risk of immunogenic reactions when used as therapeutics. They do not produce immunogenic glycans such as Galα1,3-Gal and N-glycolylneuraminic acid residues that can be produced by the NS0 cells (Goh and S. K. Ng, 2017). On the contrary, CHO cells produce highly sialylated products, although only of the α2,3 type linkage (Goh and S. K. Ng, 2017). High sialylation has been linked to the ability of a glycoprotein to be retained in blood circulation for longer and thus, decrease dosage requirements (Morell et al., 1971). Expression of the α-2,6-sialyltransferase in CHO cells could be achieved with the current genetic engineering techniques leading to anti-inflammatory responses. Previously, this has been shown in a CHO bispecific antibody producing cell line, by expressing the ST6Gal I derived from CHO itself (Onitsuka et al., 2011) (Raymond et al., 2015). The scope of using CHO cells for production of recombinant proteins is enormous, with advancements in technology being made rapidly. Not only glycosylation, but other avenues such as cell growth, protein folding and secretion can also be explored to develop even more

robust CHOs and improve production of recombinant proteins further (Lalonde and Durocher, 2017).

1.2 Introduction to Chapter 2: Comparison of two glycoengineering methods aimed at reducing fucosylation of a camelid heavy-chain monoclonal antibody

1.2.1 Antibody Glycosylation

Antibody glycosylation influences effector functions including ADCC, ADCP and CDC. Currently, most marketed as well as 'under development' monoclonal antibody therapeutics are of the IgG type, where the Fc region is glycosylated (Kaplon and Reichert, 2018). The glycans are mostly of complex biantennary type and heterogenous in nature, with varying degrees of glycosylation. In some cases, the Fab variable region is also glycosylated (Jefferis, 2005). The glycosylation of antibodies is known to be responsible for the effector functions: for example, galactosylation is also thought to affect anti-inflammatory properties. The presence of galactose residues on the antibody Fc region is known to influence the CDC by inhibiting the complement component 5a receptor 1-related (Mastrangeli et al., 2018). High levels of sialylation are known to enhance the half-life of IgG antibodies (Bas et al., 2019). The presence of sialic acids could also be responsible for the decreased ADCC activity of IgGs (W. Li et al., 2017; Scallon et al., 2007). However, this is disputed and requires further investigation (Kapur et al., 2014; Stadlmann et al., 2010; Thomann et al., 2015). The presence of a bisecting GlcNAc is known to inhibit the addition of fucose onto the core structure, thus in turn reducing fucosylation and increasing the ADCC activity of the antibody (Jefferis, 2009b). With regards to MAb therapeutics for immunotherapy where ADCC activity is important, the glycosylation

profile of the glycans on the Fc region of the monoclonal antibody therapeutics affects the efficacy of the drug (Cymer et al., 2018; Jefferis, 2009c).

Due to their highly specific nature, MAbs are extensively researched for cancer immunotherapy. This began in 1997 with Rituximab as the first IgG type MAb approved for use as a cancer therapeutic against the CD20 receptor, for treatment of non-Hodgkin's lymphoma (Neves and Kwok, 2015). However, with the ever-increasing understanding of the structure and function relationship of IgG glycosylation, there is now an avenue for improvement of MAbs to increase efficiency and decrease dosage requirements by modification of Mab glycosylation. Efforts to increase efficacy include glycoengineering, CHO cell line engineering as well as manipulation of the bioprocess parameters used for production of such therapeutics.

1.2.2 Approaches to glycoengineering

Various strategies can be applied towards manipulation of N-linked glycosylation of Mabs in CHO cells with the primary intent to decrease core fucosylation and increase the ADCC response. Chemical inhibitors such as deoxymannojirimycin, which inhibits Golgi α-mannosidases resulting in glycans with high mannose content and low fucose levels have recently been used (Shalel Levanon et al., 2018). Media supplements can also affect glycan patterns. Arabinose has been used to increase high mannose glycans in turn replacing the fucose on a recombinant IgG (Hossler et al., 2017a). Other approaches such as genetic engineering, which includes overexpression of certain glycosyltransferases, addition of glycosylation sites, inhibition of enzymes such as sialidases and mannosidases to reduce

heterogeneity, have been utilized to improve product quality (Q. Wang et al., 2017). Increasing the efficacy of the EG2-hFc antibody by specifically decreasing fucosylation and thereby potentially increasing ADCC activity and efficacy has been shown by two different methods. The first method uses a decoy substrate – 2-fluoro peracetylated fucose (2FF) and has been used to inhibit production of fucosylated antibodies (Rillahan et al., 2012) and the second involves overexpression of the GDP-6-deoxy-D-lyxo-4-hexulose reductase (RMD) gene, which deflects the fucose de novo pathway into producing GDP-rhamnose, which is a dead-end product in mammalian cells (Dekkers et al., 2016; Horsten et al., 2010). In CHO cells, FUT8 is the only gene responsible for addition of the fucose onto the core glycan structure.

1.3 Introduction: Development of a non-radioactive method for analysis of ADCC activity using an engineered effector cell line

1.3.1 Antibody-dependent Cell Cytotoxicity

As mentioned in the earlier sections, ADCC activity is an important criterion to define the efficacy of a therapeutic antibody especially for cancer treatment, defined by the ability to kill tumour tissue. Therefore, evaluation of the efficiency of ADCC activity is important, especially when modifying glycosylation at the Asn 297 site of the Fc region. Fc receptors (FcRs) are expressed on the surface of cells in the immune system such as natural killer (NK) cells (Gessner et al., 1998; Ravetch and Bolland, 2001), (Gessner et al., 1998; Ravetch and Bolland, 2001). IgGs bind to the surface of the targeted cell (eg. cancer cell) through the Fab region. This allows binding of the Fc domain of IgGs to FcγR of the effector cells. With NK cells as the effector cell, activation of the perforin/granzyme pathway occurs, leading to

apoptosis and eventually cell death of the targeted cell (Trapani and Smyth, 2002) Figure 1-5. The FcγRs are comprised of three types; FcγRI (CD64), FcγRII (CD32), FcγRIII (CD16), which are further categorised into different sub-types based on expression on cell type (Gessner et al., 1998). IgG1s have high affinity for FcγRI (CD64), comparatively lower affinity than FcγRI for FcγRIIIa (CD16a) and the least affinity for FcγRII (CD32). NK cells express the FcγRIIIA type receptor that is essential for binding to a tumour antigen and induce an ADCC response and thus it is the focus of our studies for evaluating the EG2 antibody variants.

Previously, chromium (^{51}Cr) release assays have been used to quantify the ADCC activity. ^{51}Cr release assays are still preferred over other available assays in the market, possibly due to high sensitivity. However, it is a radioactive assay and relatively difficult to set up compared to other available non-radioactive assays. It also requires a source of human blood cells (PBMC - peripheral blood mononuclear cells). This project specifically aims at developing an assay that is non-radioactive, easier to establish and can be used frequently without PBMCs.

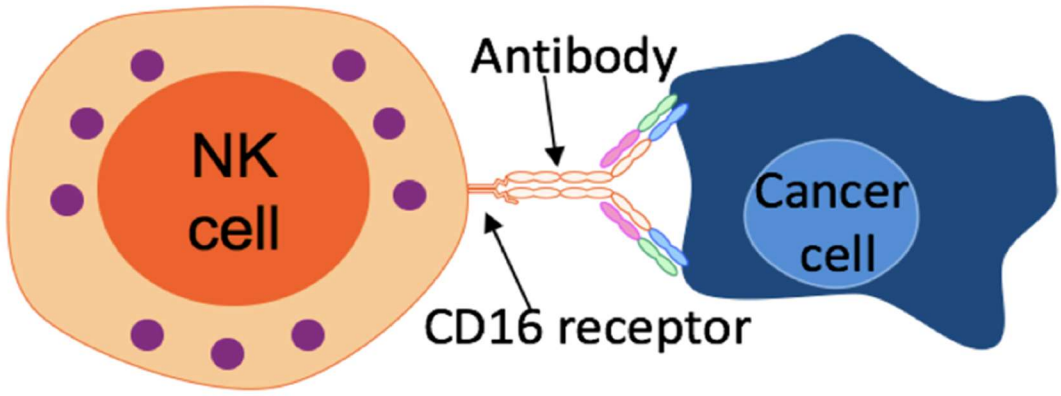

Figure 0-5: Antibody -dependent Cell Cytotoxicity mediated by NK cells: NK cells express the FcγRIIIA type receptor that is essential for binding to a tumour antigen and induce an ADCC response (adapted from Román et al., 2013)

Several non-radioactive assays were available on the market at the start of the thesis work. Assays developed by Promega and Perkin Elmer require fluorescence/luminescence measurements. Specifically, the DELFIA assay from Perkin Elmer requires time resolved fluorescence (TRF) measurements, but a major drawback is the requirement of a plate reader with TRF capabilities. Another factor to weigh in was the cost of such assays; they are much more expensive than the chromium release assays. The ideal choice was a colorimetric Lactate Dehydrogenase (LDH) release assay for which an absorbance reading could be taken at 490 nm (reference wavelength 600 nm) using a plate reader (BioTek EL808). LDH is a cytoplasmic enzyme released into cell culture supernatant upon cell membrane damage. This assay has been used in previous studies in other groups to quantify ADCC activity (Broussas et al., 2013; Shields et al., 2002). In the study described in this thesis, an attempt has been made to use NK-engineered cell lines, which has been described in detail in Chapter 3. Although LDH assays might be prone to difficulty in terms of determining whether LDH released is from the target cells or from effector cells, with appropriate controls, a robust method could be established.

1.3.2 NK-92 - novel engineered effector cell line

The novelty of this assay method development combines the commonly used LDH assay with a NK-92 effector cell line that has been generated by Dr. Kerry Campbell and his group at Fox Chase Cancer Centre, USA (Binyamin et al., 2008). The NK-92 cell line has been modified such that it expresses a CD16 (FcγRIIIA) receptor, which can bind the Fc of IgG. The cells were first discovered in the blood of a non-Hodgkin's lymphoma patient and were observed to express only activating receptors and not inhibitory receptors. It was also noted that they were able to be cultured as a cell line and thus, could be used instead of PBMCs in assays to evaluate antibodies for ADCC. The NK-92 cell lines can be modified to express any of the Fcγ receptor. For the purpose of the work described in this thesis, three different variants

were used: 1) the first NK-92 cell line, called NK-92 Parent, does not express any CD16 receptors; 2) the second variant expresses the homozygous high affinity valine variant called NK-92 V/V and 3) the third expresses the homozygous low affinity phenylalanine variant called NK-92 F/F. (Kerry S. Campbell, USA, Patent No.14/836,927, Date of Publication10-03-2016). The developed ADCC assay can be used to measure the ADCC activity of the Mab with modified glycosylation. The assay was also used to test various defucosylated antibodies generated during the course of this thesis as a proof of concept study.

1.4 Development of probes to detect intracellular redox status of glycosylation machinery

1.4.1 Redox Milieu

The ER is a highly specialized cellular organelle responsible for protein folding and protein modification such as glycosylation; therefore, assessing this environment is an important component of investigation of the glycosylation that occurs there. Enzymes involved in protein folding, calcium, ATP, and pH are all co-factors that are involved in ER homeostasis. Other factors involved in maintaining the ER environment are the redox active molecules. Redox active molecules are involved in/generated as a result of the oxidation/reduction of cysteines that form disulfide bonds or are formed due to breakage of disulphide bonds occurring during degradation of misfolded proteins (Braakman and Bulleid, 2011; Ellgaard et al., 2018). Protein Disulfide Isomerase (PDI) is known to help the formation of disulphide bonds, whereas EroI, which is an oxidoreductase, oxidises PDI and helps in maintaining continuous disulphide exchange reactions. The PDI family of proteins can be reduced by glutathione (GSH), whereas Ero1 is not. In the cytosol, a reducing environment is maintained by glutathione being oxidised to GSSG, which in turn is reduced to GSH by glutathione reductase (Braakman and Bulleid, 2011). In contrast, the ER has a more oxidising environment, conducive to protein folding. After disulfides are formed, they can be reduced either by GSH or PDI, but only if they are solvent accessible. Therefore, protein folding as well as the inaccessibility of the disulfides prevents breakage of the bonds. It is thought that the oxidised environment of ER is a result of the protein folding activities rather than being a precursor requirement.

1.4.2 Effect of Redox state on glycosylation in mammalian cells

Redox status, DO, pH and ammonia are suggested to be factors influencing the intracellular machinery, the ER and Golgi where glycan processing occurs (Kunkel et al., 1998; Muthing et al., 2003; Yang and Butler, 2002a). Studies have focused on effect of these biochemical parameters on MAb production and glycosylation. However, the interplay between the biochemical factors and the cellular machinery during MAb production and its influence on glycosylation pathway has not been explored extensively. A recent publication has highlighted the potential link between redox balance and the role it plays in glycosylation especially by producing high mannose (HM) glycans in MAbs. It was shown through metabolomics analysis that the addition of certain amino acids such as ornithine to the cell culture medium was responsible for production of HM glycans (Kang et al., 2015). Ornithine, along with other identified metabolic markers such as cystine, niacinamide, glutathione, have been known to contribute to redox regulation (Kang et al., 2015; Zanatta et al., 2013). (Meneses-Acosta et al., 2012a) have shown that reducing conditions lead to an increase in the MAb concentration and enhanced cell growth in hybridoma cell culture. Although glycan analysis was not conducted in this study, it is an important finding that can be extrapolated to study the importance and effect of redox potential in cell culture on glycosylation.

Following the results from DO (Kunkel et al., 1998) and culture reduction potentials (CRP) of hybridoma cell lines (Meneses-Acosta et al., 2012b) further studies in the Butler lab have led to investigating antibody producing mammalian cell lines. Experiments were conducted using dithiothreitol (DTT) to induce reducing conditions (Dionne et al., 2017a). Three antibody producing cell lines were studied and compared: 1) NS0 cell line producing an

IgG1 2) CHO cell line producing anti-IL8 antibody (CHO-DP12) and 3) CHO cell line producing EG2 camelid antibody (CHO EG2-hFc). It was observed that although the addition of DTT to induce reducing conditions had no effect on cell growth or antibody concentration, variations in glycan profiles occurred with a decrease in ~50% galactosylation index (GI). A comparison of CRP after DTT treatment amongst the three cell lines also established that the variation in GI is host cell line dependent. It was also noted that decrease in GI was related to a lowering of pH in the different cell lines irrespective of DTT concentration. Both NS0 and CHO-DP12 exhibit low GI whereas CHO EG2-hFc exhibits high GI.

Redox homeostasis has been a focus of many studies primarily because it affects cellular functions. The importance of redox state within ER required for protein folding has been studied extensively. The balance between glutathione and its oxidised form is considered to be crucial for disulfide bond formation in ER and it prevents hyperoxidising conditions, thus, protein misfolding (Chakravarthi and Bulleid, 2004; Chakravarthi et al., 2006). This project was consequently designed to investigate the intracellular redox state using redox sensitive green fluorescent proteins (roGFPs) and its role in MAb production and glycosylation, by integrating roGFPs into the in-house CHO cell line producing EG2hFc chimeric monoclonal antibody variant.

1.4.3 Use of GFP to detect redox states of cellular organelles:

1.4.3.1 GFP

The green fluorescent protein is 27 kDa in size with 238 amino acids (Hink et al., 2000), and was discovered in 1960s while researchers were studying *Aequorea victoria* (Kremers et al., 2011). The entire structure of the fluorescent protein is required for its fluorescent properties. Several marine species express green fluorescent proteins but the most commonly used is derived from *A. victoria*. GFP has been used as a reporter protein for various purposes which include but are not restricted to the study of gene expression, location, pH and redox state. The wild-type GFP that has been described above has two excitation peaks, 395 nm and 475 nm. However, a modified GFP with a single mutation of serine-65-threonine has been developed that has enhanced fluorescence and is thus called, enhanced green fluorescence protein (EGFP). Various other mutations have been introduced at position 65 and exhibit different properties some of which include increased/decreased fluorescence intensities and single excitation peaks. Thus, it showed that the amino acid at position 65 was important for the spectral properties of GFP.

1.4.3.2 Use of redox sensitive GFPs to measure redox state

Traditional assays to measure these ratios have been cumbersome and involved invasive studies requiring cell lysis, thus eliminating the possibility of studying redox status in live cells (Dooley et al., 2004). This has changed with the Nobel Prize winning work of Osamu Shimomura, Martin Chalfie and Roger Tsien discovering and developing GFP. Extensive

research by various groups has focused on exploring the capabilities of GFP. The potential is vast with usage ranging from gene expression detection with GFP co-transfection (Kain et al., 1995) to studying factors that affect cellular events such as pH, calcium ion concentration, and redox homeostasis (Cannon and James Remington, 2008). GFP exhibits a dual excitation behaviour that has led to the development of biosensors to study biological events via real-time imaging using fluorescence microscopy (Cannon and James Remington, 2008; Lohman and Remington, 2008; Jin Zhang et al., 2002). Studies in mammalian cells (van Lith et al., 2011) and yeast (Delic et al., 2010) have monitored the redox status of the cytosol (reducing environment) and the ER (oxidising environment) using redox sensitive GFP (roGFP) probes designed in the Remington lab, University of Oregon. The roGFPs exhibit a ratiometric change between the oxidised and reduced roGFPs occurring due to a conformational difference within the chromophore (Lohman and Remington, 2008). These studies in yeast and mammalian cell lines have indicated that the roGFP constructs are suitable for studying real-time changes in redox status in living cells, with varying oxidising or reducing conditions. In mammalian cells, it was noted that the response to DTT or 4 - 4′dipyridyl disulfide (DPS) was rapid with difference observed between fully reduced and oxidised states, with cell recovery occurring in 5 minutes after removal of either agents. This finding steered the hypothesis towards the role of genetic elements such as PrxIV and Ero1 at play that were responsible for directly or indirectly metabolizing DTT and helping cells recover (Baker et al., 2008; Tavender et al., 2010).

Glycosylation in the Golgi is mediated by enzymes such as glycosyltransferases or mannosidases present in the cis, medial or trans membranes. These enzymes are responsible for further processing of the glycoprotein that passes on from the ER, adding galactose, N-acetylglucosamine, sialic acid and fucose or cleaving mannose residues from the structure.

None of the studies conducted using roGFPs have focused on Golgi redox state and its effect on glycan processing. Results from this project will provide an insight into the organelle's redox status and how this might be affecting its role in glycosylation.

Objectives of the thesis:

The objectives of the thesis were: -

1) **Glycoengineering to improve therapeutic efficacy by decreasing fucosylation and measurement of this decrease in fucosylation and its effect, by detection of ADCC.**
2) **Examining the effect of redox potential on glycosylation, specifically the development of probes to detect intercellular redox status within the ER and Golgi.**

2

Comparison of two glycoengineering strategies to enhance the antibody-dependent cell cytotoxicity response of a camelid heavy chain antibody

2.1 Introduction

The development of biopharmaceutical monoclonal antibodies (MAbs), has been a major contribution towards treatment of many forms of cancer, and Crohn's disease (Singh et al., 2018; Weiner, 2015; Yu et al., 2017). Production of these biopharmaceuticals in mammalian cells requires certain critical quality attributes to be complied with, which include safety and efficacy, as well as quality of the protein (Jungbauer and Graumann, 2012). Safety of the protein refers to the capability of the therapeutic to avoid generating an immunogenic response, whereas efficacy could be responsible for eliciting an immune response against a pathogen and decrease dosage requirements. The efficacy of an Immunoglobulin G (IgG) type antibody for cancer immunotherapy is dependent on its ability to elicit effector functions such as the antibody-dependent cell cytotoxicity (ADCC) response via interaction with effector cells such as Natural Killer (NK) cells.

Efficacy is also related to glycosylation. Antibody glycosylation is well characterized, of which the N-linked glycosylation of the Fragment crystallisable portion (Fc) has been studied extensively(Jefferis, 2009c; 2007). This Fc region of the IgG antibody is responsible for binding to Fcγ receptors. For a majority of therapeutic IgGs available, binding to the FcγRIIIa

(CD16) receptor on natural killer (NK) cells is imperative to trigger the ADCC response (W. Wang et al., 2015). The effect of fucose on binding of the antibody Fc region to CD16 and activation of the ADCC response have been well studied, and the absence of core fucose has been found to increase ADCC (Shinkawa et al., 2003; Yamane-Ohnuki and Satoh, 2009). Numerous structural studies have shown that the presence of glycans on Fc contributes to binding of FcγR to target antigen-IgG complexes, leading to ADCC (Krapp et al., 2003; Mimura et al., 2001; Yamaguchi et al., 2006) and CDC (Leatherbarrow et al., 1985).

Our model antibody of interest, the anti- Epidermal Growth Factor Receptor (EGFR) chimeric (camelid heavy chain domain-human Fc) antibody, EG2-hFc(human Fc) is expressed in CHO cells (Bell et al., 2010). With the hFc, the antibody is expected to elicit an ADCC response via the FcγRIIIa receptor. A large molecular size such as an IgG1 for a cancer therapeutic results in inefficient tissue penetration. Moreover, larger doses of antibodies are required to be injected for adequate efficacy, leading to increased production costs (Chames et al., 2009). This has led to an exploration of antibody engineering as an option to increase specificity, reduce molecule size, increase tumor penetration and decrease production costs. Novel antibody formats have been designed to fulfill this purpose. Some of these formats include antibody-binding fragment (Fab) only antibodies, single chain fragment variable (scFv) and single domain antibodies (sdAb). Bispecific antibodies have also been generated, which are capable of recognising two different epitopes, that might be from the same or different antigens. They have been categorised into orthodox (IgG-like) and heterodox (non-IgG like) and are designed using some of the novel formats mentioned above as the base structure (Ayyar et al., 2016; Elgundi et al., 2017; Spiess et al., 2015). With the goal of engineering an antibody with increased tissue penetration, low dosage requirements and decreased production costs, the EG2-hFc chimeric (camelid heavy chain Fab-human Fc) single domain monoclonal antibody

was designed at BRI-NRC, Montreal by Dr. Yves Durocher's group. The MAb is designed such that it is devoid of the light chains (because of its derivation from camelid antibodies, which have single domain heavy chain Fab, about 12-15 kDa in size), reducing its total size to ~80 kDa (without considering glycosylation) compared to ~150 kDa seen in full-length IgG (Bell et al., 2010). EG2-hFc targets the epidermal growth factor receptor EGFR which is over-expressed in a number of cancers, most commonly in non-small cell lung cancer (NSCLC) (da Cunha Santos et al., 2011). The EG2-hFc is stably expressed in a proprietary cell line derived from the CHO-DXB11 cell line (Agrawal et al., 2012).

As the core fucose can affect the effector function of an antibody, efforts have focused on various methods that can be employed either prior to or during the production process to manipulate pathways to reduce fucosylation. Although different approaches have been developed to remove the core fucose, they have been subject to drawbacks. (Yamane-Ohnuki et al., 2004) developed a FUT8 knockout CHO cell line to produce non-fucosylated antibodies but there is a possibility of non-homologous recombination occurring over time, resulting in reversion of the cell lines. Strategies involving RNAi knockdown of enzymes responsible for fucosylation could be difficult for large-scale production. Glycoengineering methods use chemical inhibitors and cell line engineering for such purposes. Here we have investigated and present the effect of two such methods on our in-house MAb producing cell line, 1) a decoy substrate – 2-fluoro peracetylated fucose (2FF) has been used to inhibit production of fucosylated antibodies (Rillahan et al., 2012) and 2) overexpression of the GDP-6-deoxy-D-lyxo-4-hexulose reductase (RMD) gene, which deflects the fucose de novo pathway into producing GDP-rhamnose, which is a dead-end product in mammalian cells (Dekkers et al., 2016; Horsten et al., 2010) (Figure 2-1(a)). 2FF is a cell-permeable chemical inhibitor of Fucosyltransferase (FUT) activity. In CHO cells, FUT8 is the only gene product responsible

for addition of the fucose onto the core glycan structure. Using 2FF, we have shown that core fucosylation decreases by 78%. The RMD expression vector which was transfected into the antibody producing cell line showed a decrease in core-fucosylation by 68%. An ADCC assay was also used to check the effect of the changes in fucosylation on the cytotoxicity of the target cells, MDA-MB-468 cells which express an EGFR receptor. Also, electrospray ionization mass spectrometry (ESI-MS) was used to analyze the fucosylation pattern of EG2 with addition of increasing concentrations of 2FF. This showed that 2FF inhibits the addition of fucose in a concentration-dependent and specific, sequential manner with the inhibition of fucose occurring one fucose residue at a time.

Contents of this chapter have been published in the following papers:

1. Comparison of two glycoengineering strategies to control the fucosylation of a monoclonal antibody N Mishra, M Spearman, L Donald, H Perreault M Butler, Journal of Biotechnology: X, Volume 5, 2020, 100015, ISSN 2590-1559, https://doi.org/10.1016/j.btecx.2020.100015.
2. Mass spectrometric analysis of core fucosylation and sequence variation in a human–camelid monoclonal antibody, L. J. Donald, M. Spearman, N. Mishra, E. Komatsu, M. Butler and H. Perreault, *Mol. Omics*, 2020, Advance Article, https://doi.org/10.1039/C9MO00168A

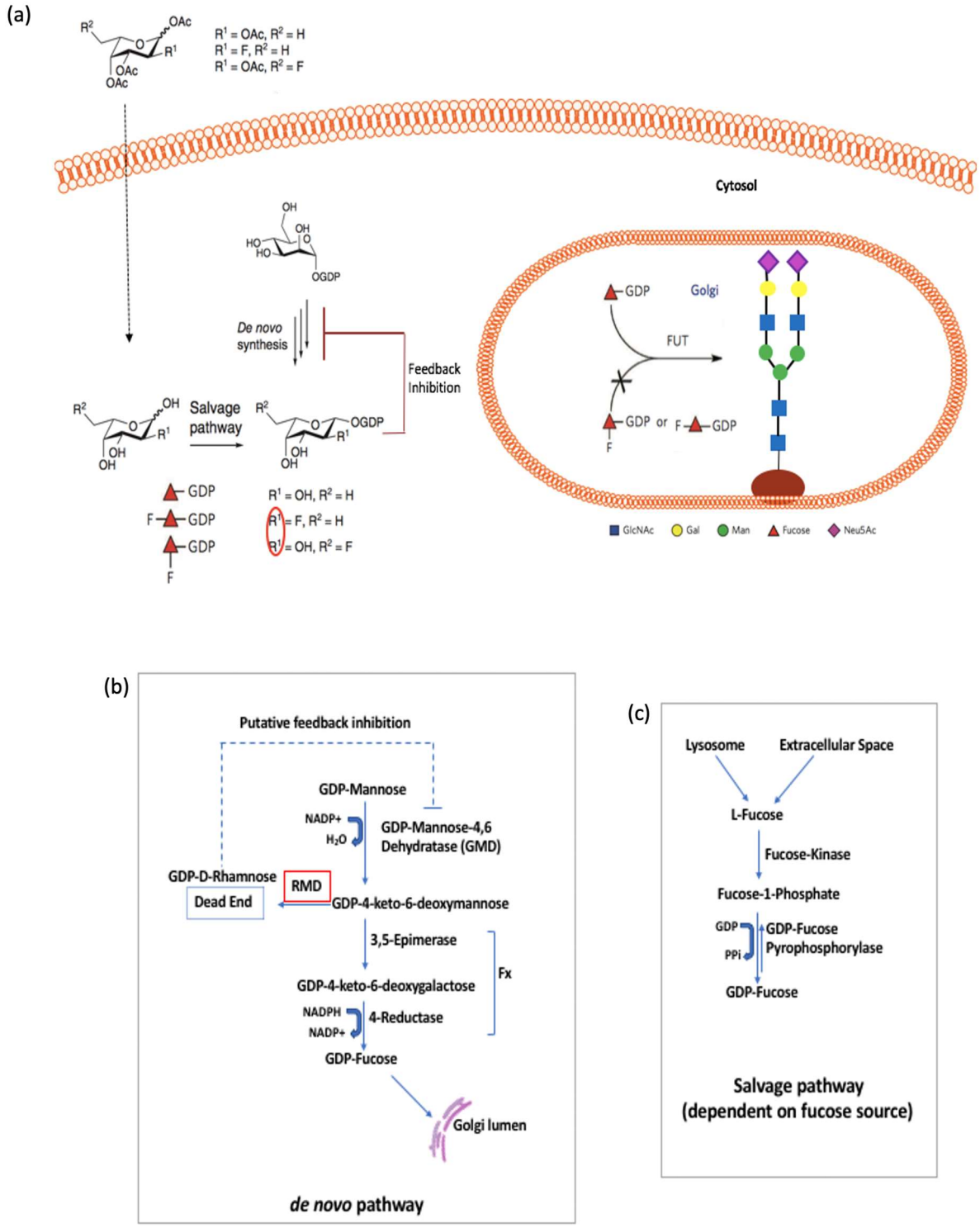

Figure 2-1: How do 2FF and RMD work at a cellular level? (a) Mechanism of action of 2-fluoro peracetylated fucose via passive diffusion through cellular membrane (b) deflection

of de novo pathway by RMD co-expression leading to production of GDP-rhamnose (c) production of GDP-fucose via salvage pathway through addition of fucose in cell culture media. Figure adapted from (Horsten et al., 2010; Rillahan et al., 2012).

2.2 Methods

2.2.1 Cell culture

CHO EG2-hFc cells (kindly provided by Dr. Yves Durocher) were cultured in baffled shaker flasks with vented caps (VWR International, Mississauga, CA). Cells were passaged every 3-4 days for maintenance and seeded at $2.5x10^5$ cells/mL in BioGro CHO CD media (BioGro Technologies, Winnipeg, CA) and further experiments were set-up using these cells. For experiments, cells were cultured at the same seeding density as above and harvested on day 4 to collect the supernatant for further analysis.

2.2.1.1 2FF addition to CHO EG2-hFc cells

2FF (kindly gifted by Dr. James C Paulson, The Scripps Research Institute, la Jolla, California) was dissolved in DMSO to prepare the required concentrations. CHO EG2-hFc cells were seeded as mentioned in section 1.2.1 and 2FF concentrations of - 0, 5, 20, 50 and 100 μM 2FF were added to the culture. The control culture (0 μM) had an equivalent amount of DMSO only added. On day 4 media was harvested and filtered through 0.2-μm filters for further analysis.

2.2.1.2 RMD transfection into CHO EG2-hFc

The RMD expression vector (kindly gifted by Dr. Volker Sandig, ProBioGen, Germany) was transfected into the CHO EG2-hFc cell line. The proprietary RMD bicistronic plasmid vector from ProBioGen also encodes the green fluorescent protein (GFP) and can thus, co-express both RMD and GFP simultaneously. Transfection was done using Xfect™ transfection reagent (Takara Bio, CA, USA) according to manufacturer's instructions. $5x10^5$ cells were set up in a 6-well plate prior to preparation of the DNA-Xfect complex. The required concentration of RMD plasmid DNA was diluted with Xfect reaction buffer to a final volume of 100 µl and mixed thoroughly. The Xfect polymer was then added to the diluted plasmid DNA and mixed again by vortexing (the protocol dictates that 0.3 µl of Xfect polymer be added per µg of DNA). The DNA-Xfect mix was incubated for 15 minutes at room temperature, following which it was added to the cells. The plate was incubated at 37°C overnight. Transfection media was replaced with fresh media the following day. Transfection was confirmed 48-hours post transfection using epifluorescence inverted microscopy. The transfected cells were then selected for, using Geneticin (concentration) (Thermo Fisher Scientific, Waltham, MA, USA). Cells were grown in the presence of the selection reagent for two weeks when the cell viability reached ≥90-95% (assessed using the trypan blue exclusion method described in 2.2.1.5) and a stable pool was thus generated.

2.2.1.3 Addition of 2FF to RMD-transfected CHO EG2

Concentrations of 10 and 50 μM 2FF were added to RMD-transfected CHO EG2-hFc cells into the starting culture (Day 0). Cells were seeded at $2.5x10^5$ cells/mL and cultured for 4 days. These were then harvested, and the cell culture supernatant collected for further studies.

2.2.1.4 Fucose titrations

Cells were cultured as previously 2.2.1, and seeded at $2.5x10^5$ cells/mL on the day of fucose addition. L-Fucose was obtained from Sigma-Aldrich (Oakville, Ontario, CA) increasing concentrations (0, 0.01, 0.05, 0.1 and 1 mM) of fucose were added to the BioGro-CHO CD media. Cells were allowed to grow for 4 days in the presence of the fucose-supplemented media. At the end of 4 days, cells were harvested, and samples purified using Protein-A mini-columns (as described in 2.2.3.1) for further glycan analysis.

2.2.1.5 Determination of cell viability using trypan blue exclusion method

Cells were checked for viability percentage and cell concentration using the trypan blue exclusion method. The measurements were taken using an automated instrument – Cedex (Innovatis AG, Bielefeld, Germany) using a mix of equal volumes of 0.4% (w/v) trypan blue (Thermo Fisher Scientific, Waltham, MA, USA) and cell samples. The results of image analysis using Cedex includes total cell concentration, viable cell concentration, viability percentage, aggregation and cell size.

2.2.2 Cell sorting using a Fluorescence activated cell sorter (FACS)

The cell sorting on the CHO EG2-hFc cells expressing GFP tagged RMD was done using BD FACSAriaIII system (BD Biosciences, San Jose, CA). The GFP transfected cells at a concentration of 10^7 cells/ml were washed with PBS and resuspended in the sorting buffer containing 1xPBS (Ca/Mg^{2+} free), 1%FBS, 25mM HEPES pH7.0 and 1mM EDTA. The cell suspension was then sorted on the BD FACSAriaIII system using 100-µm nozzle at 20 psi pressure. Sorting was categorised into high (Hi) and medium expressing cells (Med) and cells were gated before start of the sort accordingly. The sorted GFP positive cells were collected and washed in PBS. They were then transferred to BioGro CHO CD in T75 suspension flasks (Sarstedt AG & Co, Nümbrecht, Germany) overnight for recovery, before moving the cells into shaker flasks.

2.2.3 Glycan analysis

Glycan analysis was performed as per the previously published protocol (Tayi and Butler, 2015).

2.2.3.1 Protein A antibody capture and glycan release

Cell culture supernatants were collected on day 4 and filtered using 0.2-µM filters (Merck Millipore, Darmstadt, Germany). The supernatants were then concentrated such that the resulting antibody concentration was at least 100 pM for glycan detection using HPLC. Protein A mini (1 mL) columns (GE Life Sciences, USA) were first washed with 20 mM phosphate buffer (80% 20 mM Na_2HPO_4, 20% of 20 mM NaH_2PO_4). Each filtered solution was then incubated for 15 minutes at 37°C, in the respective Protein A columns to capture the EG2

antibody. The solution was then removed by centrifugation and the column washed with the phosphate buffer 3 times. To release glycans, 10 units of PNGase F (Promega, Wisconsin, USA) was then added to the column with 150 µl phosphate buffer and incubated for 24 hours at 37°C on a rotary shaker platform.

2.2.3.2 Glycan collection, 2-AB labelling and clean-up of glycans

After the 24 hours incubation, the glycans were collected by centrifugation in a 2-mL tube. The centrifugation was repeated after addition of 250 µl of water. The collected glycans were then filtered through a 10K filter (Pall corporation, USA) to remove the PNGase F and then dried in a vacuum concentrator. To elute the antibody, first 600 µl of phosphate buffer was added to the Protein A column and washed, and this was repeated twice more. 300 µl of elution buffer (100 mM glycine-HCl) was then added to the column, and the filtrate collected in a 2-mL tube. This was repeated with 100 µl of elution buffer (1 M Tris-Cl) following which the neutralization buffer was added to bring the pH to ~7.2.

To label the glycans, 5 µl of 2-AB labelling solution was added to the dried glycans and incubated at 65°C for 2 hours. The 2-AB labelling solution was prepared using 100 µl of a 30% acetic acid/70% DMSO solution and 5 mg of 2-AB, to which 6 mg of sodium cyanoborohydride was added and mixed until dissolved. To clean-up the glycans and remove excess labelling, HyperSep™ Diol cartridges were used. First, the cartridges were washed with water and then conditioned with 4 ml of acetonitrile. 40 µl of acetonitrile was then added to the labelled glycans, mixed well and then added into the cartridges. The glycans were allowed to bind to the cartridge for 15 mins and then washed with 6 ml of acetonitrile. The glycans were eluted with water and dried in the vacuum concentrator.

2.2.3.3 Glycan analysis by HILIC-HPLC

To the dried glycans from 2.2.3.2, 20 µl of Milli-Q water was added and mixed well. To prepare samples for HPLC, 6 µl of sample was mixed with 24 µl of acetonitrile in a HPLC vial. A 30 µl dextran ladder was also prepared and used to generate a standard curve for the glucose units (GU) from sample retention times. The samples were analysed using HILIC-HPLC. The GU values were compared to structures available on the GlycoStore database (https://glycostore.org/) and previous exoglycosidase digests.

2.2.3.4 Calculation of Galactosylation, Sialylation Indices and Fucosylation Percentage

Galactosylation index (GI) is calculated on the basis of number of galactose residues on glycan structures: G0 – no galactose, G1- one galactose and G2- 2 galactose residues.
The GI is calculated using the following equation:

$$GI = \frac{(G1 * 0.5) + G2}{G0 + G1 + G2} \qquad \textit{Equation 2-1}$$

Fucosylation percentage was calculated taking into consideration area of all the fucosylated species within the total area of glycans.

$$\textit{Fucosylation}\ \% = \frac{\%\ \textit{Area with Fucosylated Glycan}}{\textit{Total Area}\ \%} \qquad \textit{Equation 2-2}$$

Sialylation Index is calculated by including all the sialic acid molecules on the glycan structure. The equation is as follows:

$$SI = \frac{(S1*0.5+S2)}{S0+S1+S2} \qquad \textit{Equation 2-3}$$

2.2.4 Electrospray Ionization Mass Spectrometry

Samples were exchanged into 50 mM Aldrich NH_4OAc (99.99%) using Amicon Ultra filtration units 50K MWCO. Six centrifugations of 15 min at 5K rpm were required, in a SS34 rotor in a Sorval Centrifuge. Ideally, samples were recovered at about 45 μM. For electrospray ionization, samples were diluted to 10 μM in 1% acetic acid/50% methanol. When the sample concentration was insufficient, samples were diluted to 2 μM and nanospray ionization was used.

The declustering voltage was adjusted in order to give the best resolution of the ions, usually from 120 V to 180 V, with a spray voltage of 3000 V for ESI and 1000 V for nanospray. Spectra were acquired and analysed using TOFMA, an in-house software developed with the instrument. Spectra were very complex due to multiple species at each charge state: for this reason, only the deconvolutions of the major ions are presented here (Donald et al., 2006; Kozlovski et al., 2011)

2.2.5 ADCC assay

The efficacy of both RMD-transfected EG2 and 2FF-treated EG2 was measured using an ADCC assay that has been developed in-house based on the published method by (Broussas et al., 2013) (described in detail in Chapter 3). Briefly, the assay was performed using an LDH based assay method (Roche, Switzerland). The NK-92 effector cells used were provided by Dr. Kerry Campbell (Fox Chase Cancer Centre, PA, USA) and the MDA MB 468 cell line was provided by Dr. Spencer Gibson's lab (University of Manitoba, Winnipeg, CA). Both NK-92 and MDA-MB-468 cells used were ≥90% viable. First, optimization assays were performed to establish the number of effector and target cells required to obtain the best and most consistent signal. Subsequent experimental assays with the EG2-hFc antibody, both RMD-transfected and 2FF treated, were then performed using these cell numbers. The cytotoxicity percentage was calculated using the following equation:

$$\textit{Cytotoxicity}\ (\%) = \frac{[Exp-(SR_{NK+468\ cells})]}{MR_{468\ cells} - SR_{468\ cells}} \times 100 \qquad \textit{Equation 2-4}$$

where, Exp = experimental conditions after addition of antibody; $SR_{468\ cells + NK}$ = spontaneous LDH released from untreated cells; $MR_{468\ cells}$ = Maximum LDH activity in the target cells that can be released; $SR_{468\ cells}$ = Spontaneous LDH release from untreated target cells.
The equation takes into account the spontaneous release by target cells as well as combination of target and effector cells, thus, considering the no antibody control.

2.3 Results

2.3.1 Effect of 2FF

Varying concentrations of 2FF (0-100 μM) were added to CHO EG2-hFc cells. Cells were cultured with 2FF over 4 days and then harvested. The supernatant collected from the 2FF-treated cultures were passed through a 0.2 μm filter and glycan analysis was performed on these. 2FF did not affect the growth of cells, viability or productivity as compared to the control, when concentrations up to 50 μM were tested Figure 2-2 (a) and (b). At a concentration of 20-50 μM, the effect was maximum and fucosylation decreased to 17.5%. Between 15-50 μM, the decrease in fucosylation was not as significant as the lower concentrations Figure 2-2(c) which could be due to the uptake of 2FF reaching saturation. With respect to the glycan profile, addition of 2FF showed a shift towards the non-fucosylated species, with increase in area % for A2G1(20%) and decrease in F(6)A2G2. An increase in the A2 peak was also observed with increasing concentrations of the inhibitor. The galactosylation index (GI) was also reduced from 0.65 to 0.5 with little effect on sialylation with decrease in area% by 6% Figure 2-3.

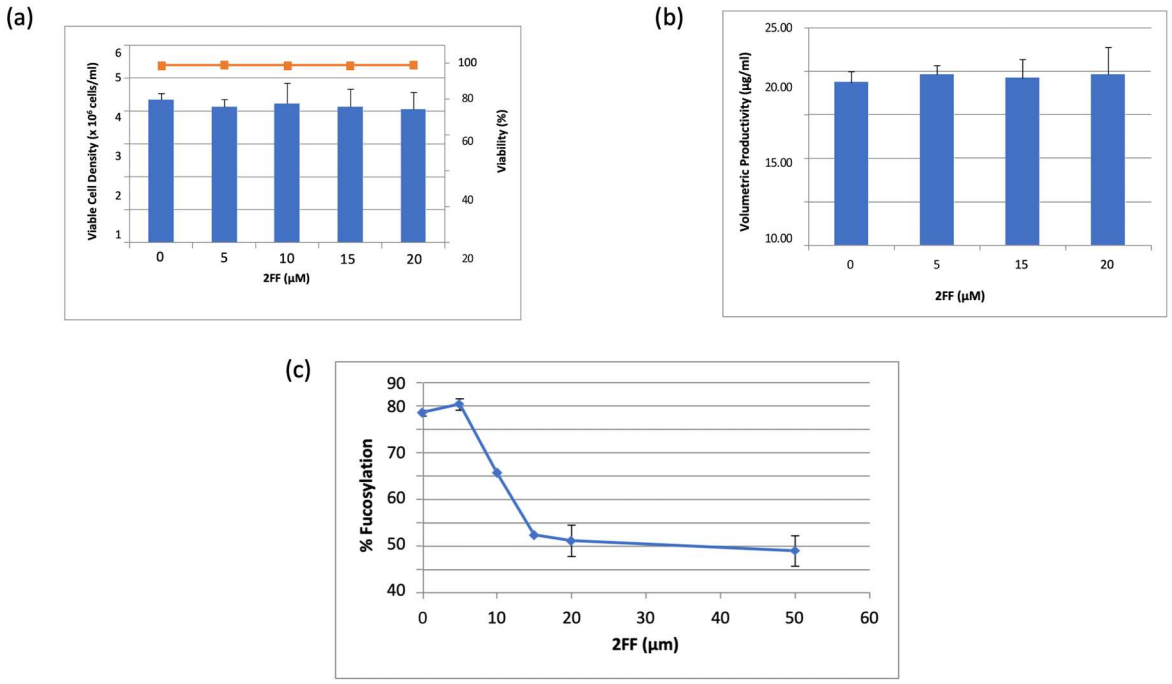

Figure 2-2: Effect of 2FF on (a) viability (b) productivity (c) fucosylation percentage of CHO EG2-hFc cells: CHO EG2-hFc cells were inoculated at 2.5x105 cells/ml into 100 ml media containing varying concentrations of 2-F-peracetylated fucose (0-20 µM). The cultures were maintained in 250 ml shake flasks for 4 days at which point the viable cells were enumerated by the trypan blue exclusion method. The antibody was harvested from the cell-free media and glycans isolated following PNGase F release prior to anlaysis by hydrophilic column separation by HPLC. The panels above show: (a) the viable cell density (cells/ml) and % viability. (b) Volumetric concentration of antibody (µg/ml) and (c) the % fucosylation of the associated glycans (Mishra et al., 2020).

*Table 2-1: List of main glycan peaks and percentage area observed in the 2FF added CHO EG2-hFc experiment. This is a representative table for two experiments conducted with 2FF addition to CHO EG2-hFc cells. (*isomer forms of F(6)A1G1, ** isomer forms of F(6)A2G1)*

	0µM		5µM		10µM		15µM		20µM	
Structures	***GU value***	***% Area***	***GU value***	***% Area***	***GU value***	***% Area***	***GU Value***	***% Area***	***GU value***	***% Area***
M3	4.35	0.48	4.35	0.54	4.35	0.79	4.35	0.76	4.35	0.85
F6M3	4.89	1.39	4.89	2.54	4.91	2.66	4.91	3.12	4.90	3.64
F(6)A1/A2	5.36	2.01	5.36	3.3	5.39	7.64	5.40	15.02	5.39	18.48
A1G1	5.60	1.48	5.60	1.33	5.61	1.99	5.61	1.93	5.60	2.09
A1G(4)1									5.72	1.6
F(6)A2G0	5.81	11.16	5.80	16.98	5.81	8.77	5.81	5.38	5.80	4.69
*F(6)A1G1	6.03	0.86	6.01	0.23	6.04	1.53	6.03	1.06	6.02	1.86
A2G1	6.14	2.32	6.13	2.38	6.16	9.94	6.17	18.75	6.16	21.24
F(6)	6.27	1.37	6.25	0.62	6.26	5.68	6.26	7.97	6.25	8.64
*F(6)A1G1	6.36	1.15								
**F(6)A2G1	6.56	19.92	6.55	23.39	6.56	14.11	6.57	7.78	6.56	5.8
**F(6)A2G1	6.68	7.42	6.66	7.16	6.68	4.86	6.68	2.3	6.67	1.79
A2G2	6.98	4.27	7.00	2.85	7.04	11.42	7.04	15.08	7.03	14.22
A4G1	7.21	1.9	7.19	1.09						
F(6)A2G2	7.44	27.13	7.42	24.11	7.45	17.81	7.45	6.86	7.44	4.05
F(6)A1G1S1							7.58	3.5	7.57	2.74
F(6)A2G2S1	7.94	7.65	7.93	5.94	7.95	4.11	7.95	1.8	7.94	0.92
A2G2S2					8.14	1.2	8.14	1.45	8.13	0.99
A2G2S1	8.27	0.56								
F(6)A2G2S2	8.45	2.94	8.44	2.31	8.46	1.56	8.45	0.7	8.44	0.32
A2G2S2	8.76	0.98	8.74	0.27						

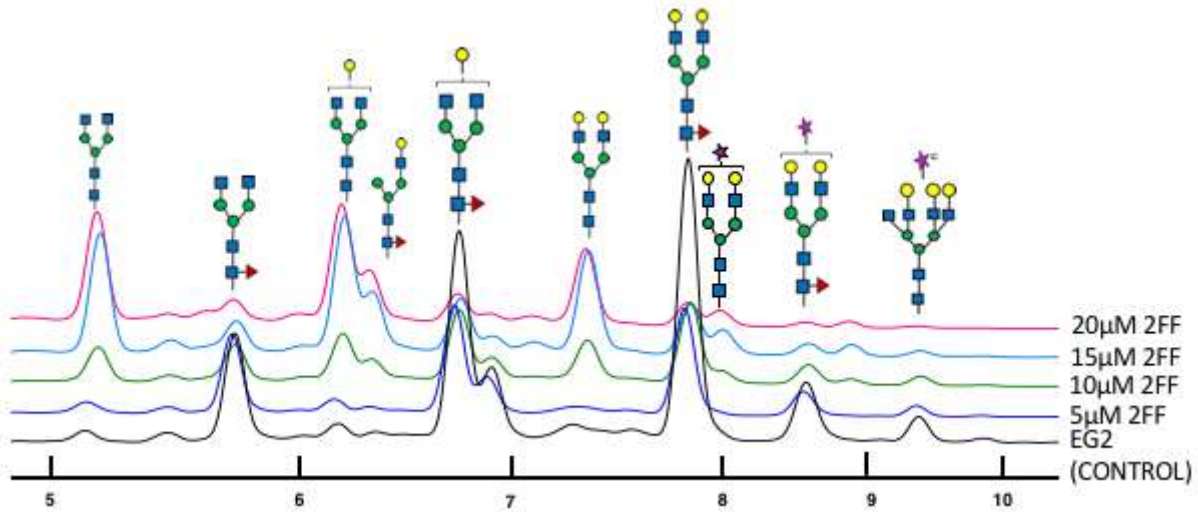

Figure 2-3: Glycan profiles of CHO EG2-hFc after addition of 2FF: Profiles of the glycans isolated from each of the cultures described in Figure 2-2 are shown. Glucose unit (GU) values were determined for each of the major peaks by reference to a standard dextran ladder run. Structures were then assigned by reference to the Glycostore database (https://glycostore.org/

2.3.2 Effect of RMD

RMD plasmid was transfected into the CHO EG2-hFc cell line with increasing concentrations of the plasmid DNA (2.5, 5, 7.5, 10, 15 and 20 μg) and stable pools of cells were generated. HILIC-HPLC was used to analyze the glycan profile of the antibody. RMD transfection resulted in a decrease in fucosylation, with the largest decrease (37.5%) in RMD at 7.5 μg. The glycan profile was similar to the profile observed with addition of 2FF. There was a shift towards the non-fucosylated species that included an increase in the peak areas for, A2G0, A2G1, A2G2and A2G2S1, and a decrease in the fucosylated peak areas including A2G0F, A2G1F, A2G2F and A2G2S1F. The effect was most pronounced in RMD at 7.5 μg (Figure 2-4) (with a 37.5% area reduction of fucosylated species. It was expected that with increasing concentrations of transfected DNA, an increasing effect of RMD would be observed by decrease in fucosylation. However, it was noted that with increasing concentrations of RMD plasmid DNA (RMD 7.5 μg compared to RMD 20 μg), the effect was reduced (Figure 2-5).

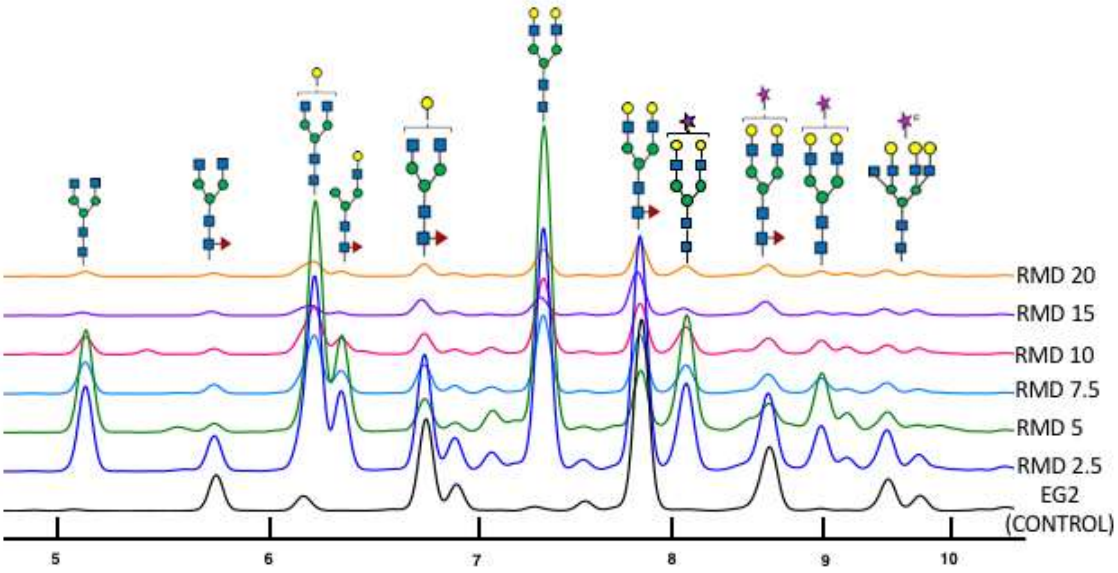

Figure 2-4: Glycan profiles of RMD transfected CHO EG2-hFC cells: HPLC profiles are shown for glycans isolated from antibodies isolated from cultures of cells transfected with RMD plasmid DNA at various concentrations. The conditions of cell culture and antibody isolation was as described for Figure 2-3.

*Table 2-2: List of main glycan peaks and percentage area observed in RMD transfected CHO EG2-hFc experiment. This is a representative table for two experiments conducted with transfection of RMD (2.5, 5 and 7.5 µg) into CHO EG2-hFc cells. (*isomer forms of F(6)A2G1)*

	Control		RMD 2.5µg		RMD 5µg		RMD 7.5µg	
Structures	***GU value***	***% Area***	***GU value***	***% Area***	***GU value***	***% Area***	***GU value***	***% Area***
M2	3.38	0.07	3.38	0.04	3.38	0.02	3.38	0.14
M3	4.40	0.3	4.40	0.15	4.40	0.09	4.40	0.29
A1	4.94	0.04	4.95	0.13	4.95	0.21	4.95	0.22
M4	5.28	0.15	5.27	0.03	5.27	0.06	5.28	0.1
F(6)A1/A2	5.40	0.36	5.44	0.05	5.45	7.69	5.45	6.95
A1G1			5.66	0.07			5.66	0.04
A1G(4)1			5.77	5.61	5.75	0.64	5.76	0.29
F6A2G0	5.86	6.51	5.86	0.05	5.87	0.76	5.87	2.1
M5	6.17	2.97	6.21	0.04				
F6A1G1	6.31	0.12	6.31	0.19	6.31	7.22		
A2G1	6.49	0.41	6.50	2.48	6.51	0.22	6.22	15.79
***F6A2G1**	6.62	16.58	6.62	14.78	6.62	2.77	6.32	5.19
***F6A2G1**	6.74	5.03	6.74	5.32	6.74	0.79	6.63	6.74
A2G2	7.05	1.03	7.09	0.18	7.10	23.77	7.10	18.45
A4G1	7.25	2	7.25	7.83	7.26	0.58	7.26	0.85
F6A2G2	7.50	35.53	7.50	2.24	7.50	5.65	7.51	13.65
A2G2S1	7.69	0.47	7.69	1.44	7.70	10.3	7.70	7.26
F6A2G2S1	8.07	14.36	8.07	16.89	8.08	4.35	8.08	6.25
A2G2S1	8.32	0.57	8.32	0.9	8.32	5.03	8.33	3.84
F6A2G2S2	8.43	0.18	8.45	16.12	8.46	1.53	8.46	1.15
A2G(4)2S(3,6)2	8.64	6.42	8.64	6.59	8.65	2.04	8.65	2.84
A2G2S2	8.81	2.93	8.81	6.81	8.81	0.69	8.82	1.65

*Table 2-3: List of main glycan peaks and percentage area observed in RMD transfected CHO EG2-hFc experiment. This is a representative table for two experiments conducted with transfection of RMD (10,15 and 20 µg) into CHO EG2-hFc cells. (*isomer forms of F(6)A2G1)*

	Control		RMD 10µg		RMD 15µg		RMD 20µg	
Structures	***GU value***	***% Area***	***GU value***	***% Area***	***GU value***	***% Area***	***GU value***	***% Area***
M2	3.38	0.07	3.39	1.2	3.39	0.29	3.38	0.2
M3	4.40	0.3	4.40	0.4	4.40	0.3	4.40	0.46
A1	4.94	0.04	4.91	1.36	4.93	0.21	4.95	0.27
M4	5.28	0.15	5.28	0.15	5.28	0.17	5.28	0.21
F(6)A1/A2	5.40	0.36	5.44	4.23	5.44	2.02	5.44	2.76
A1G1			5.64	1.19				
A1G(4)1			5.76	0.14			5.75	0.14
F6A2G0	5.86	6.51	5.87	1.47	5.86	2.52	5.87	1.93
M5	6.17	2.97						
F6A1G1	6.31	0.12	6.31	4.71	6.31	2.09	6.31	2.91
A2G1	6.49	0.41	6.21	15.1	6.21	8.48	6.21	12.17
***F6A2G1**	6.62	16.58	6.74	1.19	6.62	9.89	6.62	7.28
***F6A2G1**	6.74	5.03	6.88	1.8	6.74	2.25	6.74	1.68
A2G2	7.05	1.03	7.09	20.16	7.09	11.76	7.09	16.3
A4G1	7.25	2	7.26	0.84	7.26	1.28	7.26	1.13
F6A2G2	7.50	35.53	7.50	13.04	7.50	26.81	7.50	19.56
A2G2S1	7.69	0.47	7.70	7.87	7.69	4.9	7.70	6.68
F6A2G2S1	8.07	14.36	7.94	1.1	8.07	10.94	8.07	9.14
A2G2S1	8.32	0.57	8.32	3.67	8.32	2.39	8.32	3.09
F6A2G2S2	8.43	0.18	8.45	1.89	8.45	1.32	8.46	1.83
A2G(4)2S(3,6)2?	8.64	6.42	8.65	2.6	8.64	4.42	8.65	3.75
A2G2S2	8.81	2.93	8.81	2.19	8.81	3.83	8.82	3.54

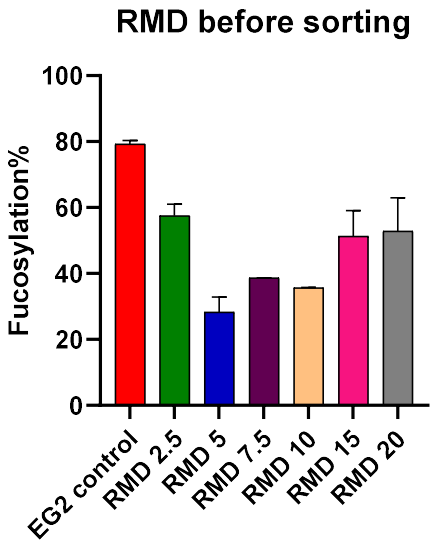

Figure 2-5: Fucosylation percentages of RMD transfected CHO EG2-hFc cells before cell sorting: Fucosylation percentages of glycans from MAbs produced from RMD transfected CHO EG2-hFc cell pools. The data was extracted from the peak areas of the profiles in Figure 2-4 and based on two independent experiments. Values shown are means ± SD (n=2).

2.3.3 Fluorescence Activated Cell Sorting (FACS) to sort RMD transfected CHO EG2-hFc cells into high and medium RMD expressing cells

Following the results from glycan analysis on RMD transfected cells, and the observations that the increasing concentrations of RMD plasmid DNA transfection did not show a proportional decrease in fucosylation, the CHO EG2-hFc RMD cells were sorted into high and medium RMD expressing cells using the GFP expression which would also co-relate to high and medium RMD expression which were gated on FACS relative to the baseline (with background removed) Figure 2-7. Glycan analysis was performed after cell sorting to compare levels of fucosylation Figure 2-6 between unsorted and sorted cells. Fucosylation was decreased most effectively in RMD 7.5_med, amongst all sorted cell lines with 16% fucosylation. In RMD 5, the fucosylation% decreased by 10% after sorting for both medium

and high RMD expressing cells. Between, RMD 7.5_med and 7.5_hi, there is a higher % decrease in the RMD 7.5_hi than in the RMD 7.5_med sample. However, it was also observed that sorted CHO EG2-hFc RMD 2.5µg did not show a lower fucosylation percentage. It is also important to note that during RMD 2.5 µg cell sorting, we were unable to isolate high expressing GFP/RMD-CHO EG2-hFc cells. Some low GFP expressing cells were collected, but since the effect on fucosylation was minimal, these cells were not used in further experiments. It is possible that during passaging of RMD 2.5µg cells for maintenance, the expression of RMD decreased over time, leading to no effect of RMD on the cell line and thus, increased fucosylation.

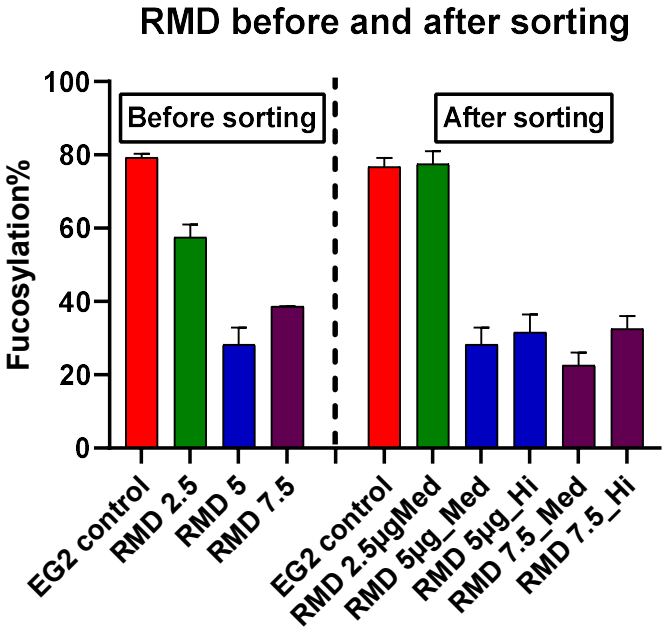

Figure 2-6: Comparison of fucosylation percentages of unsorted and sorted RMD transfected CHO EG2-hFc cells: The cell pools following RMD plasmid transfection (2.5 - 7.5 ug DNA) were sorted into clones by fluorescence-activated cell sorting (FACS). The sorting was based upon the co-transfected GFP and resulted in clones that were identified with high or medium fluorescence. Each pool was then grown as described in 2.2.1 and the resulting glycan profiles of the Mabs analysed for the percentage fucosylation. Values shown are means ± SD for two independent experiments (n=2).

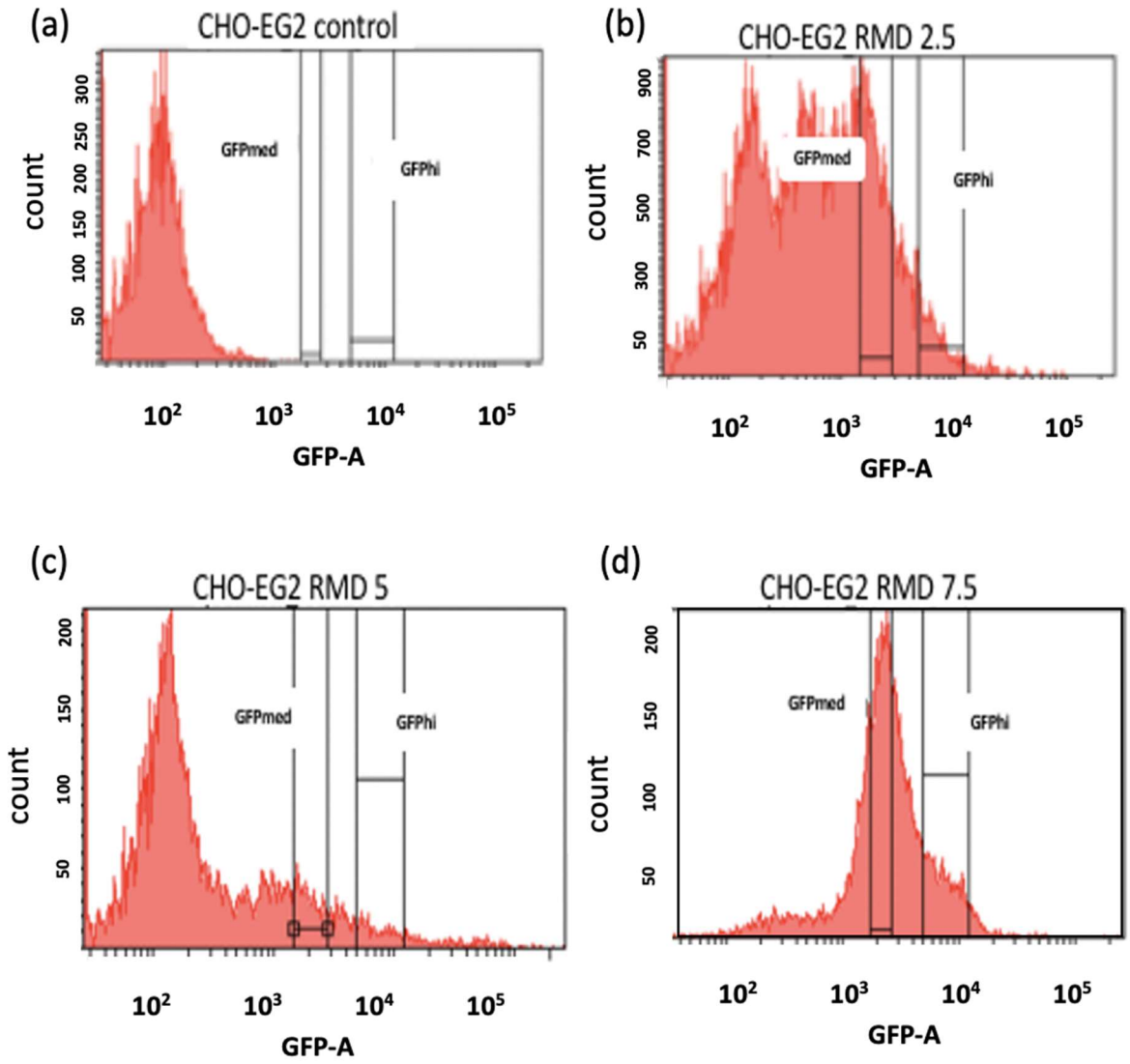

Figure 2-7: Flow cytometry histograms for RMD transfected CHO EG2-hFc cell sorting: CHO EG2-hFc RMD cells were sorted into high and medium RMD expressing cells using the GFP expression which would also co-relate to high and medium RMD expression which were gated on FACS relative to the baseline (with background removed). RMD 2.5_hi cells could not be isolated, however for RMD 5 and RMD 7.5, both high and medium GFP/RMD expressing cells could be isolated.

2.3.4 Analysis of 2FF + RMD

2FF (10μM or 50μM) was added to stable pools from RMD_CHO EG2-hFc transfections to investigate the effect of addition of the inhibitor on fucosylation. Glycan analysis performed on samples collected 4 days post addition of 2FF exhibited a further decrease in fucosylation (up to ~40% more compared to the control RMD 2.5 μg and 20 μg with no 2FF added) in RMD cells to which 50 μM 2FF was added compared to only RMD transfected cells (Figure 2-6). However, the addition of 2FF to RMD_CHO EG2-hFc did not result in generation of completely non-fucosylated products with at least 3-6% fucose remaining (in RMD 2.5 and 20 μg with 50 μM 2FF).

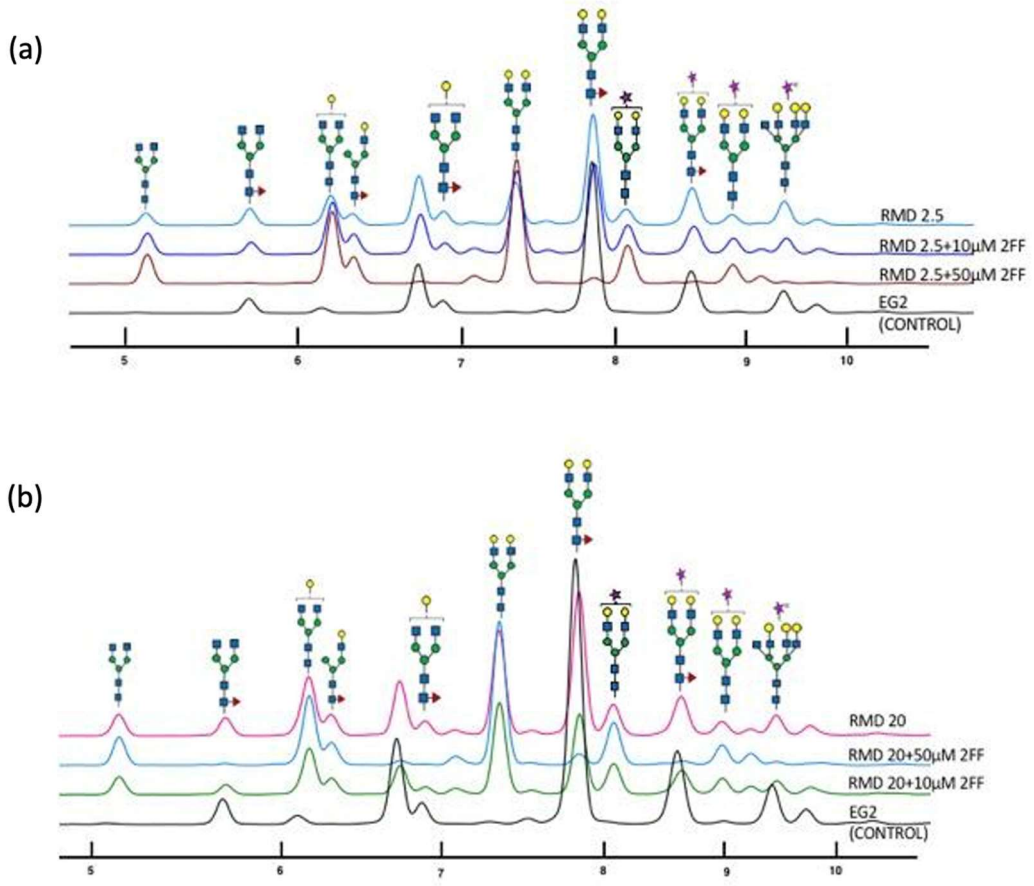

Figure 2-8: Glycan profiles following 2FF treatment of RMD transfected cells: 2-F-peracetylated fucose at 10μm and 50μm was added to two clones of cells transfected with RMD- (a) 2.5 μg and (b) 20 μg DNA. The resulting glycan profiles of the isolated MAbs was compared with untreated transfected cells and non-transfected controls.

2.3.5 Fucose titrations

GDP-Fucose is produced in cells either via the de novo pathway or via the salvage pathway. The de novo pathway however produces 90% of the GDP-Fucose that is utilized by the FUT8 enzyme for fucose addition onto the glycan structures. The salvage pathway is a minor pathway within cells which utilizes fucose in the cell culture media to produce GDP-Fucose. The salvage pathway is also known to correct fucosylation defects in cell lines where the de novo pathway is incapable of generating required fucose (Becker and Lowe, 2003). The fucose titration experiments were conducted to investigate whether the RMD_CHO EG2-hFc cell line would be able to divert towards the salvage pathway for production of fucosylated glycan species. Using the sorted RMD_CHO EG2-hFc cells, increasing concentrations of fucose (0, 0.01, 0.05, 0.1 and 1 mM) were added to the BioGro CHO-CD media and the cells cultured in the fucose-added media for 4 days. The supernatants collected after 4 days were then Protein-A purified and glycan analysis was performed on the purified samples. The glycan profiles of the RMD_CHO EG2-hFc cell lines found fucosylation percentages increase with an increase in fucose concentrations. Specifically, for RMD 7.5_med, which also showed the lowest fucosylation, there was a consistent increase in fucosylation (Table 1, 16% to 87%) with respect to increasing concentrations of fucose in the media (Figure 2-8). The glycan analysis for control EG2-hFc cultured in fucose-added media shows a small increase (up to 10%) in in the control samples (*Table 2-1*). These results show that in the absence of availability of fucose from the de novo pathway as with the RMD cells, the salvage pathway can utilise the fucose available in cell culture media to generate fucosylated products. Also, as seen in the control CHO EG2-hFc samples, when fucose is added to the media, the salvage pathway can utilise it to increase fucosylation percentage, even when the de novo pathway is available.

Table 2-4: Fucosylation percentages following fucose titration in cell culture media

Cell lines ↓	**0mM Fucose**	**0.01mM Fucose**	**0.05mM Fucose**	**0.1mM Fucose**	**1mM Fucose**
EG2-hFc	78.35%	88.28%	86.99%	86.53%	84.65%
RMD 5_med	23.58%	46.61%	77.90%	88.82%	86.70%
RMD 5_hi	25.20%	37.04%	52.33%	54.25%	64.94%
RMD 7.5_med	16.06%	39.74%	71.78%	79.08%	87.42%
RMD 7.5_hi	26.31%	72.68%	71.65%	42.73%	86.03%

(a) EG2-hFc (Control)

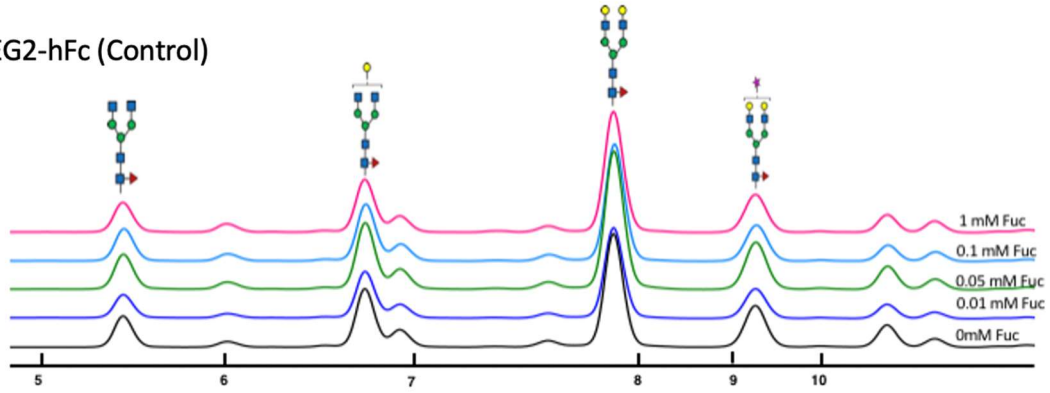

(b) RMD 5_med

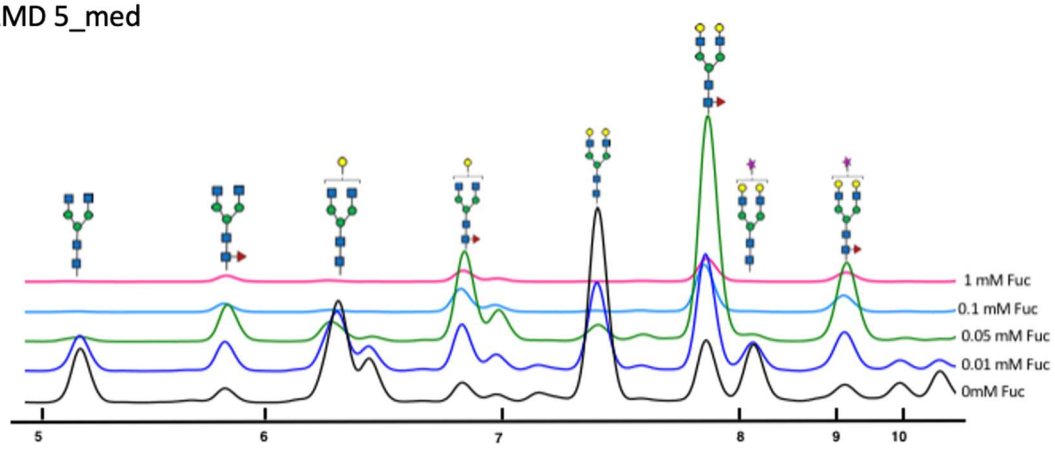

(c) RMD 5_hi

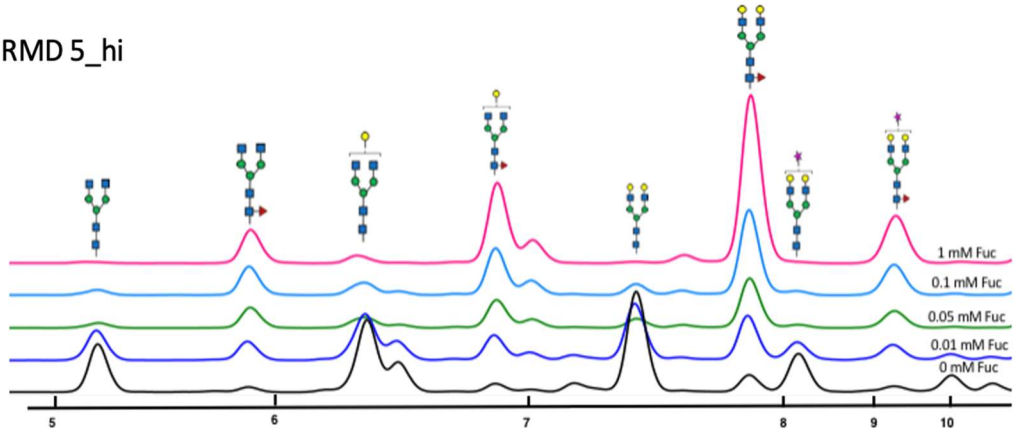

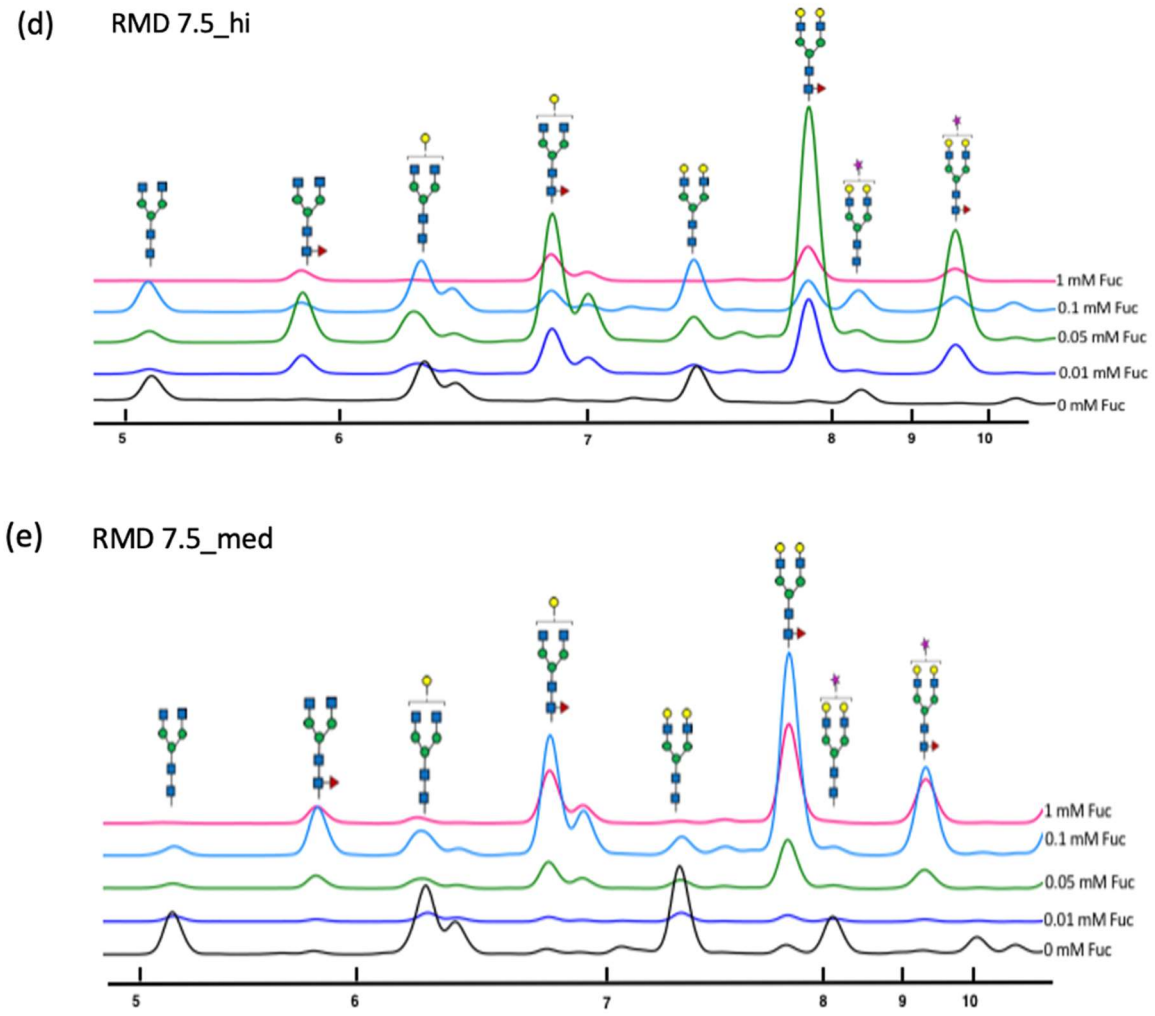

Figure 2-9: Glycan profiles of RMD CHO EG2-hFc to which different concentrations of fucose has been added. FACS sorted cells from RMD transfected CHO EG2-hFc cells were grown over 4 days in media containing fucose concentrations (figure a→e: 0-1mM). The figure shows the shift of peaks towards fucosylated species of the glycans.

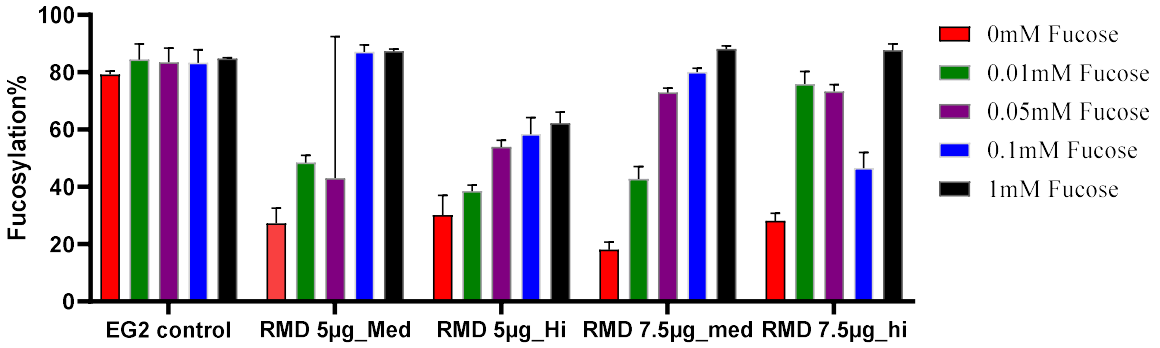

Figure 2-10: Comparison of fucose titrations of RMD CHO EG2-hFc cells after sorting. Various FACS sorted cells of RMD transfected cells were grown over 4 days in media containing fucose concentrations (0-1mM). The figure shows the % fucosylation of the glycans isolated from the Mabs produced from each culture. Values on means of two independent experiments ± SD (n=2).

2.3.6 ADCC assay to assess efficacy of the 2FF treated and RMD transfected CHO EG2-hFc cell line

To test the efficacy of the 2FF treated and RMD transfected CHO EG2-hFc cell lines, an ADCC assay that has been developed and described in this thesis, with NK-92 engineered cell lines as effector cells, was used. Details of the assay have been described in Chapter-3. A control IgG1 antibody, Cetuximab was used as positive control along with the EG2 antibody. The NK-92 VV cell line is a high affinity variant of the FcγRIIIa receptor whereas the NK-92 FF is a low affinity variant.

As can be noted from Figure 2-11, the results from the assay with NK-92 VV show that the best ADCC activity is observed in RMD 5 (both med and hi); as well there is a marginal

increase over Cetuximab. However, RMD 7.5_med, which has 16% fucosylation, shows lesser activity. The assay with NK-92 FF presented an interesting result. As expected, with NK-92 FF effector cells, decreased ADCC activity was observed with Cetuximab. However, RMD 5 (med and hi) shows an increased response. 2FF, although with similar fucosylation percentages as RMD 7.5_med, exhibits decreased ADCC response.

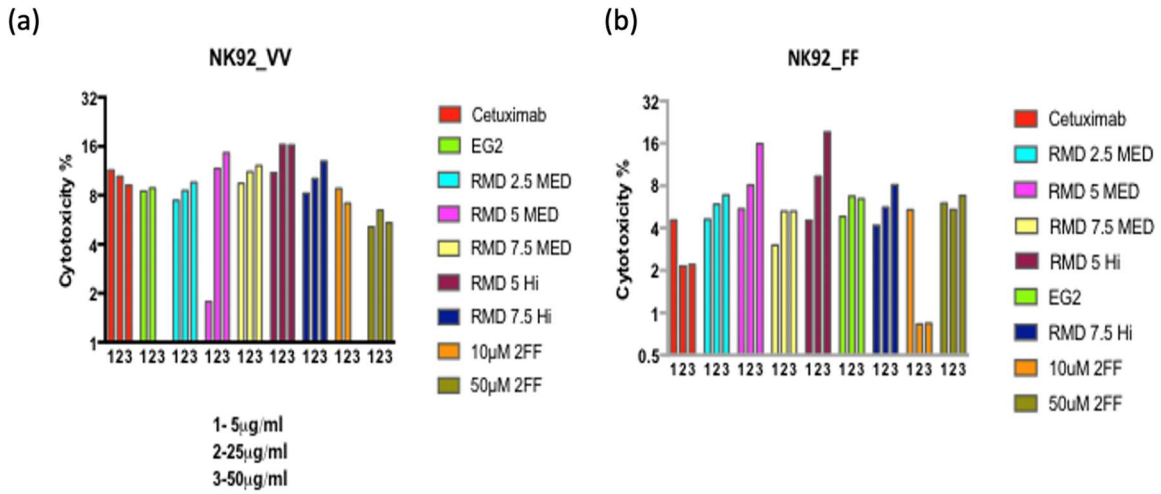

Figure 2-11: ADCC assay plots comparing cytotoxicity percentages of RMD transfected and 2FF treated CHO EG2-hFc cells. The assays were performed across three technical replicates (of each concentration tested) with (a) NK-92 VV and (b) NK-92 FF effector cells. The cytotoxicity percentage was calculated using the equation 1.2.5. The equation also takes into consideration the spontaneous release by target cells without addition of antibody.

2.3.7 ESI-MS to elucidate fucosylation pattern of CHO EG2-hFc

The aim of this experiment was to analyze the fucosylation pattern of EG2-hFc. Denatured EG2-hFc was treated with different concentrations of 2FF and then EndoS digested to remove all residues except core GlcNAc and fucose. Analysis was done using electrospray time – of – flight mass spectrometry (Kozlovski et al., 2011) . When analysed by ESI-MS, the

EG2-hFc protein used in our experiments, when treated with EndoS, has two major species of masses 80095 ± 13 and 79842 ±24 Da. This can be explained by the presence of two extra lysine residues on the larger, more abundant species. The same protein, treated with PNGase F, also has two major species, of masses 79397 ± 17 and 79151 ± 25 Da; these also differ in mass by two lysine residues. The difference in mass between the two larger and two smaller isoforms following PNGaseF treatment is about 700 Da, equivalent in mass to two GlcNac (2 x 203 Da) and two fucose residues (2 x 146 Da). The addition of 2FF resulted in a change in the spectra, with two new species appearing with masses 146 and 292 Da less than the full-size protein as shown in Figure 2-12. When increasing concentrations of 2FF were added, the major species was 79800 ± 17 Da, equivalent to the loss of two fucose residues, and the original, larger protein was no longer detectable. This leads to the conclusion that 2FF inhibits the addition of fucose in a concentration-dependent manner. The prevention of the simultaneous addition of fucose to glycans on both heavy chains, would result in a species 292 Da smaller than the full-length protein. Since there are two species of protein observed, we also conclude that the addition of fucose must be sequential.

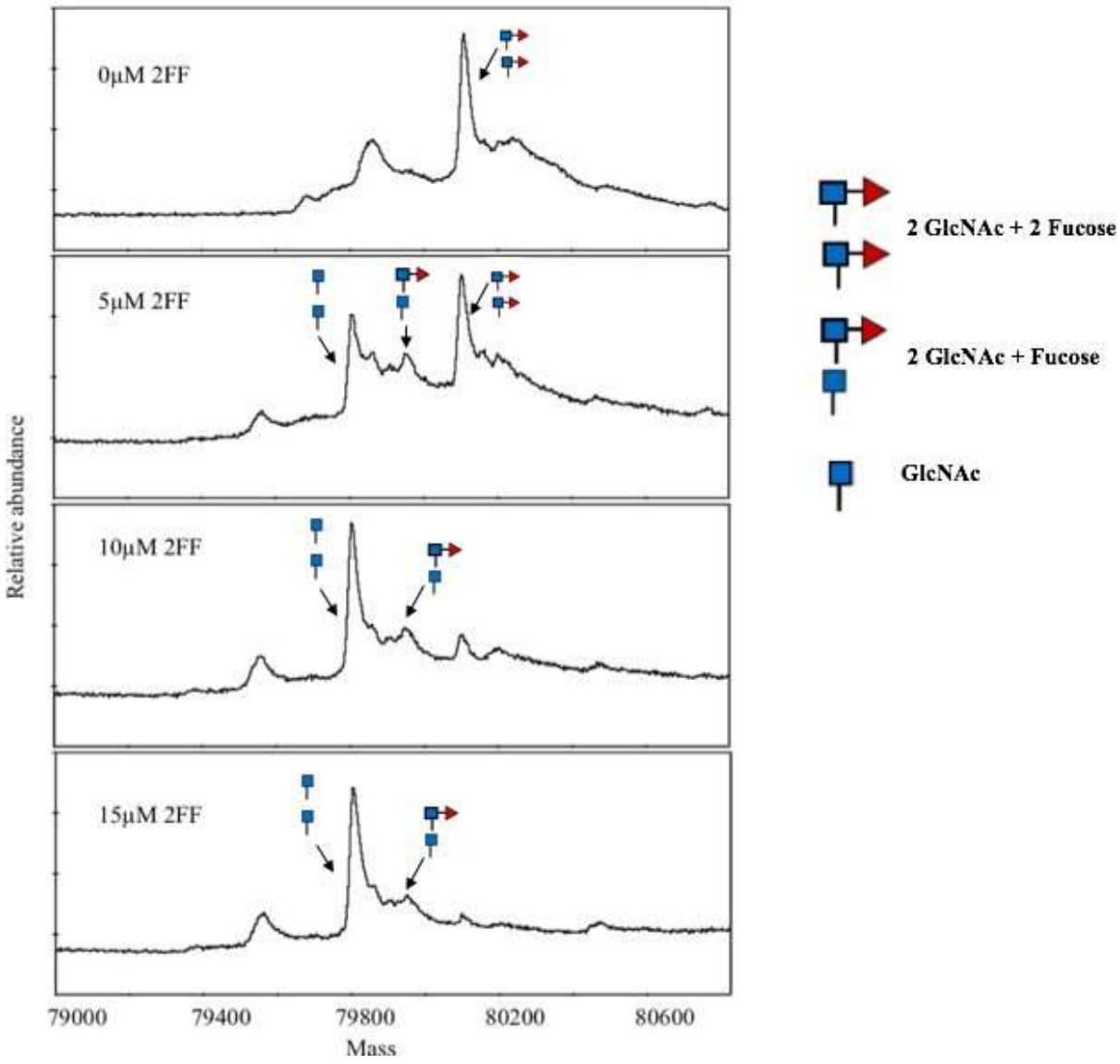

Figure 2-12: Electrospray time-of-flight spectra for 2FF added to CHO EG2-hFc cells. (Figure courtesy: Dr. Lynda J Donald) To elucidate the fucosylation pattern of CHO EG2-hFc, specifically sequence of addition of fucose to the glycan post-addition of 2FF, ESI-MS was used. The addition of fucose is sequential with increasing concentrations of 2FF, which is observed by the addition of one fucose at a time on a glycan. Comparing the 0μM 2FF sample (control) and 5μM 2FF added sample, there is a shift in mass from ~80000 towards ~79800. Similarly, as the concentration of 2FF is increased to 15μM, the mass shifts to 79800, indicating the absence of fucose in this sample.

2.4 Discussion & Conclusion

Two methods to reduce fucosylation of a heavy chain camelid antibody produced in CHO cells have been compared and discussed in this chapter - 1) using 2FF, a chemical inhibitor to stop addition of core fucose onto the glycan structure and 2) by co-expression of RMD to deflect the de novo pathway into producing a dead-end product, GDP-rhamnose. Previous studies have shown that GDP-rhamnose does not affect cell growth and productivity (Dekkers et al., 2016; Horsten et al., 2010). In our experiments, we report a decrease in fucosylation to 17.5% for the 2FF and 34.01% for the RMD 7.5 µg CHO EG2-hFc unsorted cells and 16.06% for RMD 7.5 µg_med CHO EG2-hFc sorted cells. From the results, it is evident that both 2FF and RMD are equally efficient at reducing fucosylation to comparable levels. It is also worth noting that the RMD transfection method does require stringent selection and thus, stable cell line generation/enrichment of stable pools is required for effective results.

In order to investigate the effect of 2FF, which is designed to inhibit the addition of fucose to the core-glycan structure, increasing concentrations of 2FF were added to the CHO EG2-hFc cell cultures. The addition of 2FF to CHO EG2-hFc did not affect cell viability and growth (Figure 2-2 a and b). There was a steep decline in fucosylation up to a concentration of 20µM and no significant decrease in fucosylation was observed in higher concentrations (50 and 100µM) (Figure 2-2c). The glycosylation profile of EG2 after addition of 2FF also shifted towards non-fucosylated glycans. 2FF has been known to effectively decrease fucosylation in HL-60 as well as CHO cells (Rillahan et al., 2012) and our results support this. As this inhibitor can be added to cells in culture, it is a convenient method of reducing fucosylation. The inhibitor has also been tested in vivo, and it has been shown that it has no significant effect on

the health of the mice the compound was injected in. This means that it could be a viable option to quickly and effectively reduce fucose as well as use the MAbs produced in clinical applications.

In the case of RMD, a previous study has reported complete non-fucosylation (Horsten et al., 2010) of the MAb tested. In another study by (Dekkers et al., 2016), where RMD was transiently transfected in a HEK293 cell line producing IgG1, the effect was different in terms of percentage decrease in fucosylation. Although, the RMD co-transfection method has been shown to achieve the desired effect to some extent in the experiments discussed here, there are considerable differences in decrease in fucosylation amongst the different RMD transfections, with none resulting in completely non-fucosylated antibodies. The reasons could be due to differences in cell lines, transfection efficiency or generation of stable cell line vs. stable pool leading to heterogeneous population of RMD expressing cells. It is now known that generation of a stable cell line for a particular characteristic by applying selection results in a more homogenous population of cells with that characteristic (Vcelar et al., 2018).

The difference between the study in this thesis and the previous study which resulted in completely non-fucosylated products (Horsten et al., 2010) is the generation of stable pool vs. stable cell line post transfection. This could be an important parameter for the use of the RMD transgene co-transfection as a glycoengineering method. In an attempt to resolve this, FACS was used to sort RMD-transfected CHO EG2-hFc cells into high expressing and low expressors. On comparing the sorted and unsorted cells, it was observed that there was a further decrease in fucosylation in RMD 5µg_Med (23.5%) and RMD 7.5µg_Med sorted cells (16.06%) (Figure 2-6). An interesting observation is that the sorted high expressing RMD cells exhibit higher fucosylation than the medium expressors. Although the unsorted RMD 2.5µg

cells exhibited lower fucosylation, the sorted cells exhibited higher fucosylation. During cell sorting, a lower number of medium expressors, compared to the RMD 5 μg and 7.5 μg was sorted which could be due to the loss/silencing of the GFP/RMD transgene. We were also unable to sort high expressors (Figure 2-7).

In order to investigate if addition of 2FF to the RMD transfected cells had an additive effect, we tested two concentrations of 2FF, 10 and 50 μM on the RMD 2.5 and RMD 20. The results showed that although there was a further decrease in the fucosylation, it was not a significant change and thus, not an additive effect (Figure 2-8).

It is known from previous studies that the salvage pathway is able to restore fucosylation defects in cell lines as well as mouse models (Becker and Lowe, 2003; B. G. Ng et al., 2018). In order to investigate if the RMD transfected CHO EG2-hFc cell line will be able to restore fucosylation with fucose titrations into the cell culture media, the BioGro CHO CD media was supplemented with increasing concentrations of fucose. The glycan analysis of fucose titrations on RMD transfected CHO EG2-hFc showed that the salvage pathway does restore fucosylation to the original levels in the antibody (Figure 2-9). In the control, non-transfected CHO EG2-hFc cells, the fucose titrations increase fucosylation further. However, as noted from Table 2-1 and Figure 2-10 the titration does not result in an increase proportional to the increase in fucose concentration, suggesting that the enzymatic activity of FUT8 might be restricted even with availability of substrate. This experiment established that in cell lines where fucosylation has been depleted to negligible amounts using genetic manipulation, fucosylation can be restored via the salvage pathway and would be useful in cases where completely eliminating fucosylation results in genetic defects (Freeze, 2002), which has been observed in mouse models in a previous study. In this study the FX gene in *de novo* fucose pathway was knocked

out resulting in mice lacking in normal fucosylation that led to decrease of survival rates. However, supplementation of fucose resulted in the recovery of these mice, leading to the observation that external sources of fucose may restore normalcy via the salvage pathway.

To investigate whether the defucosylation methods affect ADCC activity of the EG2 antibody, an assay developed using LDH based method was used. Both 2FF-added EG2 and RMD-transfected EG2 were purified and three different concentrations of 5, 25 and 50 μg/ml were used. The ADCC activity was calculated using the equation in 1.2.5. In the NK-92 VV variant assay, compared to the positive control Cetuximab, RMD-transfected EG2 shows an increase in cytotoxicity percentage, although not a significant difference. However, it was interesting to see that although 2FF decreased fucosylation more efficiently than RMD, the ADCC activity was enhanced for RMD. Although it is not known if a minimum amount of fucosylation is required to be retained in order to increase ADCC activity, from the results seen here, it is likely that might be the case. Further investigation using different antibodies would be required to confirm this hypothesis. In case of the NK-92 FF variant, which are low affinity effector cells for the FcγRIIIa receptor, the Cetuximab sample does not exhibit ADCC activity. However, interestingly the RMD-transfected EG2 samples do show an increased response. This leads to the possibility that with defucosylated antibodies, NK-92 FF low affinity variants can also be recruited to elicit an immune response (Figure 2-11).

We have also attempted to elucidate the fucosylation pattern of CHO EG2-hFc, specifically sequence of addition of fucose to the glycan post-addition of 2FF using ESI-MS. The addition of fucose is sequential with increasing concentrations of 2FF, which is observed by the addition of one fucose at a time on a glycan. Comparing the 0 μM 2FF sample (control) and 5 μM 2FF added sample, there is a shift in mass from ~80000 towards ~79800. Similarly,

as the concentration of 2FF is increased to 15 μM, the mass shifts to 79800, indicating the absence of fucose in this sample (Figure 2-12).

This chapter focuses on two methods that can be employed to improve efficacy of a MAb. It was shown that both 2FF and RMD can be effective methods, albeit each with its advantages and disadvantages. There are other methods to decrease fucosylation. A recent study has used a mannosidase inhibitor Deoxymannojirimycin (DMJ) to generate defucosylated IgG1 in a CHO-DXB11 cell line, although the decrease was from 92% down to 73% (Shalel Levanon et al., 2018). Yet another study, used arabinosylation to replace fucose, which resulted nearly 100% defucosylated antibodies (Hossler et al., 2017b). Other methods include using gene editing technologies such as Zinc Finger Nuclease (Malphettes et al., 2010b) and CRISPR-Cas9 (Ronda et al., 2014) to knock-out the FUT8 gene and thus, generate non-fucosylated products. The advantage of using such technologies is that it would result in targeted biallelic knockouts and could be established as cell lines that can be used for generating multiple MAbs. These could be further used to design MAbs according to therapeutic requirements of various diseases (Schulz et al., 2018). However, currently, due to patent restrictions gene editing can be used only for research and development. Thus, a viable option could still be to use an inhibitor such as 2FF or DMJ for production of defucosylated MAbs for therapeutic applications.

3

Development of a non-radioactive method for analysis of ADCC activity using an engineered effector cell line

3.1 Introduction

Antibody-dependent Cell Cytotoxicity (ADCC) activity is an important criterion to define the efficacy of a therapeutic antibody, especially for monoclonal antibody-based cancer therapeutics, which are defined by their ability to target and trigger apoptosis in tumour tissues (Zahavi et al., 2018). Therefore, evaluation and quantification of ADCC activity is important. Fc receptors (FcRs) are expressed on the surface of natural killer (NK) cells (Gessner et al., 1998; Ravetch and Bolland, 2001). FcγRs bind to the Fc domain of IgGs, inducing NK cells (effector cells) to activate the perforin/granzyme pathway leading to apoptosis and eventually cell death (Trapani and Smyth, 2002). The FcγRs are comprised of three types; FcγRI (CD64), FcγRII (CD32), FcγRIII (CD16), which are further categorised into different subtypes based on expression on cell type (Gessner et al., 1998). IgG1s have high affinity for FcγRI (CD64), comparatively lower affinity for FcγRIIIa (CD16a) and reduced affinity for FcγRII (CD32). NK cells express the FcγRIIIa type receptor that is essential for binding to an IgG-bound tumour antigen and inducing an ADCC response. Our antibody of interest, CHO EG2-hFc, targets the epidermal growth factor receptor (EGFR), a transmembrane tyrosine kinase receptor that is the hallmark of cancer cells. EGFR is overexpressed in a number of cancers including those of the breast, head and neck, and pancreas (Martinelli et al., 2009).

Previously, chromium (^{51}Cr) release assays have been used to quantify the ADCC activity. Briefly, target cells are incubated with ^{51}Cr. Effector cells are then added to the labelled cells, and due to the lysis of the target cells by effector cells, the ^{51}Cr is released and is detected using a gamma counter (Wallace et al., 2004). ^{51}Cr release assays are still preferred over other available assays in the market, possibly due to their relatively high sensitivity. However, it is a radioactive assay and requires a specific set up within the laboratory area, which is different from other available non-radioactive assays. It also requires peripheral blood mononuclear cells (PBMCs) (González-González et al., 2019). Due to genetic variability from donor to donor, assays with PBMCs do not produce consistent and accurate results (Mata et al., 2014), and more and more researchers are turning to other cells, such as stable cell lines, that can be cultured in the lab.

In order to investigate the options available for ADCC detection, a literature review was conducted, which revealed a few different assays. Thomann et al. have utilized a NK cell line *in vitro* assay to quantify the ADCC response, wherein Time-Resolved Fluorescence (TRF) was used to measure the release intracellular proteins that were fluorescently labelled prior to the assay (Thomann et al., 2016). Assays developed by Promega (ADCC Reporter Bioassay) and Perkin Elmer (DELFIA) also require fluorescence/luminescence measurements of the release of fluorescently labelled proteins to measure ADCC activity. The DELFIA assay from Perkin Elmer in particular, requires TRF measurements, which was a major drawback due to the unavailability of a plate reader with TRF capabilities, within the university facilities. Another assay that has been reported previously using stable 'thaw and use' Jurkat cell lines as effectors also demonstrates higher sensitivity than a PBMC-based assay that detects cell cytotoxicity through the loss of signal from a luciferase reporter protein (Cheng et al., 2014). However, another factor to weigh in was the cost of such assays; they are relatively more

expensive than the chromium release assays. The ideal choice for our use was thus, a colorimetric Lactate Dehydrogenase (LDH) release assay for which an absorbance reading could be taken at 490 nm (reference wavelength 600 nm, which is used to normalize for the background) using a microplate reader (BioTek ELx808; BioTek USA). The absorbance reading at 490 nm measures the amount of formazan released, which is directly proportional to the LDH released. LDH is a cytoplasmic enzyme released into cell culture supernatant upon cell membrane damage. This assay has been used in previous studies in other groups to quantify ADCC activity (Broussas et al., 2013; Shields et al., 2002). Although LDH assays might be prone to errors in terms of determining whether LDH released is from the target cells or from effector cells, with appropriate controls, a robust method can be established. The work described here specifically aims at developing an assay that is non-radioactive, easier to establish than ^{51}Cr release assays and can be used frequently without PBMCs, using engineered NK-92 cells as the effector cell line (Binyamin et al., 2008).

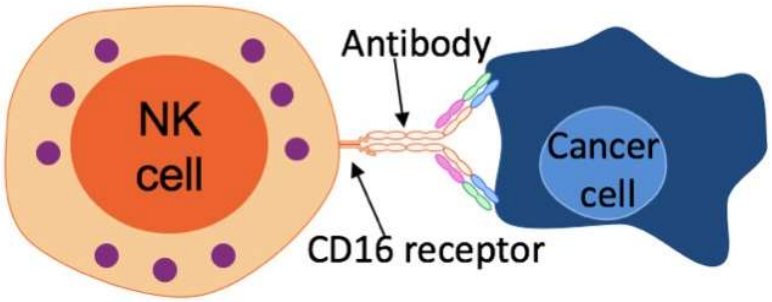

Figure 3-1: Antibody -dependent Cell Cytotoxicity (ADCC) mediated by NK cells: ADCC response on a cancer cell via CD16 receptor on NK cell, triggered with the help of a MAb (figure adpted from (Román et al., 2013)).

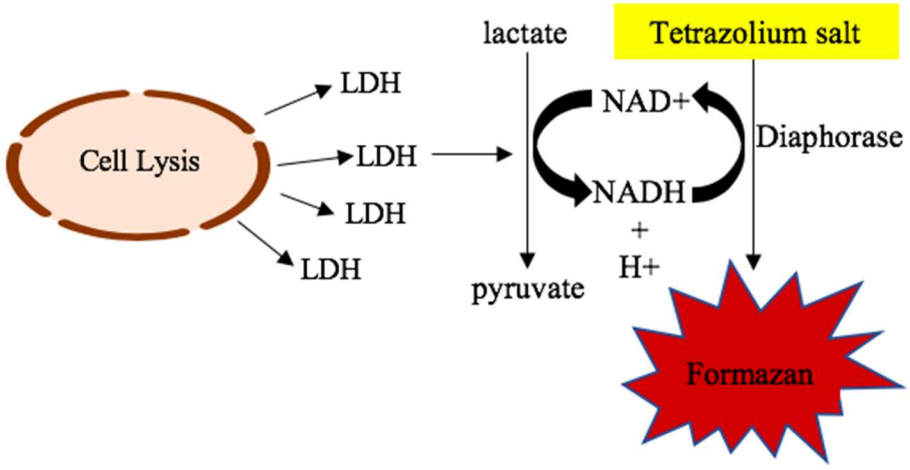

Figure 3-2: Mechanism of action of a LDH assay: the assay occurs via a two-step reaction wherein during conversion of lactate to pyruvate, NAD^+ is reduced to $NADH^+$ and H^+ via LDH. In the second step the H+ released is transferred to the tetrazolium salt by diaphorase, which in turn is reduced to Formazan. The amount of LDH is directly proportional to Formazan absorbance reading and thus, the number of lysed cells.

Assay principle

The assay works via a 2-step reaction. The reaction mixture that consists of a catalyst (diaphorase) and dye (tetrazolium salt) is added to the supernatant and incubated for 30 minutes. The stop solution is added after incubation to stop the reaction from progressing any further. LDH that has been released into the supernatant can be measured using a plate reader at 490 nm. The amount of LDH is directly proportional to Formazan absorbance reading and thus, the number of lysed cells.

Assay set-up for measuring cytotoxicity

The LDH assay was set up using a commercially available cytotoxicity detection kit (Roche Diagnostics, Que, Canada). Samples were set up in triplicates. Briefly, target cells were seeded 2 days before the assay. They were incubated along with the antibody to be tested in 96-well plates on the day the assay was carried out. The effector cells were seeded in 96-well plates to which the target cells treated with antibody were added and incubated. To measure LDH, the reaction mixture was added to supernatant collected from the target/antibody – effector cells to which the lysis solution had been added. The reaction mixture-supernatant was incubated following which the stop solution was added to stop reaction from progressing any further. The absorbance was read at 490 nm with a reference wavelength of 600 nm.

3.2 Methods

3.2.1 Cell culture

3.2.1.1 *MDA-MB-468*

MDA-MB-468, an adherent breast cancer cell line with EGFR expression (received from Dr. Spencer Gibson's laboratory, Manitoba Institute of Cell Biology) was used as a source of target cells. The cells were grown in Dulbecco's Modified Eagle Medium (DMEM), (Sigma Aldrich, St. Louis, Missouri, USA) with 10% Fetal Bovine Serum (FBS), (Life Technologies, Carlsbad, CA, USA) in the presence of Penicillin-Streptomycin (1%), (Life Technologies, Carlsbad, CA, USA) and passaged every 4 days as the cells reached 70-80% confluency. Cells were grown in T75 flasks for adherent cells (Fisher Scientific, New Hampshire, USA). To detach cells from surface of the flask, 4 mL of TrypLE Select (Thermo Fisher Scientific, Waltham, MA, USA) was added and the flasks incubated for 7-9 minutes at 37 °C. For experiments, cells with viability ≥95% were used. MDA-MB-468 cells were plated 2-3 days before day of assay.

3.2.1.2 *NK-92 engineered cells*

The effector cells used were 'engineered' NK-92 176V (also referred to as NK-92 VV cells, high affinity variant) and NK-92 176F (low affinity variant) cells (received from Dr. Kerry Campbell, Fox Chase Cancer Centre, Philadelphia, USA). As a control, a cell line without CD16a expression was used (NK-92 Parent). They are suspension cells cultured in Minimum Essential Eagle Media with alpha modifications (αMEM), (Sigma Aldrich, St. Louis, Missouri, USA), Penicillin-Streptomycin (1%) and inactivated 10% FBS and 10% Horse serum

(Life Technologies, Carlsbad, CA, USA), also passaged every 4 days at a seeding density of $2x10^6$ cells/ml. Cells were grown in T75 flasks for suspension cells (Sarstedt, Nümbrecht, Germany).

3.2.2 Assay set-up

3.2.2.1 *Antibodies and MDA-MB-468 target cells set-up*

On the day of experiments, MDA-MB-468 cells were detached using 4 mL of TrypLE Select and washed with Dulbecco's phosphate-buffered saline solution (DPBS) (Gibco/Thermo Fisher Scientific, Waltham, MA, USA) to remove all serum containing DMEM media. The cells were then spun down and resuspended in 10 ml of assay medium. The assay medium consisted of serum-free Roswell Park Memorial Institute (RPMI) 1640 media (Lonza, Basel, Switzerland), to which 4 mM GlutaMAX (Gibco/Thermo Fisher Scientific, Waltham, MA, USA) and 1% Bovine Serum Albumin (Sigma Aldrich, St. Louis, Missouri, USA) were added. The cells were then counted using the trypan blue (Thermo Fisher Scientific, Waltham, MA, USA) exclusion method on the Cedex (Innovatis AG, Bielefeld, Germany) and assays were always set-up when viability of the cells was ≥95%. For all experimental assays (excluding the optimization assay described in section 1.2.2.3, where two different concentrations of target cells were tested ($5x10^3$ cells/well and $1x10^5$ cells/well), $5x10^3$ MDA-MB-468 cells/well were used. Thus, the total cells per ml used was $1x10^5$ cells. 1 ml of target cells were transferred into each of five 1.5-ml microcentrifuge tubes. Appropriate concentrations of control and experimental antibodies were then added to the target cells and incubated at room temperature for 10 minutes. As a positive control, Cetuximab, which is also

an anti-EGFR antibody, was used, the reason being that Cetuximab was readily available for comparison from our collaborators who have also used it for ADCC assays. Along with the EG2-X0 model antibody for the studies conducted in this thesis, variants of this EG2 antibody were also tested. These variants were kindly provided by Dr. Jamshid Tanha, National Research Council, Ottawa. The differences amongst these EG2 variants are detailed in Table 1 (D'Eall et al., 2019). Since the EG2 variants are modified within the Fc region by swapping the hinge regions or by introducing mutations within the region, they are expected to exhibit varying degrees of binding to the effector cells, thus, resulting in varying levels of cytotoxicity.

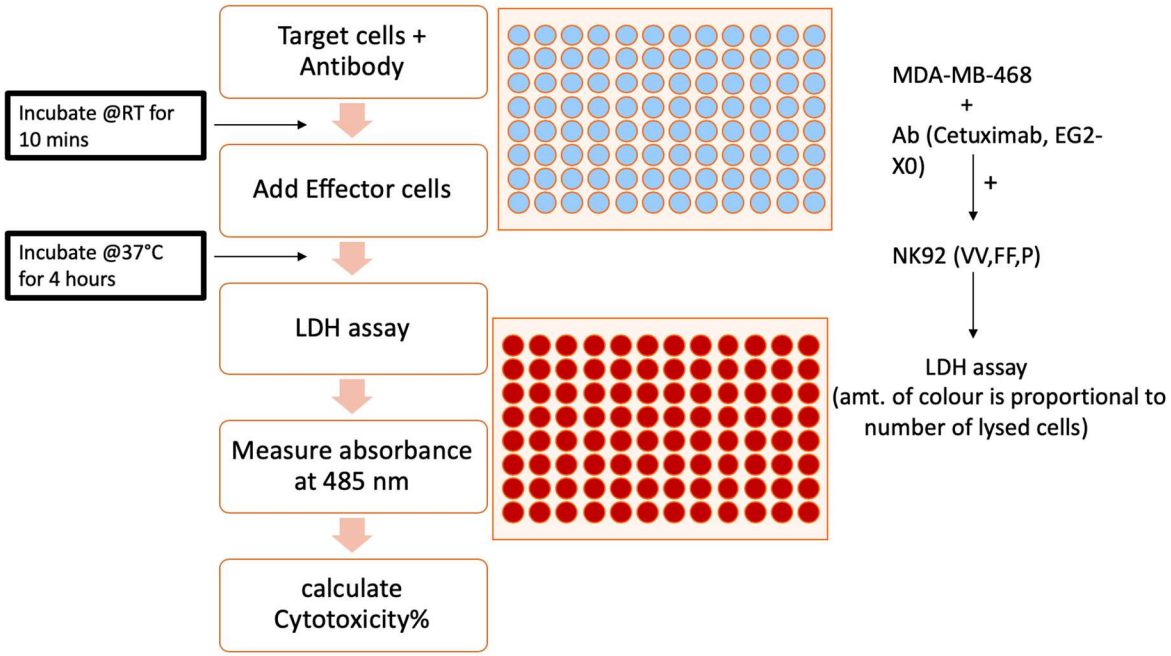

Figure 3-3: Step-by-step schematic representation of the assay set-up: Target cells are plated in a 96-well plate to which the antibody samples are added. Effector cells added next after allowing the target cells to be opsonized and the plate is further incubated for 4 hours at 37°C. The LDH assay is then performed following manufacturer's instructions and the percent cytotoxicity calculated as per Equation 3-1

Table 3-1: Differences between the EG2 variants used in the development of the LDH-based assay. (D'Eall et al., 2019). This table included variants developed by D'Eall et al. and were kindly provided by the Tanha lab (NRC-Ottawa).

EG2-X0	mutated Fc; D270G, Y268H – (this variant has been used for the purpose of the studies in this thesis)
EG2-X1	Wild type format Camelid Fab-Human IgG1 Fc
EG2-X2	truncated hinge
EG2-X5	upper-hinge cysteines replaced with serine residues
EG2-X6	IgG1 hinge replaced with camelid long-hinge
EG2-X8	human IgG3 hinge – Human IgG1 Fc
EG2-X9	Flipped format – Human IgG1 hinge with a spacer between EG2 and Human IgG1 Fc (EG2 on C terminal)

3.2.2.2 *NK-92 cells preparation and assay plate set-up*

All assays were set-up in 96-well tissue culture plates (Fisher Scientific, New Hampshire, USA). For all experimental assays (excluding the optimization assay described in section 1.2.2.3, where two different ratios of Effector-Target cells were tested, 10:1 and 25:1), an Effector-Target cells ratio of 10:1 was used. A total of $5x10^4$ cells were seeded into each well. Viability of the NK-92 cells was always ≥95%.

3.2.2.3 *Optimization assay*

In order to establish the number of target and effector cells required for the assay so that a clear distinction could be made between spontaneous release (LDH release without addition of lysis reagent) vs. maximal release (LDH release with addition of lysis reagent), first an optimization step was conducted. It was also important to determine the minimum number of target cells required to observe a response in the assay. To determine the optimal number of target cells, concentrations ranging from 0-10,000 cells/well were tested at incubation times of 15 minutes and 30 minutes. The number of MDA-MB-468 cells required was determined to be 5000 cells/well. Both the 15-minute and 30-minute assays exhibited the same response and thus an incubation time of 15 minutes was chosen. It is to be noted that the optimal number of cells has to be determined for each target cell being used in an assay. The next step was to determine the number of effector cells required. For this, two different ratios of cells (Effector:Target) 10:1 and 25:1 were tested with a range of antibody concentrations. With the 10:1 ratio, a relatively more consistent result was observed than with the 25:1 ratio (Figure 3-5) and thus, the 10:1 ratio of effector/target cells was used for further experiments.

Table 3-2: Set of experimental and control conditions used in the assay.

1. Background control (BC)	LDH activity of assay media, subtract BC from other values
2. Spontaneous release ($SR_{468\ cells}$)	Spontaneous LDH release from untreated target cells
3. Maximum release ($MR_{468\ cells}$)	Maximum LDH activity in the target cells that can be released
4. Spontaneous release of both cells ($SR_{468\ cells + NK}$)	Spontaneous LDH released from untreated cells
5. Positive control	Reference antibody (Cetuximab)
6. Experimental conditions (Exp)	LDH release of effector and target cells treated with antibody

3.2.3 Data analysis

The measurements were taken at 490 nm with a reference wavelength of 600 nm. After calculating average values from triplicate samples as well as controls, the absorbance value obtained from background control was subtracted from the average absorbance values of samples and the cytotoxicity percentage calculated using the following equation:

$$\boldsymbol{Cytotoxicity}\ (\%) = \frac{[\boldsymbol{Exp} - (\boldsymbol{SR_{NK+468\ cells}})]}{\boldsymbol{MR_{468\ cells}} - \boldsymbol{SR_{468\ cells}}} \times \mathbf{100} \ldots\ldots\ldots\ldots\ldots\ldots\ldots\ldots \textit{Equation 3-1}$$

where,

Exp = Experimental samples

SR = Spontaneous release of LDH without addition of lysis buffer

MR = Maximal release of LDH with addition of the lysis buffer

NK = NK 92 effector cells

468 = MDA MB 468 target cells

3.3 Results

3.3.1 Optimization assay

ADCC activity was measured using an LDH assay. In order to determine the number of effector (E) and target (T) cells to be used in the assay, first two different sets of optimization assays were set-up. NK-92 engineered effector cells were used with MDA-MB-468, EGFR-expressing target cells to test the cytotoxicity of in the presence of EG2-Xs. The number of target cells required was determined to be 5000 cells/well, where the maximum separation between the maximal and spontaneous release could be observed (Figure 3-4). The maximal release was obtained by addition of the lysis buffer and the antibody to the target cells, to

measure the maximum amount of lysis that can occur. Another optimization assay was set-up to determine the number of effector cells required for the assay. The assay was tested with varying concentrations of antibody, first with 5, 10, 50 and 100 μg/ml and consequently with lower concentrations ranging from 2-10 μg/ml (Figure 3-5). At 2 μg/ml (Figure 3-5(b)), the EG2-X0 does not induce cytotoxicity, as most likely the concentration of antibody is low. This same effect is also observed with higher effector/target (E/T) cell ratio Figure 3-5(a) as the antibody concentration is low for the number of cells used. Ratios of 10:1 and 25:1 of E/T cells were tested. For the optimization assay, NK-92 parent cells (as a control) and NK-92 VV variants were used. However, with the NK-92 VV high affinity variant, Cetuximab showed an increase in the ADCC response with increasing concentrations of the antibody (up to 40% cytotoxicity), but only with the 10:1 E/T ratio. In the 25:1 E/T experimental set, the correlation between antibody concentration vs. ADCC response was not as clear (Figure 3-5). It is possible that the assay does not have the same sensitivity with increased number of NK-92 VV cells. With the EG2-X0 and X1, there was again an increased ADCC response with increasing concentrations of the antibodies, but as with the control Cetuximab antibody, the E/T ratio of 10:1 gave a more consistent result than with the E/T ratio of 25:1. This was further confirmed with the antibody concentrations ranging from 2-10 μg/mL. Thus, the number of NK-92 cells required was chosen to be at a 10:1 ratio i.e. 50,000 effector cells/well. The assay was then performed with NK parent cells and it was observed that with the NK-92 parent cells, which do not express the CD16a receptors, there was less LDH released, in comparison to that from the NK-92 VV cells, which was as expected (Figure 3-6). This effect would be due to lack of CD16a receptors on the effector cells, the binding of antibody to induce cytotoxicity on the target cells would not be possible.

As the results from the optimization assay showed variability in terms of the concentrations used, the replicate values for the experiment was also checked. As shown in Figure 3-7 and Figure 3-8, both with antibody concentrations ranging from 5-100 µg/ml and 2-10 µg/ml, the absorbance values are consistent. Therefore, it is likely that the variations in cytotoxicity effect was due to the number of cells being tested, rather than an experimental error.

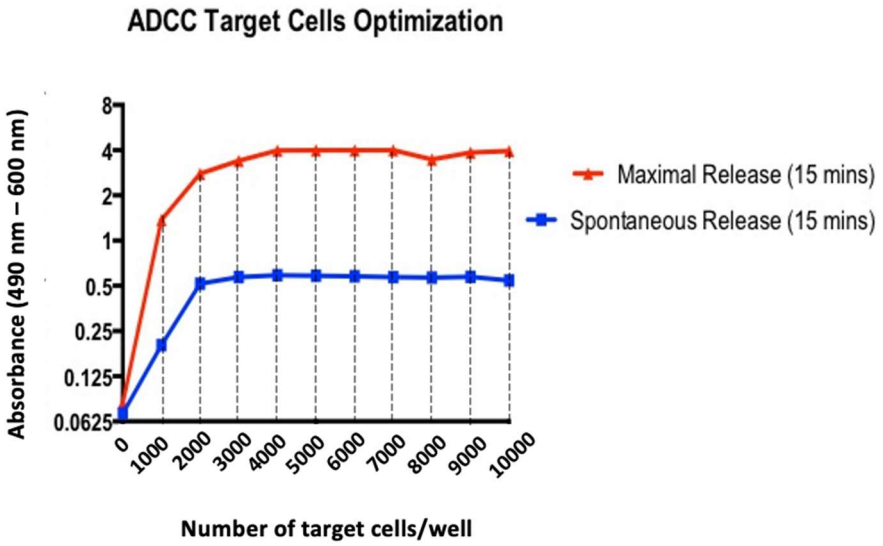

Figure 3-4: Optimization to determine the number of target cells required for the ADCC assay: An assay was set-up with 5000 cells/well and 10,000 cells/well. Lysis buffer was added to cells that were being measured for Maximal release of LDH (shown in red). This measurement was compared to the spontaneous release of LDH from cells without lysis (no addition of lysis buffer; shown in blue). The number of cells chosen for further experiments was 5000 cells/well. At this concentration, maximum release of LDH was observed (in the plateau). This number was also used in other studies ((Broussas et al., 2013)) and therefore allows comparison of the methods.

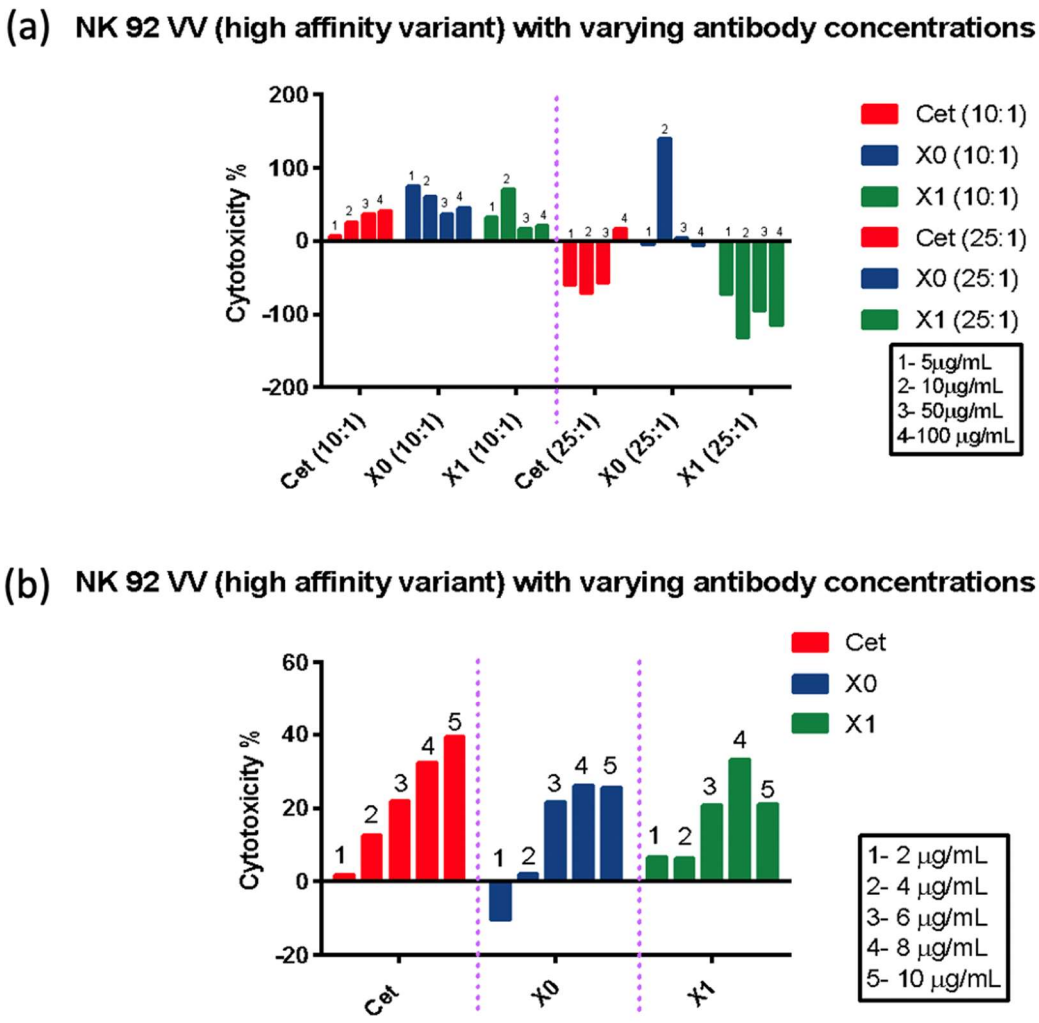

Figure 3-5: ADCC optimization assay on EG2-X0, EG2-X1 and Cetuximab, which is used as a control antibody: These sets of assays were done using the high affinity variant of the NK cells i.e. NK VV. (a) Effector:Target cell ratios of 10:1 and 25:1 were also tested. Concentrations of antibody tested ranged from (a) 5-100 µg/mL and (b) 2-10 µg/mL (effector:target cell ratio of 10:1), to determine the range of antibody concertation that can be tested within the assay. In the final assays, concentrations tested were 5, 25 and 50 µg/mL with an effector to target ratio of 10:1.

(a)

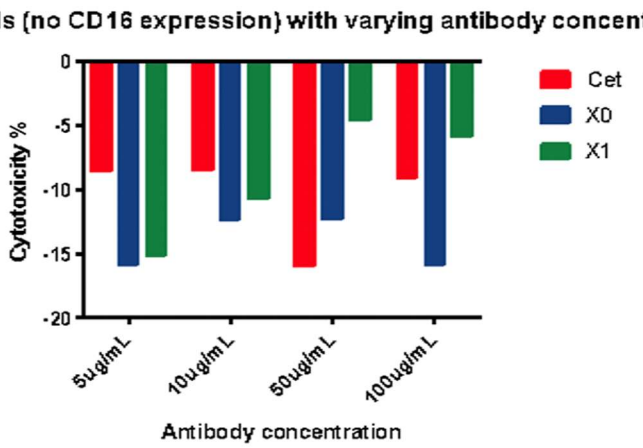

(b)

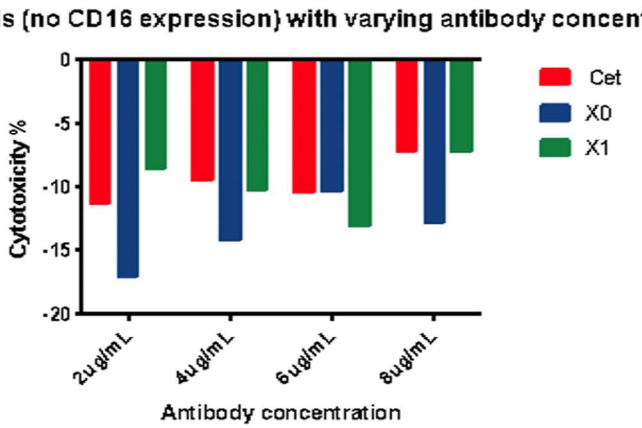

Figure 3-6: Optimization of LDH assay with NK parent cells: NK parent cells tested with antibody concentrations ranging from (a) 2-8 µg/ml and (b) 5-100 µg/ml. Along with the control, Cetuximab, neither X0 nor X1 exhibited any cytotoxicity response, as would be expected with a cell line that does not express CD16 receptor. Data are from a single experiment for each condition.

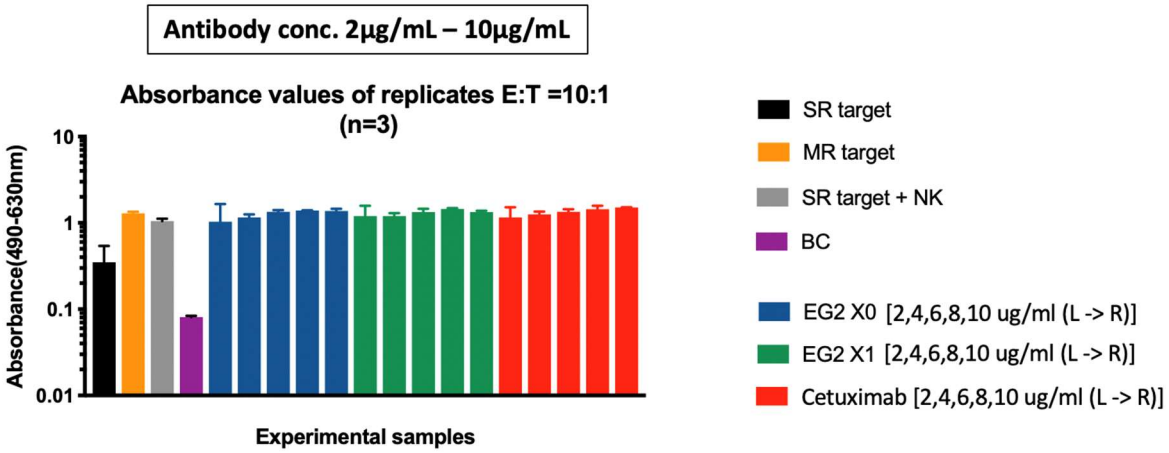

Figure 3-7: Absorbance values of replicate samples with E:T ratio of 10:1and antibody concentration ranging from 2-10 µg/ml: Samples in triplicate analysed showed a consistent result amongst the set of replicate samples. All samples were measured at a concentration ranging from 2 µg/ml to 10 µg/ml. The average of three technical replicate samples was then used to compare the cytotoxicity. Error bars indicate standard errors.

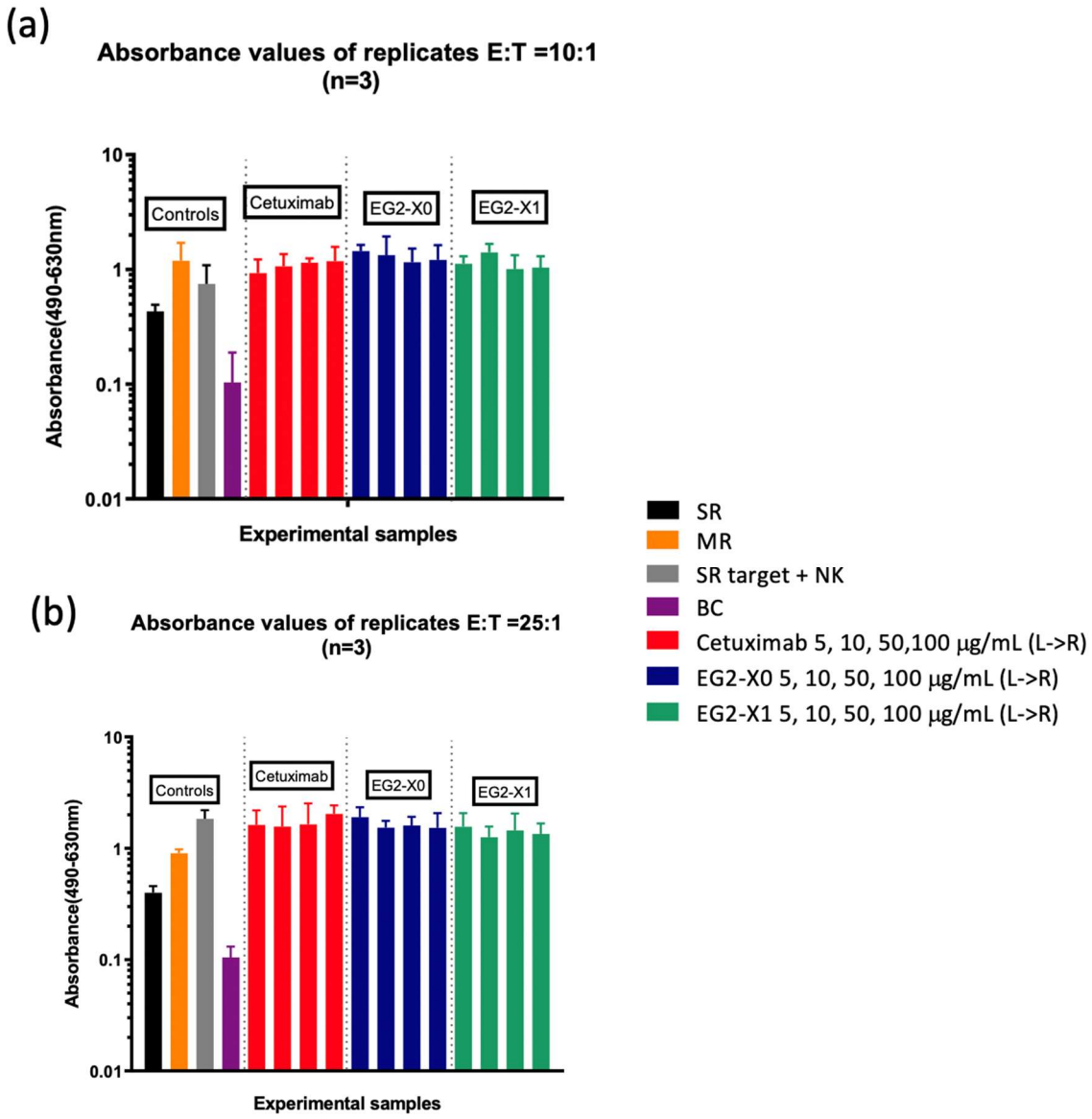

Figure 3-8: Absorbance of formazan released post-addition of antibody: Absorbance values of replicate samples with E:T ratio of 10:1and 25:1 with antibody concentration ranging from 5-100 µg/ml- (a) shows the absorbance values of replicates with E:T of 10:1 and (b) shows absorbance values of replicates with E:T of 25:1. Absorbance of formazan released post-addition of antibody at the concentrations tested (ranging from 5-100 µg/ml as in the previous Figure 3-7).

3.3.2 Determination of ADCC activity of EG2 variants

To further test the efficiency of the assay to measure cytotoxicity post-addition of the different concentrations of antibody, different variants of the EG2 antibody were used (Figure 3-9). Details of the differences amongst the EG2 antibodies are listed in Table 1. For the EG2 variants, the assay was performed with 5000 cells/well of target cells, using an E/T ratio of 10:1 as per the optimization assay results. The antibody concentrations tested were 5, 25 and 50 μg/mL. For the NK-92 parent cells, with the control Cetuximab antibody and NK92 parent cells, there is a "negative cytotoxicity" effect observed, as was the case in the optimization assay. There were low levels of cytotoxicity observed in all samples. An EG2-deglycosylated control was also included in this experimental set in order to be able to assess the sensitivity of the assay. In this case, LDH released was below detection when compared to the EG2-X0 (fully glycosylated) sample. However, with certain EG2 variants, including the wild-type EG2 antibody, there was relatively higher cytotoxicity observed, when compared to that in the presence of the control MAb Cetuximab. This should not be the case in a NK-92 parent cell line, as the cells do not express the CD16a receptor. Similarly, for the NK-92 FF variant of effector cells, the Cetuximab antibody was not associated with any effect, whereas the EG2 variants caused low levels of cytotoxicity. The overall pattern was again similar to that seen with the NK-92 parent cells. For the NK-92 VV variant of effector cells, although the cytotoxicity levels were higher when compared to the parent and FF cells, the levels of cytotoxicity were still low when compared to the optimization assay. The assay using the EG2 deglycosylated antibody displayed a cytotoxicity of 5% whereas, that with Cetuximab had a cytotoxicity close to 9%, although this was not a statistically significant difference. The EG2-X1 wild type antibody, however, did lead to a higher level of cytotoxicity when compared to

Cetuximab. The highest percent cytotoxicity was observed with the X9 variant, which has a human IgG1 hinge with a spacer between EG2 and a human IgG1 Fc. The EG2 segment is on the C terminus (D'Eall et al., 2019).

3.3.3 Determination of ADCC activity of RMD-EG2 variants

For the variant Mab from the RMD-EG2 and 2FF-treated experiments (described in Chapter 2 in detail), the assay was set-up as previously established by the optimization assay. Both EG2-RMD and 2FF treated antibodies are defucosylated (to various degrees, also detailed in Chapter 2). It was therefore hypothesised that the percent cytotoxicity would be higher than that associated with the EG2-X0 and the Cetuximab antibodies. From the NK-92 VV effector cell cytotoxicity assays, it was observed that the Mab from the RMD 5 Hi and Med cells induce a relatively higher percent cytotoxicity than do the control Cetuximab and the EG2-X0 antibodies. However, the difference was not significant. Similarly, in case of the NK-92 FF cells, the Mab from the RMD 5 Hi sample, led to a higher percent cytotoxicity than did the control antibodies. Interestingly, although the Mab from both the RMD-transfected cells, as well as from the 2FF-treated cells are defucosylated up to a certain level, antibodies resulting from 2FF-treated cells, at both 10 and 50 μM concentrations do not cause the same intensity of cytotoxicity as do the RMD-EG2 antibodies. For the NK-92 parent cells, as was observed with previous experimental sets as well as the optimization assay, a reduction in cytotoxicity was observed. However, the percent cytotoxicity for all samples in all effector cells was not as high as was observed in the optimization assay (approx. 40% cytotoxicity) (Figure 3-10). It is possible that the sensitivity of the LDH assay is not high, due to the effector cells that have been used here. In order to see if there was a trend that could be detected from all the assays performed with RMD-EG2 and 2FF-treated antibody samples, a correlation analysis was

performed to compare the % fucosylation vs. % cytotoxicity of NK92 effector cells (VV, FF and parent) and 2FF-treated and RMD-EG2 MAb samples (Figure 3-11). As expected for the 2FF-treated EG2 samples, a strong correlation was observed in the NK 92 parent cells (R^2 = 0.888). For the NK92 FF cells also, a weaker correlation was observed (R^2 = 0.582). However, for the NK92 VV cells, no correlation was observed (R^2 = 0.022). In case of the NK92 FF cells tested with RMD-EG2 samples, again, no correlation was observed (R^2 = 0.0203). With the NK 92 Parent cells (R^2 = 0.3188), a positive correlation was observed whereas with the NK 92 VV cells, again no correlation was observed (R^2 = 0.088). It is therefore possible that the sensitivity of the assay is dependent on the NK cell variant type and that it should be optimized further for the NK-92 VV variant.

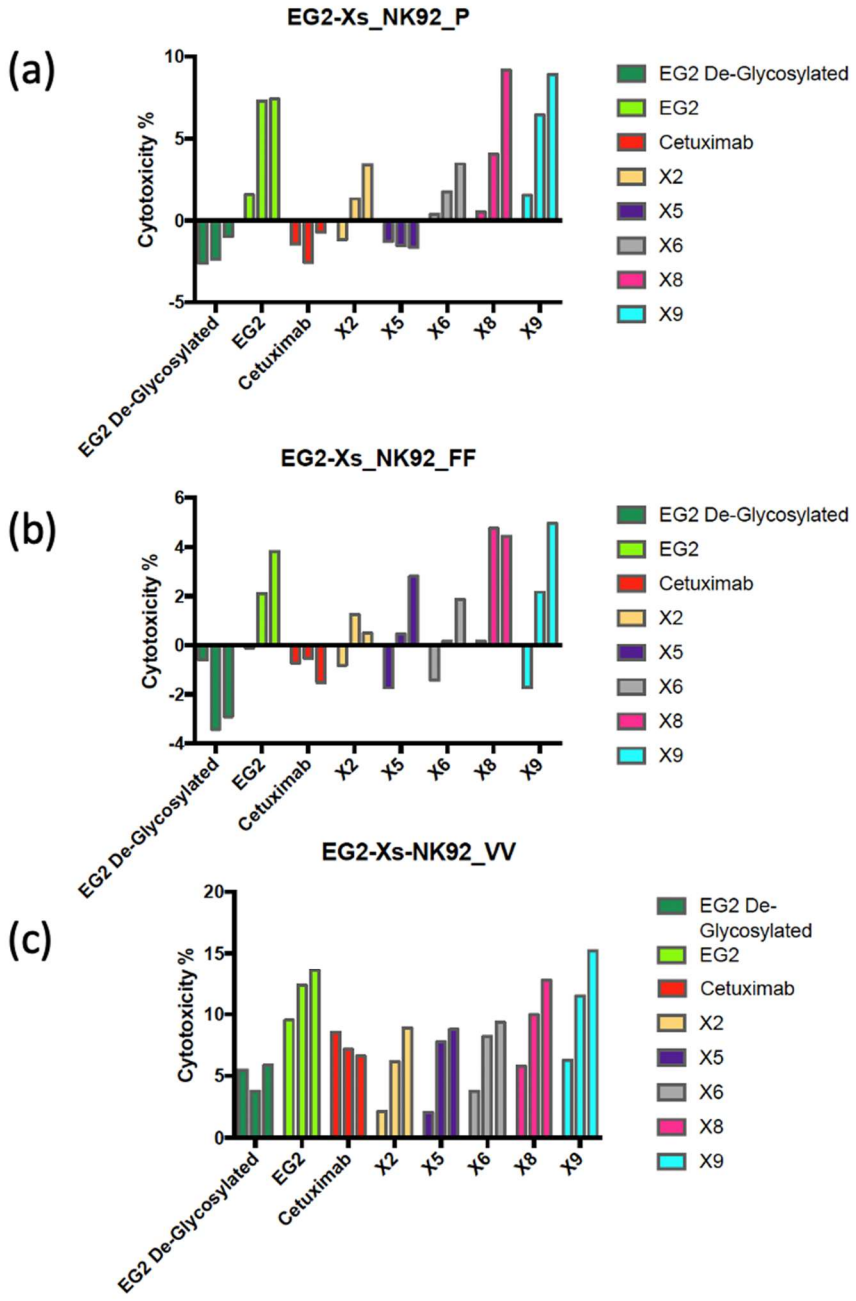

Figure 3-9: ADCC assay performed with EG2-Xs: The variants of EG2 antibody were tested in the same assay to check (a) with NK 92 Parent cells (b) NK 92 FF cells and (c) NK 92 VV effector cells. Along with all the EG2 variants, a deglycosylated EG2 antibody was also used, to test if the assay is able to detect cytotoxicity of the deglycosylated antibody. As expected, the deglycosylated antibody exhibited lower cytotoxicity.

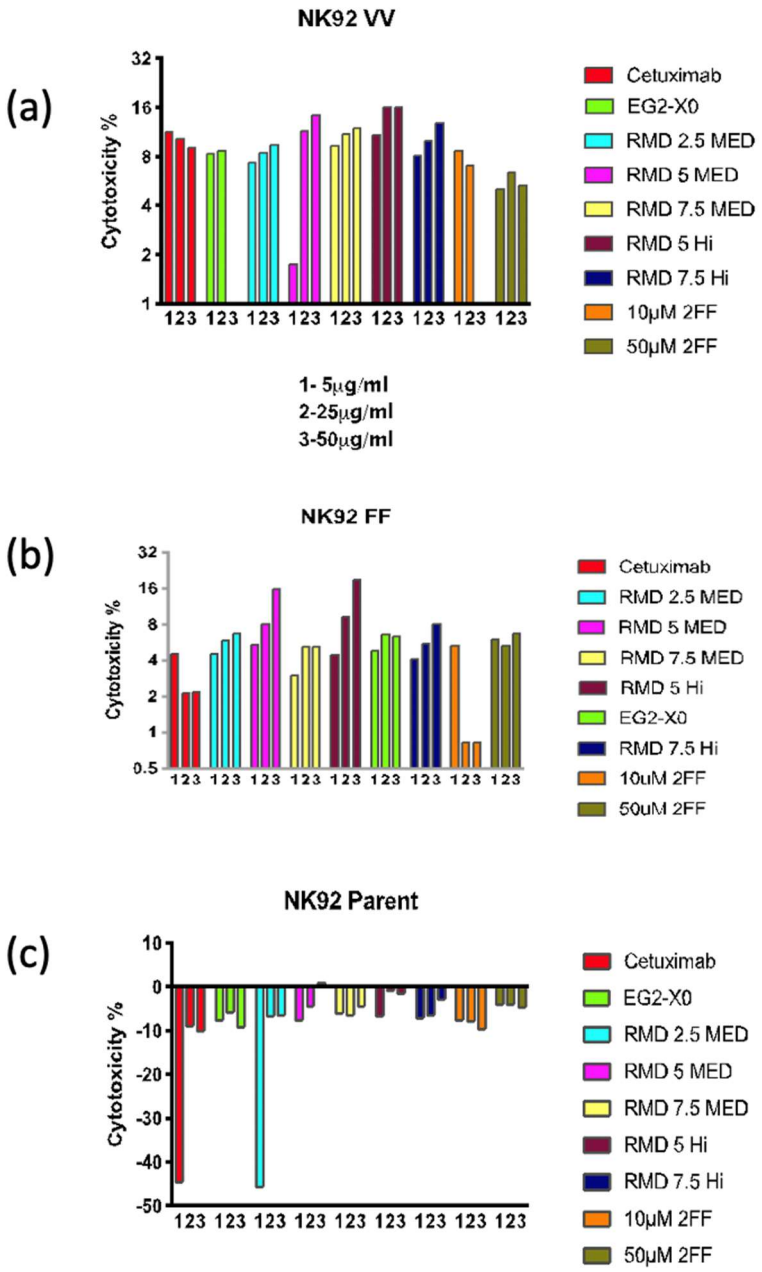

Figure 3-10: ADCC assay performed with EG2 antibody generated from RMD-transfected CHO-EG2 cells and 2FF-treated cells: The RMD-EG2 and 2FF-treated EG2 were tested with the LDH-based ADCC assay. Antibody concentrations of 5, 25 and 50 μg/mL were tested with (a) NK 92 VV (b) NK 92 FF and (c) NK 92 parent effector cells. The results of three technical replicates are shown.

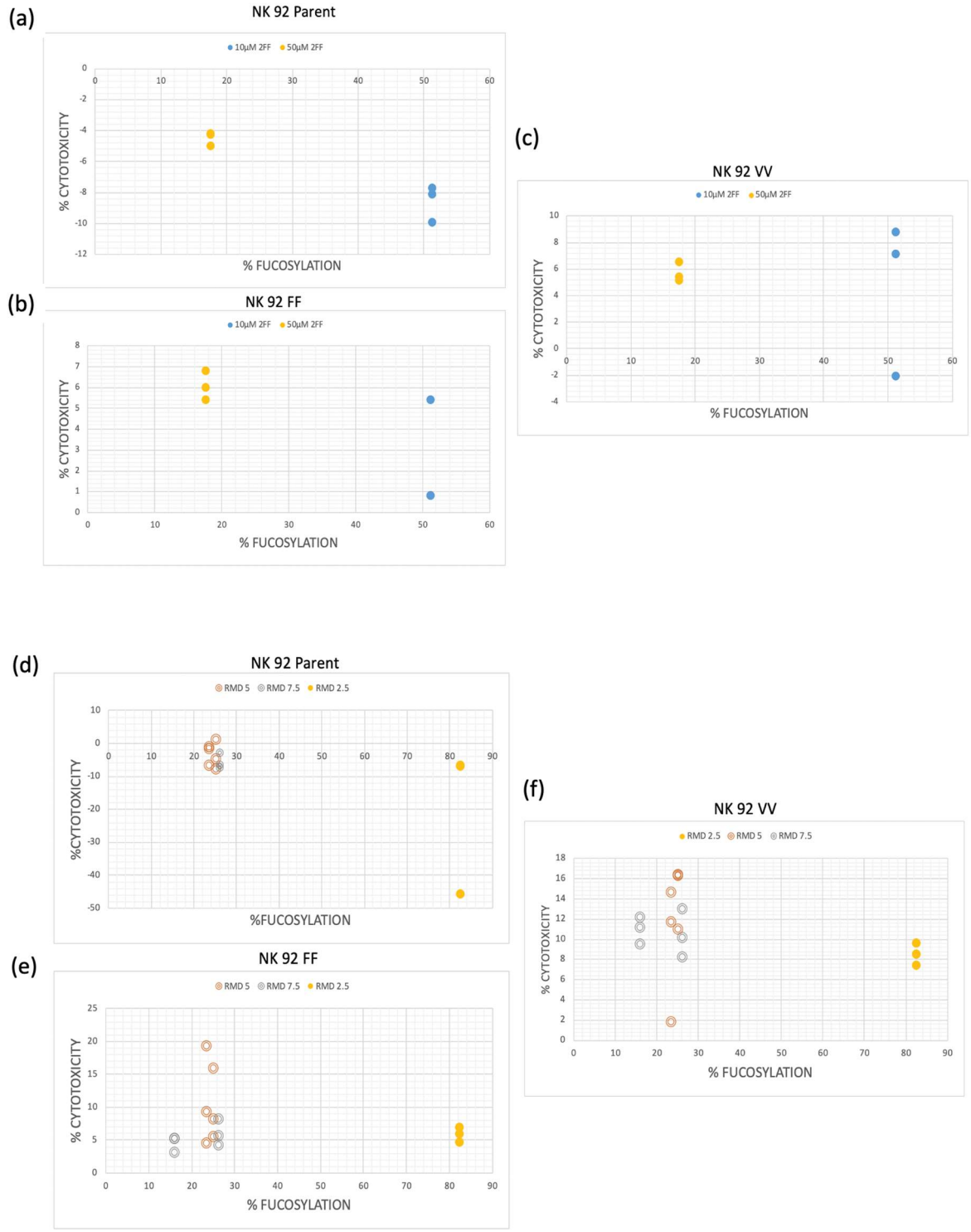

Figure 3-11: Correlation between all the test samples of each NK-92 variant: The sample set shown includes all of the tests conducted with NK-92 cells. A strong correlation is observed in the parent cells. However, in the VV variants, no correlation was observed and in FF variants, the correlation was relatively significant.

3.4 Discussion

The purpose of the experiments described in this chapter was to design and establish an ADCC assay that would not require the use of radioactive substances nor the use of PBMCs as effector cells. An LDH based assay was used along with an engineered NK -92 cell line as effector cells. A number of optimization assays were performed to establish number of effector and target cells as well as concentration of antibody to be used. Following the optimization assays, the EG2 antibody was tested in varying concentrations against the control antibody, Cetuximab.

Although the optimization assays performed as expected, with the percent cytotoxicity increasing with the increasing concentrations of antibody, assays set up with the EG2 Mabs did not result in the same conclusions, in terms of the cytotoxicity detected. There was little to no correlation observed in NK 92 VV cells that were tested with the 2FF treated antibody samples, and the same trend was observed for the NK 92 FF cells tested with RMD-EG2 antibodies. Ideally, this trend should be confirmed with biological replicates (as well as technical replicates within the experiment) to collect more data points and assess reproducibility. However, it is worth noting that although the cytotoxicity induced by the EG2 antibodies (both 2FF treated and RMD-EG2) was not high (<10%), it was higher than that seen in the Cetuximab control. With the EG2 antibody samples from 2FF-treated cells, a higher percent cytotoxicity was observed, which could be the result of less fucosylation in these samples leading to higher affinity for the FcγR. In a ^{51}Cr assay, the cytotoxicity achieved with the EG2 variants ranges from 20-80% (D'Eall et al., 2019). Also, in experimental sets where the deglycosylated EG2 antibody was used, cytotoxicity was much lower, below detection levels. It is possible to still use the LDH-based assay, as long appropriate controls are also

included to get a relative value for the cytotoxicity. However, the assay requires more optimization to be able to establish it as a standard for measuring the ADCC of an antibody. To further assess the sensitivity of the LDH-based assay, PBMCs derived from donors could be used and the result compared to ^{51}Cr assay. More controls such as a different IgG1 anti-EGFR antibody like Panitumumab (García-Foncillas et al., 2019) could be used to investigate whether the cytotoxicity induced is specific to Cetuximab or if it could be applied to other IgG1 antibodies.

4

Elucidating the redox status of intracellular glycosylation machinery - ER and Golgi, using roGFP-iX probes

4.1 Introduction

Eukaryotic cells are compartmentalized and contain different organelles in which the cells perform specific reactions such as post-translational modifications glycosylation. Each organelle has a defined environment, which helps the machinery function (Kellokumpu, 2019). Specifically, for glycan processing, redox status, dissolved oxygen (DO), pH and ammonia in particular are suggested to be factors influencing the intracellular machineries in the endoplasmic reticulum (ER) and Golgi (Kunkel et al., 1998; Muthing et al., 2003; Yang and Butler, 2002). Studies have focused on effect of these biochemical parameters on MAb production and glycosylation but the the interplay between the biochemical factors and the cellular machinery during MAb production has not been explored extensively. A recent publication highlighted the potential link between redox balance and the role it plays in glycosylation, especially in the generation of high mannose (HM) glycans in Mabs (Kang et al., 2015). It was shown through metabolomics analysis that the addition of certain amino acids such as ornithine to the cell culture medium was responsible for production of HM glycans (Kang et al., 2015). Ornithine, along with other identified metabolites such as cystine, niacinamide, and glutathione, have been known to contribute to redox regulation (Kang et al., 2015; Zanatta et al., 2013). Meneses-Acosta *et al*. (Meneses-Acosta et al., 2012) have shown that reducing conditions lead to an increase in the concentration of secreted MAb and enhanced

cell growth of hybridoma cell culture. Although glycan analysis was not conducted in this study, it is an important finding that can be extrapolated to study the importance and effect of redox potential in cell culture on glycosylation.

Following the results relating to DO (Kunkel et al., 1998) and culture reduction potentials (CRP) of hybridoma cell lines (Meneses-Acosta et al., 2012), further studies in the Butler lab have led to investigating antibody producing mammalian cell lines (Dionne et al., 2017). Experiments were conducted using dithiothreitol (DTT) to induce reducing conditions. Three antibody-producing cell lines were studied and compared: 1) a NS0 cell line producing an IgG1 2) a CHO cell line producing an anti-IL8 antibody (CHO DP12, anti-IL8) and 3) a CHO cell line producing EG2 camelid antibody (CHO EG2-hFc). It was observed that although the addition of DTT (at concentrations of 0.25, 0.50 and 0.75 mM) to induce reducing conditions had no effect on cell growth or antibody concentration, variations in glycan profiles occurred with a decrease of ~50% in the galactosylation index (GI). A comparison of CRP after DTT treatment amongst the three cell lines also established that the variation in GI is host cell line dependent. It was also noted that the decrease in GI was related to a lowering of the pH in the cell cultutre media different cell lines, irrespective of DTT concentration. Ab from both NS0 and CHO-DP12 cells exhibit low GI, whereas that from CHO EG2-hFc exhibits high GI.
To this end, this project was designed to investigate the intracellular redox state using redox-sensitive green fluorescent proteins (roGFPs) and its role in MAb production and glycosylation. This was done by integrating roGFPs into the in-house CHO cell line producing EG2-hFc chimeric monoclonal antibody variants.

Redox homeostasis has been a focus of many studies primarily because it affects cellular functions. Previous studies have led to the conclusion that the cytosol has a reducing environment whereas the ER has an oxidising environment (Figure 4-1). The importance of

redox state within ER required for protein folding has been studied extensively. The balance between glutathione and its oxidised form (GSSG/GSH) is considered to be crucial for disulfide bond formation in the ER and prevents hyperoxidising conditions and thus, protein misfolding (Chakravarthi et al., 2006; Chakravarthi and Bulleid, 2004). Previously reported GSSG/GSH ratios suggest that in the secretory pathway, ratios may be 100 times higher than in the cytosol (Hwang et al., 1992).

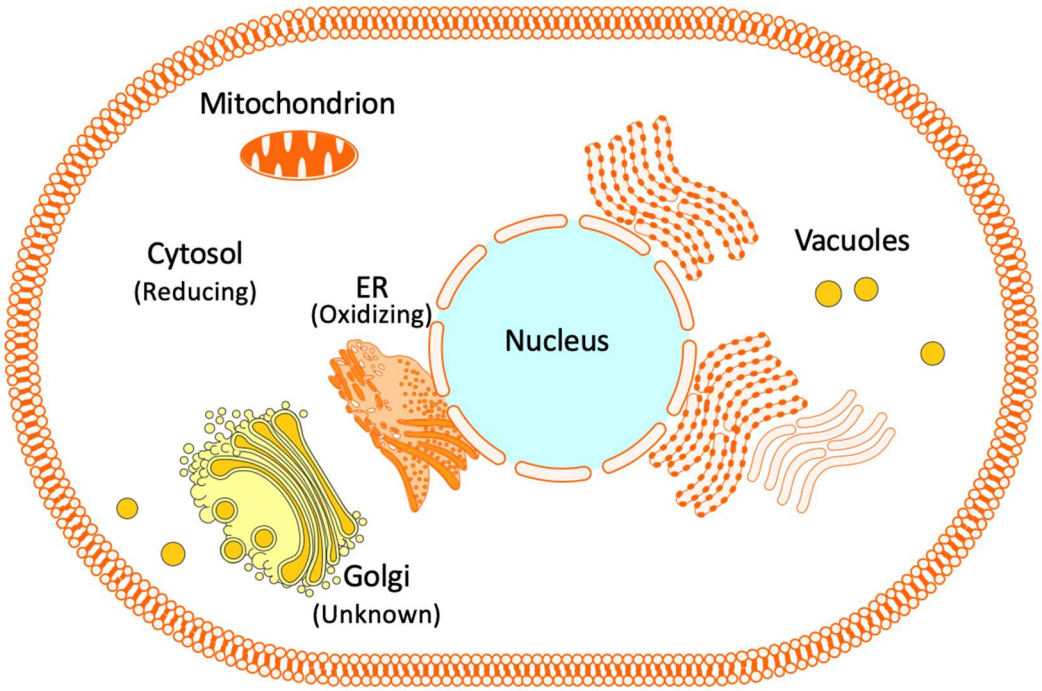

Figure 4-1: The cellular organelles within a eukaryotic cell: redox state of the machinery involved in post-translational modifications such as glycosylation is largely known except for the Golgi. ER has an oxidising environment which helps the formations of disulphide bonds within a protein. However, in the Golgi, glycosylation enzymes reside which are involved in the glycosylation of proteins, but the redox status of this organelle is unknown according to the literature reviewed.

Traditional assays to measure these ratios have been cumbersome and involved invasive studies requiring cell lysis, thus eliminating the possibility of studying redox status in live cells (Dooley et al., 2004). This has changed with the Nobel Prize winning work of Osamu Shimomura, Martin Chalfie and Roger Tsien, who discovered GFP and developed it as a research tool. Extensive research by various groups has focused on exploring the capabilities of GFP. The potential is vast with usage ranging from gene expression detection with GFP co-transfection (Kain et al., 1995) to studying factors that affect cellular events such as pH, calcium ion concentration, and redox homeostasis (Cannon and Remington, 2008). GFP exhibits a dual excitation behaviour that has led to the development of biosensors to study biological events via real-time imaging using fluorescence microscopy (Cannon and Remington, 2008; Lohman and Remington, 2008; Zhang et al., 2002). Studies in mammalian cells (van Lith et al., 2011) and yeast (Delic et al., 2010) have monitored the redox status of the cytosol (reducing environment) and the ER (oxidising environment) using redox sensitive GFP (roGFP) probes designed in the Remington lab, University of Oregon. The roGFPs exhibit a ratiometric change between the oxidised and reduced roGFPs occurring due to a conformational difference within the chromophore (Lohman and Remington, 2008). Studies in yeast and mammalian cell lines have indicated that the roGFP constructs are suitable for studying real-time changes in redox status in living cells, with varying oxidising or reducing conditions. In mammalian cells, it was noted that the response to DTT or 4 - 4′dipyridyl disulfide (DPS) was rapid with the difference observed between fully reduced and oxidised states, and with cell recovery occurring in 5 minutes after removal of either agents. This finding steered the hypothesis towards the role of the enzymes peroxiredoxin and ER oxidoreductases at play that were responsible for directly or indirectly metabolizing DTT and helping cells recover (Baker et al., 2008; Tavender et al., 2010).

Different variants of redox sensitive fluorescence proteins have been developed over the years. The redox sensitive probes are designed to detect changes in the reduced and oxidised forms of glutathione (GSH/GSSG ratio). In all the variants, redox reactive, surface-exposed cysteine pairs have been introduced into the structure of the fluorescent protein, on the β-strands. Redox-sensitive yellow fluorescent protein (rxYFP) was one of the first such probes. However, rxYFP is not a ratiometric probe and has a single excitation peak at 512 nm and single emission peak at 523 nm. Such probes are also not convenient for live cell imaging as the probes are not ratiometric and levels of expression would affect the values (Bilan and Belousov, 2017; Lohman and Remington, 2008). roGFPs also have been made more efficient over the years, which has led to improved efficiency of detection. In all the roGFP variants, redox active, surface exposed cysteines have been introduced into the β-strands at positions 147 and 204, which results in formation of a disulphide bridge, leading to protonation of the chromophore. The roGFP1 variant contains a Cysteine-48-Serine replacement, whereas the roGFP2 variant has an additional Serine-65-Threonine mutation. Also, for roGFPs, the pH of the cellular environment does not affect the read-out of the redox status, because an effect would decrease the fluorescence intensity from both the oxidised and reduced forms of the chromophore but would not affect the ratio.

Glycosylation in Golgi is mediated by enzymes such as glycosyltransferases or mannosidases present in the cis, medial or trans membranes. These enzymes are responsible for further processing of the glycoprotein that passes on from the ER, adding galactose, N-acetylglucosamine, sialic acid and fucose or cleaving mannose residues from the structure. None of the studies conducted using roGFPs have focused on Golgi redox state and its effect on glycan processing as the focus has been on protein folding and ER. It was hypothesized that results from this project would provide an insight into the organelle's redox status and how this

might be affecting its role in glycosylation. The reducing and oxidising buffers used are DTT and DPS, respectively, which have been used successfully for determination of redox state in mammalian cells (van Lith et al., 2011). DTT is a strong reducing agent and is cell-permeable (van Lith et al., 2011), whereas DPS is a highly reactive thiol oxidant, which is also membrane permeable and thus can be used in intact live cells (van Lith et al., 2011; pez-Mirabal et al., 2007)

4.2 Methods

4.2.1 Construct Design

Five different constructs were designed using the mammalian expression vector, pDREAM 2.1/mcs (7159 bp) (GenScript) (Figure 4-3) and the redox sensitive GFPs (roGFPs; 759-828 bp) to target to cytosol, endoplasmic reticulum (ER) and Golgi (Figure 4-2):

Table 4-1:List of roGFP probes designed for targeting to each organelle.

	probe	**Target organelle**
1	pDREAM- *roGFP*	cytosol
2	pDREAM-ERp57- *roGFPiL*-KDEL	Endoplasmic Reticulum
3	pDREAM – ERp57 – *roGFPiE*-KDEL	Endoplasmic Reticulum
4	pDREAM- βGalT4 – *roGFPiL*	Golgi
5	pDREAM- βGalT4 – *roGFPiE*	Golgi

roGFP (828 bp), roGFP-iL (759 bp) and ro-GFP-iE (759 bp) (iL and iE have one amino acid difference between them; L-leucine, E- Glutamic acid), have been designed to target the cytosol, ER and Golgi. To target the constructs to ER the ERp57 signal peptide was fused to the N-terminus, and the ER retention signal KDEL was added to the C-terminus (van Lith et al., 2011). Alternatively, the N-terminal 81 amino acid residues of β-1, 4 galactosyltransferase was used to target proteins to the Golgi (Llopis et al., 1998).

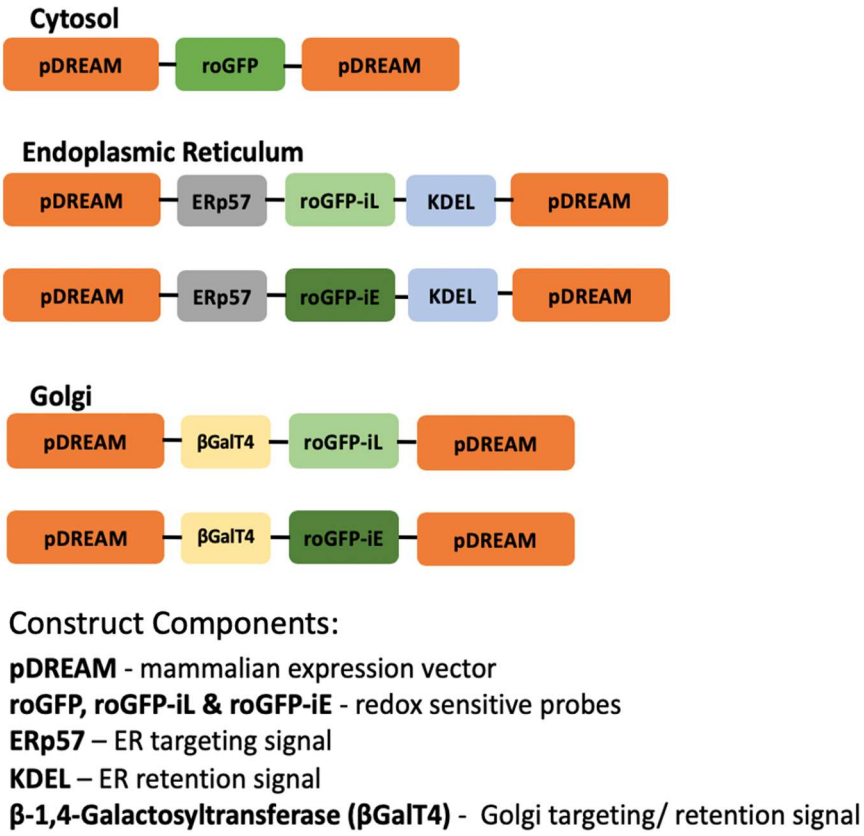

Figure 4-2: Design of the roGFP constructs roGFP-iL/iE along with the targeting and retention signals: In the final vector design, the pDREAM mammalian expression vector (orange) was used, into which synthesised roGFP probes (green) were cloned. ERp57 targeting grey) and KDEL retention (blue) signals for the ER were used, whereas, for the Golgi, β-1,4-Galactiosyltransferase targeting/retention signal (yellow) was used. (The different components of the gene fragments are depicted as individual blocks but are infact ligated together).

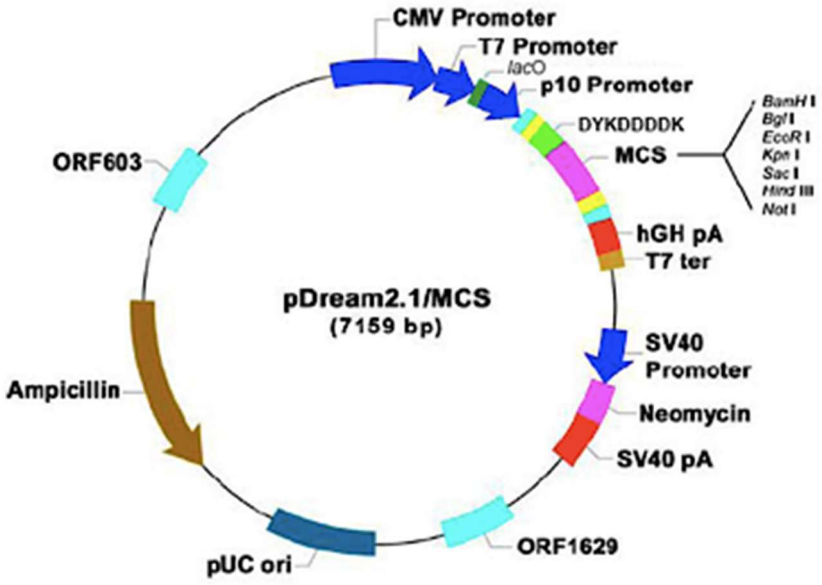

Figure 4-3: Vector map of pDREAM: The mammalian expression vector pDREAM2.1/MCS was used for cloning the roGFP fragments (Genscript). The constructs were cloned between the EcoRI and BamHI sites. The neomycin-resistance gene was used for selection.

4.2.2 Cloning

The plasmid DNAs for roGFPs (roGFP, roGFP-iL and roGFP-iE) were kindly provided by Dr. Jim Remington (University of Oregon, USA). The roGFP vectors were for expressions in bacterial systems and could not be used for mammalian expression, and thus, pDREAM (Genscript), a mammalian expression vector, was used for this purpose. The roGFPs were removed from the bacterial expression vector using restriction digestion with two different enzymes (EcoRI and BamHI), gel extracted and purified before being used for ligation. At first, T4 DNA ligase (Thermo Fisher Scientific) was used in a fast ligation - dependent method to generate the roGFP constructs with pDREAM. The targeting and retention signals – ERp57, KDEL (ER) and β-1,4-Galactosyltranferase (Golgi) were generated using GeneArt Synthesis (Thermo Fisher Scientific). Different insert/vector ratios were used (2:1, 3:1, 5:1, 6:1).

However, with this first attempt only the pDREAM - roGFP construct with an insert/vector ratio of 3:1, was generated and all other constructs were unsuccessful. The next attempt was to then PCR amplify roGFP-iL and roGFP-iE, gel extract and purify before using a ligation-independent method for cloning. In this case, the InFusion method (Clontech, Takara Bio, USA) was used. Various ratios of the insert/vector were tried as before, with no success. Finally, the roGFP sequences along with the targeting and retention signals were synthesised using GeneArt Synthesis so that a single fragment could be cloned into the vector (Figure 4), which would increase the likelihood of ligation of the vector-insert. This attempt was successful, and all the constructs generated were identified by colony PCR and verified by sequencing.

4.2.3 Cell line

The Chinese Hamster Ovary cell line CHO EG2-hFc (also described in chapters 2 and 3) was transfected with the pDREAM-roGFP, and pDREAM-roGFPiL/iE constructs. CHO-EG2hFc-X0 is a suspension cell line cultured in the proprietary chemically defined Biogro medium. Cells were passaged every 3 days with a seeding density of 2.5 x 10^5 cells/mL and incubated at 37 °C, 10% pCO_2 on a shaker platform.

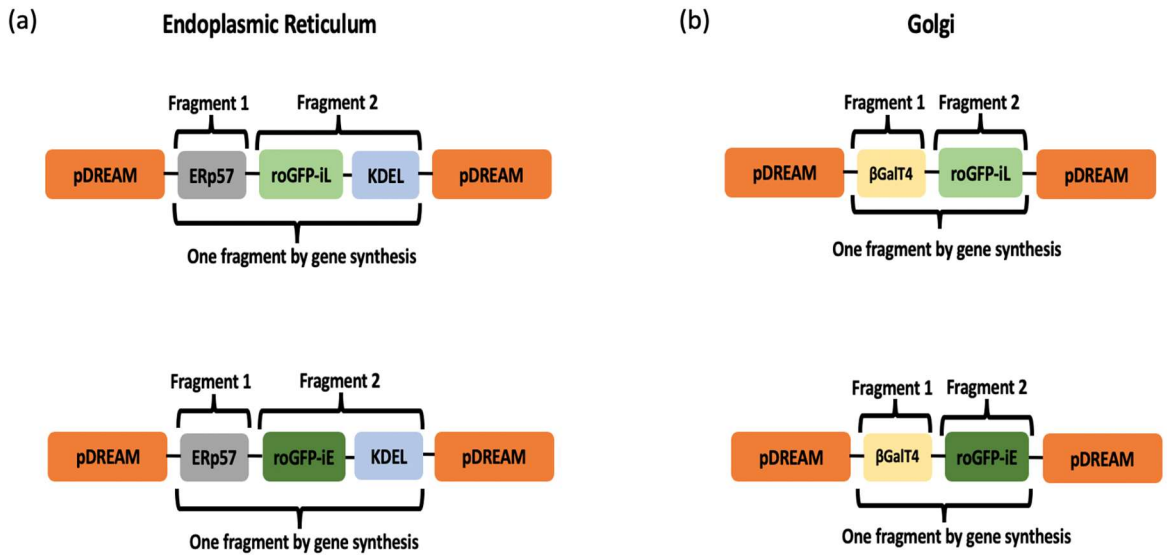

Figure 4-4: Design of the gene fragments generated by synthesising single fragments to improve ligation into pDREAM2.1/MCS. Fragments were designed for (a) ER and (b) for Golgi.

4.2.4 Transfection and generation of stable pools of cells expressing roGFP variants

Following successful cloning of all five constructs, these were transfected into the MabNet antibody producing CHO cell lines using a chemical transfection reagent, XFect (Clontech, Takara Bio, USA), using manufacturer's instructions. Briefly, cells were seeded one day prior to transfection at a density of $3x10^5$ cells per well in a 6-well plate in Pluronic® free media (to promote cell attachment and avoid inhibition of transfection). Purified plasmid (5-20 µg) was prepared in sterile deionized water to which the chemical transfection reagent was added. A range of DNA:reagent ratios were tried: 3:1, 6:1, and 10:1. The DNA:reagent mix was incubated for 15 minutes to allow complex formation, following which time this complex was added to cells. The cells were then kept at 37°C for 16 hours and the medium was changed

after 16 hours. G418 (800µg/mL) was added to select for antibody-producing pools of cells with integrated redox sensitive constructs.

4.2.5 Immunofluorescence Staining and Microscopy

$4x10^4$ cells/ chamber well were seeded in each well of a 4-well chamber slide (Thermo Scientific™ Nunc™ Lab-Tek™ II Chamber Slide). The cells were then left overnight for staining. 12-16 hours later, cells were gently washed twice with 1 mL of PBS, ensuring that cells did not detach from the surface of the wells. 36% formaldehyde (Sigma-Aldrich, St. Louis, USA) was diluted to 4% in PBS. 1 mL of the 4% of formaldehyde solution was added to the cells and incubated for 10 minutes at room temperature. Following fixing, cells were washed with PBS twice. For permeabilization, cells were then incubated with 0.1% Triton X-100 for 10 minutes and washed three times post-incubation. Cells were then blocked with 1% (w/v) goat serum in PBS for 1 hour to avoid nonspecific binding with antibodies and then incubated with the appropriate primary antibodies, which were diluted in blocking buffer (1% (w/v) goat serum in PBS).

For co-localization studies, two different primary and secondary antibodies were used for each of the constructs (Figure 4-5). For the GFP (common to all roGFP constructs), a goat polyclonal primary antibody (Santa Cruz Biotechnology, USA) was used with a donkey anti-goat secondary antibody coupled to Alexa Fluor® 405 (Abcam, UK). For detection of PDI (an ER resident protein), a rabbit polyclonal Ab and a donkey anti-rabbit polyclonal secondary (Alexa Fluor® 555) (Abcam, UK) was used. For the 58K Golgi protein (Golgi resident protein), a mouse polyclonal primary with donkey anti-mouse polyclonal (Alexa Fluor® 594) (Abcam, UK) was used. Before use all the antibodies were diluted to the required working concentrations as per manufacturer's instructions. A mixture of antibodies was used (GFP+PDI and GFP+58K Golgi protein) for simultaneous staining.

The cells were incubated for 1 hour at room temperature with the primary antibodies, following which the cells were washed three times, with PBST (PBS+Tween) for 10 minutes each wash. Secondary antibodies, which were diluted in blocking buffer, were then added to the washed chambers and left at 37°C in dark, for at least 40 minutes. Following incubation with secondary antibodies, the cells were washed again with PBST for 10 minutes each wash in the dark. After the washes, the holder of the chambered slide was removed so that the slide could be used for observation under the confocal microscope. After removing the holder, a coverslip was added and sealed using nail polish. Slides were stored at 4°C until ready for imaging. A Zeiss LSM 700 confocal microscope (Zeiss Microscopy, Jena, Germany) was used to observe the cells and the images analysed by the Zeiss integrated software as well as ImageJ ((Rueden et al., 2017).

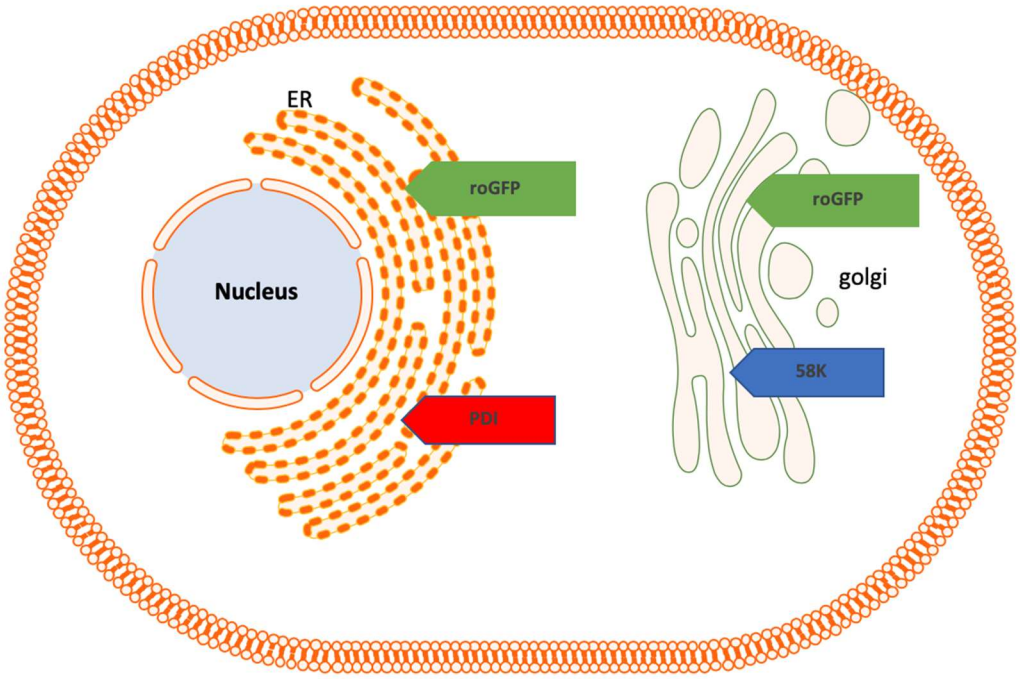

Figure 4-5: Immunofluorescence assay design: The coloured arrows indicate the different fluorescence antibodies used and the targeted organelles for each. The primary antibodies used for localization in the ER were against PDI (a molecular chaperone protein resident in ER) and the primary antibodies used for localization in Golgi were against the 58K protein resident in Golgi along. Anti- roGFP antibodies were also used. All antibodies were sourced from either Abcam or Cell Signalling Technology.

4.2.6 Flow cytometry analysis for detection of redox status

To analyse the redox status of ER and Golgi in the redox-sensitive GFP probe integrated cell lines, flow cytometry was used. A BD FACSCanto-II digital flow cytometry analyser system (BD Biosciences, San Jose, USA) was used to detect the required wavelengths. The GFP transfected cells were grown in baffled shaker flasks. On the day of experiment, cells at a concentration of 10^6 cells/ml were washed with Dulbecco's phosphate-buffered saline solution (DPBS) (Gibco/Thermo Fisher Scientific, Waltham, MA, USA) and resuspended in the sorting buffer containing 1x DPBS (Ca/Mg^{2+} free), 1% FBS, 25 mM HEPES pH 7.0 and 1

mM EDTA. At the flow cytometry facility (Rady Faculty of Health Sciences, University of Manitoba, Canada), the cells were passed through round bottom tubes with 35-μM cell strainer caps just before being treated with required concentrations of DTT and DPS. The samples were then run through the cytometer and analysed, at 5- and 15-minute time points post treatment with the compounds. Concentrations of DTT and DPS used were – 0 mM (control), 0.25 mM, 0.5 mM, 0.75 mM and 1 mM. The cells were excited sequentially at wavelengths of 405 nm and 488 nm and the fluorescence intensity emitted at 510 nm were recorded. The intensity values from 405 nm were divided by the values from 488 nm to calculate the florescence intensity ratios. These ratios were then normalized to untreated controls. Log2 ratios were then used to distinguish between the increasing (values from DPS induced oxidising conditions) and decreasing (values from DTT induced reducing conditions) values.

4.3 Results

The process of stable pool generation has been depicted in Figure 4-6 and individual steps are described in the individual sections below. Briefly, the roGFP-expressing constructs were transfected into the CHO-EG2 cells, following which GFP expression was observed using fluorescence microscopy. A selection pressure was then applied to the transfections and roGFP signals were monitored over time using fluorescence microscopy. Cells that survived the selection were then expanded and cultured as stable pools.

4.3.1 Design and Cloning of the roGFP constructs

The roGFP constructs were targeted to Cytosol, ER and Golgi by retention signals. For the cytosolic probe, roGFP, targeting and retention signals are not required. For ER, the

targeting and retention signals were ERp57 and KDEL respectively (van Lith et al 2011). For Golgi, the N-terminal 81 amino acids of βGalT4, which is a type II membrane protein and has been used previously as a marker of Golgi, were added as both targeting and retention signals (Llopis et al., n.d.). The multiple fragments of roGFP and targeting signal sequences were synthesized as one fragment with terminal restriction sites BamHI and EcoRI, by Life Technologies using GeneArt Strings. The fragment was then ligated to the expression vector by restriction digestion cloning method and transformed using *E. coli* Top10 competent cells (Invitrogen). Positive colonies were identified using colony PCR and confirmed by DNA sequencing.

4.3.2 Transfection of the roGFP constructs in the CHO EG2-hFc cell line to generate stable pools

CHO EG2-hFc cells were transfected with the roGFP constructs and stable pools were established using G418 selection. GFP expression was confirmed using fluorescence and all of the transfected cells exhibited GFP expression (Figure 4-7) as expected. As the cells were transfected with the roGFP plasmid, it was observed that the cells exhibited GFP expression as expected (Figure 4-7).

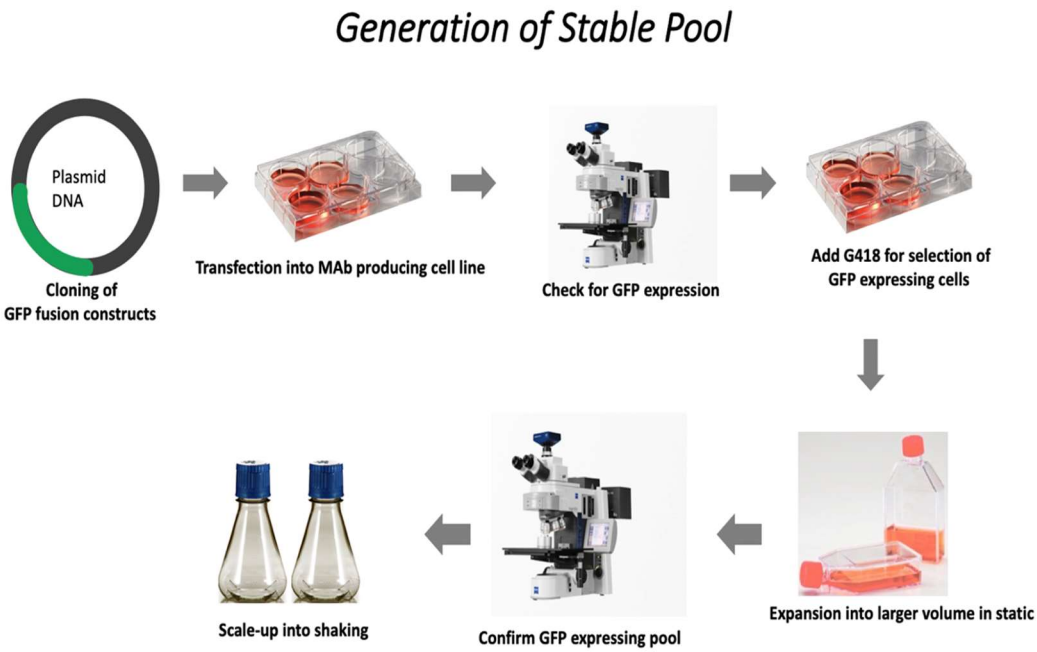

Figure 4-6 : Generation of stable pool of transfected roGFP pools: The process started with cloning of the GFP constructs followed by transfection into the CHO-EG2 hFc cells. The cells were checked for GFP expression using inverted fluorescence microscopy, following which a selection pressure, G418, was applied. The cells were kept under selection until recovery and then expanded into Erlenmeyer disposable shake flasks.

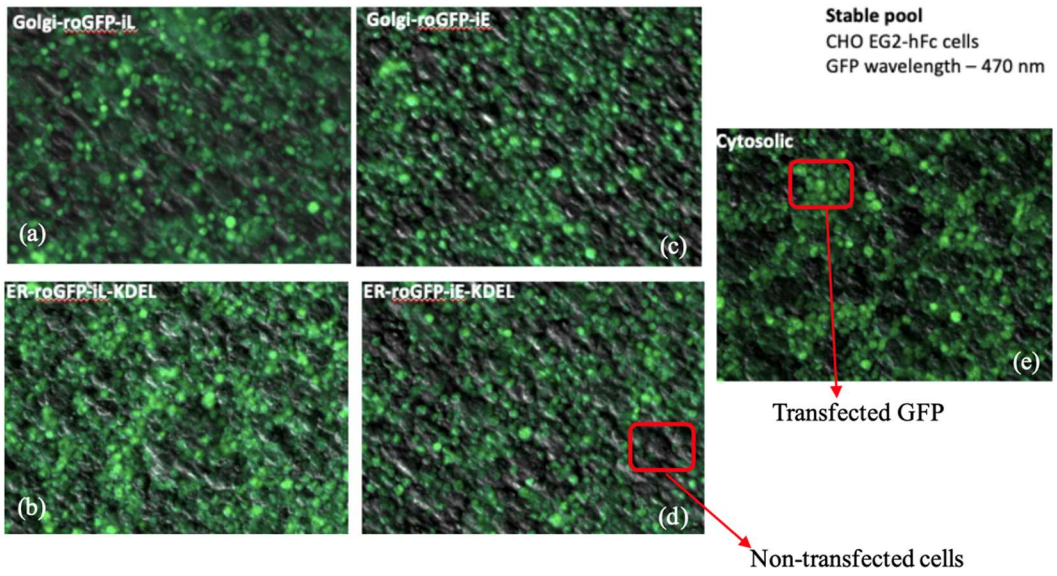

Figure 4-7: Fluorescence microscopy to detect GFP expression post-transfection and selection: The selected pools of cells were plated onto a glass-bottom 35-mm dish (MatTek corporation, MA, USA) which is optimized for imaging. GFP expressing cells were visualized with a filter set with excitation/emission of 470 nm/520 nm using a Zeiss Axio Observer Z1 at 20x magnification. (a) roGFP-iL targeting to Golgi (b) ER targeted with roGFP-iL (c) roGFP-iE targeted to Golgi (d) roGFP-iE targeted to ER. (e) roGFP targeting cytosol.

4.3.3 Co-localization studies by immunofluorescence microscopy to confirm the targeting of the constructs into the cellular organelles

In order to confirm that the constructs were correctly targeted to the intended cellular organelles, an immunofluorescence staining approach was used. The ER and Golgi resident proteins, Protein Disulphide Isomerase (PDI), a molecular chaperone resident in the ER, and 58K Golgi protein were used in co-localization experiments in cells expressing roGFP-iL or roGFP-iE constructs. Images were obtained using a Zeiss LSM 700 confocal microscope and

were analysed using the integrated software and ImageJ. As seen in Figure 4-8 (b &c), images of cells transfected with ER targeted roGFP-iL/iE (in blue) when merged with PDI (in yellow), reveal co-localization of both proteins in ER whereas, the 58K Golgi protein (in red) co-localized in the Golgi with the Golgi targeted roGFP-il/iE. For roGFP (in blue) expressed in the cytosol, as expected, the GFP expression was detected throughout the cells. It is worth noting that although the staining for PDI worked quite well as evident from the image, but the 58K Golgi protein is not as abundant within these particular cells. The staining was repeated multiple times with varying antibody dilutions, with the same result. This could merely be due to the fact that the primary antibody used for staining may have lower affinity than the PDI primary antibody. Nevertheless, the immunofluorescence staining was able to confirm the targeting of the organelles with the roGFP constructs.

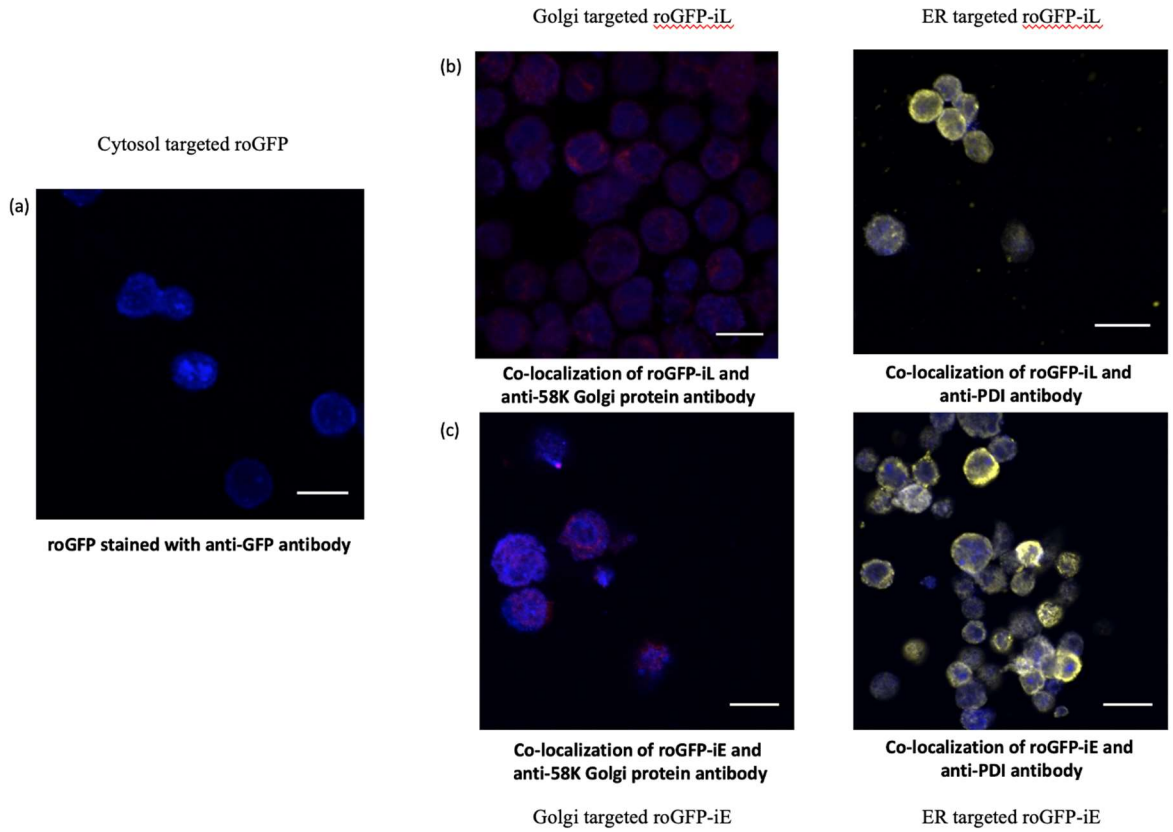

Figure 4-8: Co-localization studies of roGFP variants to show targeting to the cytosol, ER and Golgi of CHO EG2-hFc cells: The PDI and 58K Golgi protein antibodies were used for immunofluorescence studies, to co-localize to (a) Cytosol (b) ER and (c) Golgi. ER targeted roGFP-iL/iE (in blue) when merged with PDI (in yellow), reveal co-localization of both proteins in ER whereas, the 58K Golgi protein (in red) co-localized in the Golgi with the Golgi targeted roGFP-il/iE. For roGFP (in blue) expressed in the cytosol, as expected, the GFP expression was detected throughout the cells.

4.3.4 Redox status studies using flow cytometry analysis

In order to determine the efficiency of the roGFP-iL and iE probes to measure redox states within the intracellular organelles, a flow cytometry method was applied. This method to measure fluorescence in single cells was adapted from a previous study that was conducted with 3T3-L1 fibroblasts, wherein flow cytometry was used to validate the system (Sarkar et

al., 2013). Analysis of the changes in redox conditions in cytosolic, ER and Golgi probes were done using DTT and DPS as reducing and oxidising buffers. The concentrations of DPS and DTT were selected were based on concentrations used in (Sarkar et al., 2013) as well as previous work in Butler lab on culture redox potential of antibody producing CHO cells (Dionne et al., 2017a) where a range of concentrations were used (0-0.75 mM). The experimental set-up involved cells at a concentration of 10^6 cells/ml that had been washed DPBS and resuspended in the sorting buffer. The cells were passed through round bottom tubes with 35-µM cell strainer caps just before being treated with required concentrations of DTT and DPS. The samples were then run through the cytometer and analysed, at 5- and 15-minute time points post treatment with the compounds. Being ratiometric probes, the excitation wavelengths used were 405 nm and 488 nm and emission recorded at 510 nm. The intensity values from 405 nm were divided by the values from 488 nm to calculate the florescence intensity ratios. These ratios were then normalized by dividing them by the ratios for the untreated controls. Log2 of the ratios were then used to distinguish between the DPS-induced oxidising conditions and DTT-induced reducing conditions thus indicating the redox states of the cells (further explanation of the calculations described here is included in the **7 appendix** section).

roGFP-iE had a wider range of detection between fully oxidised and reduced states as has also been previously reported (Delic et al., 2010). The roGFP probe itself has a low reduction potential and can detect changes in reducing conditions such as those that occur in the cytosol. However, in more oxidising conditions such as those found in the ER, the original roGFP probe is always fully oxidised (Delic et al., 2010a) (Schwarzer et al., 2007) and cannot be used to detect changes in this environment that has a redox state that is more tightly controlled. This led to the development of the roGFP-iX family of redox sensors, which differ

in their midpoint potential. Therefore, both roGFP-iL and roGFP-iE were used to compare efficiency of measurement of both probes.

For cells expressing roGFP in the cytoplasm, there were minimal changes towards the negative ratios in the fluorescence ratio 5 and 15 minutes after addition of DTT, but a correlation between concentration of DTT or time of exposure, and the degree of change in the ratio was not observed (Figure 4-9, a,b). The addition of DPS induced a significant decrease in the ratio, in the range (log2) of -0.4 to -0.6; again, there was no correlation between DPS concentration or time and the change in ratio. This is an unexpected result when compared to past literature since addition of DPS should ideally change the fluorescence ratios towards positives. Therefore, under the conditions tested, cytosolic roGFP can detect changes due to the addition of an oxidizing agent, but not in a concentration-dependent manner over the concentrations tested.

A similar pattern of changes in fluorescence was observed for cells expressing ER-iE and G-iE in the presence of DTT; there were small, concentration-independent fluctuations in the ratio (Figure 4-9 c,d,e,f). Thus, roGFP-iE did not detect any pH changes in the ER or Golgi associated with the addition of DTT. In contrast, low concentrations of DPS (0.25 mM) were associated with changes in the fluorescence ratios of between -0.4 and -0.6 (log2). The amount of change decreased, but remained negative, with increasing of DPS in cells expressing ER-iE (15 min treatment, panel c) and G-iE (5 min panel e). In the other two experiments, the log2 change was slightly positive under the highest concentrations of DPS (panels d and f. The concentration dependence of the relative change in signal indicates that there is a range of oxidation states detectable with the roGFP-iE variant in the ER and Golgi.

roGFP-iL was also tested (Figure 4-9, g, h, i, j), and the results differed from those of the roGFP-iE constructs in both the Golgi and ER. In both compartments, there was a detectable reduction in the ratio for the roGFP-iL constructs in the presence of DTT. The general trend was one of larger decreases in the presence of higher concentrations of DTT and the maximum difference was about -0.1 (log2). Upon the addition of DPS, however, there were large, concentration-independent decreases in the fluorescence ratios; the differences were in the range of -0.8 to -1.0 (log2). This suggests a limitation of roGFP-iL, and that it may not be able to detect changes in redox beyond a certain point. Thus, its range of detection is very limited. Previous studies have reported that roGFP-iE has a better range of fluorescence (Delic et al., 2010a) than roGFP-iL, which also was observed in the experiments conducted herein.

In summary, the roGFP-iE construct was the only one associated with concentration-dependent changes in the fluorescence ratios in the presence of both oxidizing and reducing agents. When comparing the results observed in the experiments conducted here, with results reported in Sarkar *et al*., 2013 , there is a clear difference. In Sarkar *et al.*, the values observed change towards positive and negative values with addition of diamide (oxidising) and DTT (reducing), respectively. In the experiments conducted in this chapter following the flow cytometry method, definite positive and negative values are not seen due to addition of DPS and DTT. Although, changes are noted post-addition, they are most likely affected by the time of exposure to reagents or the concentration of reagents used. It could be likely that the time required for the cells to react to the reagents is more than the time of exposure in the experiments conducted. Ideally in this case, a real-time visualisation of the cells after exposure to the reagents over a period of time (starting from 0 mins to 15 mins at consistent increments of 1min longitudinally) would be able to provide a better idea of effect of time. It is also possible that the concentrations of DTT used did not generate sufficient changes in redox state

to be detected by the probes. It is also important to note that the cells used in both studies are also different; the CHO cells are expressing cell lines whereas cells used in Sarkar *et.al* are 3T3-L1 fibroblasts; however, this may be less likely to cause an effect.

In all the control samples where there was no addition of reducing or oxidising reagents, no changes in the fluorescence ratios were detected, indicating that the changes in the fluorescence ratios in the treated samples were indeed due to the changes in the redox state of the cellular organelles. It is important to note that this method represents the overall redox state in a population of cells that could be in various physiological states, rather than in a single cell and thus, may not be an accurate representation, but an overall estimate of the redox state (these results have been further discussed in Section 4.4 - Discussion).

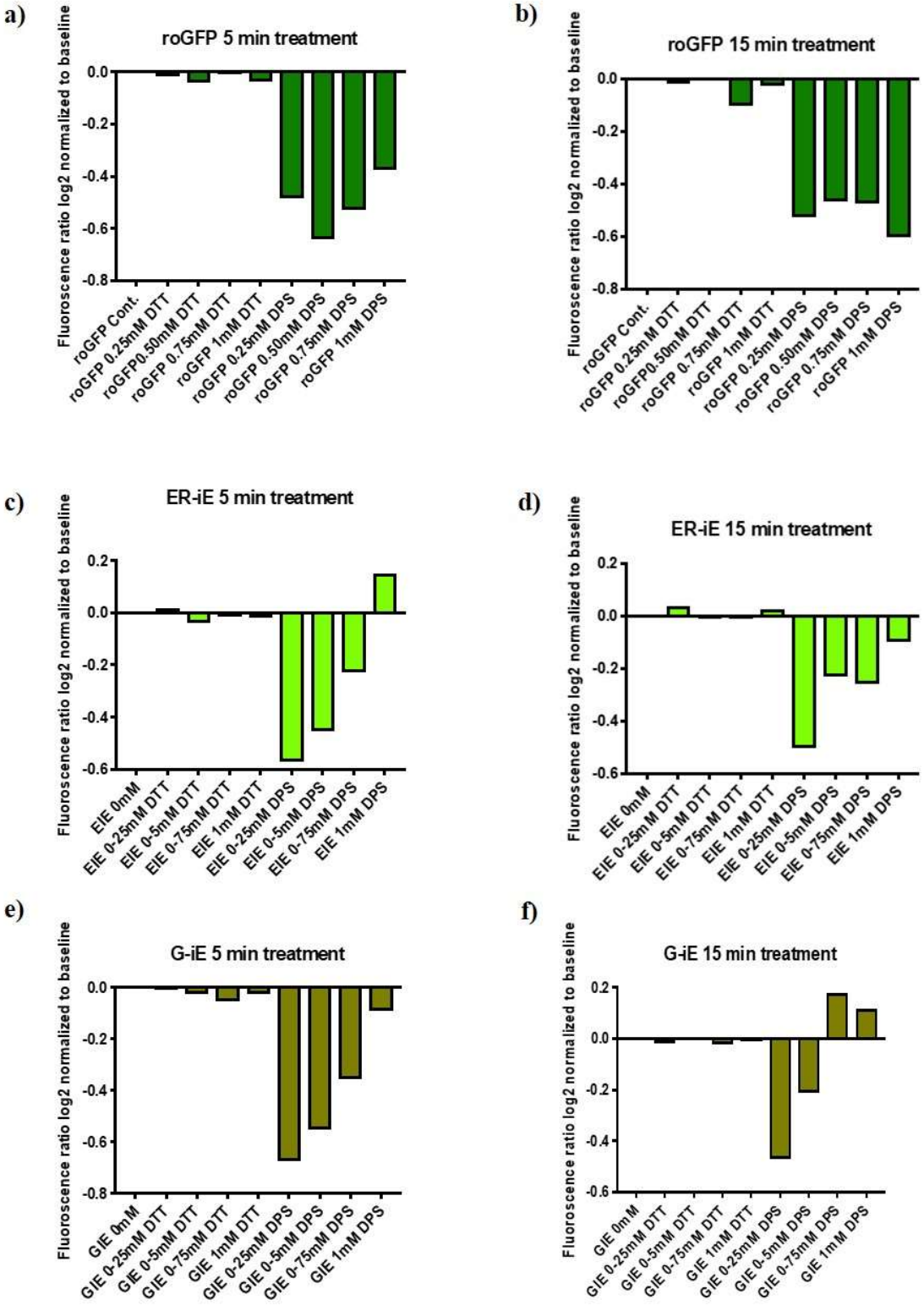
a)
roGFP 5 min treatment
Fluoroscence ratio log2 normalized to baseline
0.0
-0.2
-0.4
-0.6
-0.8
roGFP Cont.
roGFP 0.25mM DTT
roGFP0.50mM DTT
roGFP 0.75mM DTT
roGFP 1mM DTT
roGFP 0.25mM DPS
roGFP 0.50mM DPS
roGFP 0.75mM DPS
roGFP 1mM DPS
b)
roGFP 15 min treatment
Fluoroscence ratio log2 normalized to baseline
0.0
-0.2
-0.4
-0.6
-0.8
roGFP Cont.
roGFP 0.25mM DTT
roGFP0.50mM DTT
roGFP 0.75mM DTT
roGFP 1mM DTT
roGFP 0.25mM DPS
roGFP 0.50mM DPS
roGFP 0.75mM DPS
roGFP 1mM DPS
c)
ER-iE 5 min treatment
Fluoroscence ratio log2 normalized to baseline
0.2
0.0
-0.2
-0.4
-0.6
EIE 0mM
EIE 0-25mM DTT
EIE 0-5mM DTT
EIE 0-75mM DTT
EIE 1mM DTT
EIE 0-25mM DPS
EIE 0-5mM DPS
EIE 0-75mM DPS
EIE 1mM DPS
d)
ER-iE 15 min treatment
Fluoroscence ratio log2 normalized to baseline
0.2
0.0
-0.2
-0.4
-0.6
EIE 0mM
EIE 0-25mM DTT
EIE 0-5mM DTT
EIE 0-75mM DTT
EIE 1mM DTT
EIE 0-25mM DPS
EIE 0-5mM DPS
EIE 0-75mM DPS
EIE 1mM DPS
e)
G-iE 5 min treatment
Fluoroscence ratio log2 normalized to baseline
0.0
-0.2
-0.4
-0.6
-0.8
GIE 0mM
GIE 0-25mM DTT
GIE 0-5mM DTT
GIE 0-75mM DTT
GIE 1mM DTT
GIE 0-25mM DPS
GIE 0-5mM DPS
GIE 0-75mM DPS
GIE 1mM DPS
f)
G-iE 15 min treatment
Fluoroscence ratio log2 normalized to baseline
0.2
0.0
-0.2
-0.4
-0.6
GIE 0mM
GIE 0-25mM DTT
GIE 0-5mM DTT
GIE 0-75mM DTT
GIE 1mM DTT
GIE 0-25mM DPS
GIE 0-5mM DPS
GIE 0-75mM DPS
GIE 1mM DPS

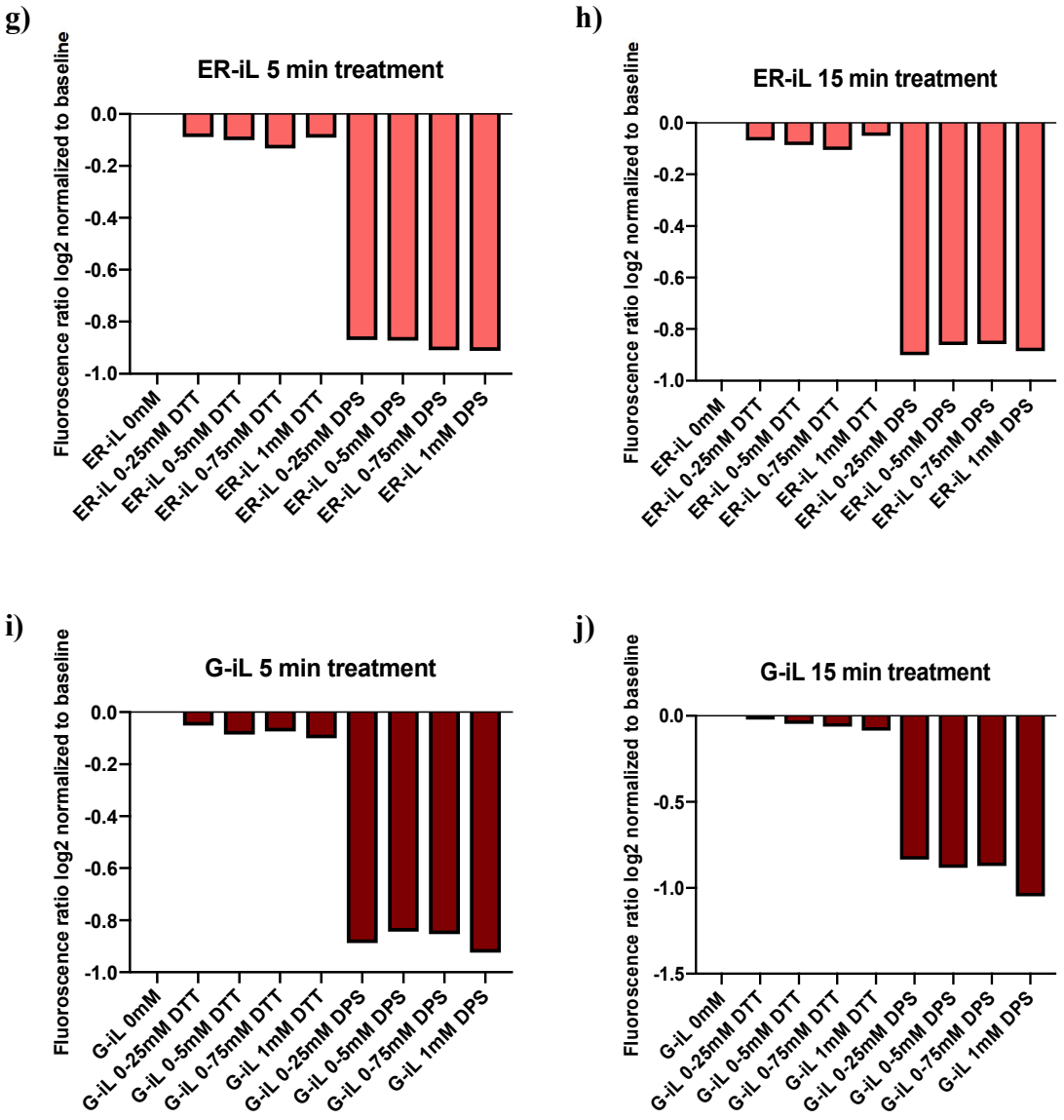

Figure 4-9: Measurement of fluorescence ratios in cells post-addition of DTT and DPS: (a) & (b) show the changes in fluorescence ratio after addition of DTT and DPS in the roGFP probe intended to measure changes in the cytosol; (c), (d), (e) & (f) show changes in the fluorescence ratio in roGFP-iE and; (g), (h), (i) & (j) show changes in fluorescence ratio in roGFP-iL. roGFP-iE exhibits a better detection range over roGFP-iL, with a log2 ratio above 0.1 with respect to the baseline.

4.4 Discussion

To investigate the redox status of ER and Golgi, redox sensitive GFPs, roGFP-iL and iE were targeted to the organelles of CHO EG2-hFc cells. The constructs were designed with targeting and retention signals ERp57, KDEL (ER) and β-1,4, GalT4 (Golgi). Co-localization studies confirmed the targeting to the intended organelles.

The next step was to monitor the changes in redox, ideally by using live cell imaging to visualize and detect real-time changes within the cellular compartments. This approach has been used previously in other studies such as in yeast and mammalian cells (Dooley et al., 2004; van Lith et al., 2011). In (van Lith et al., 2011) the roGFP-iL probe has been used to monitor redox state of ER by addition of redox buffers. They were able to detect minute changes with this probe by visualising the changes with real-time microscopy. With the studies conducted in this thesis, we were able to validate that the addition of reducing and oxidising agents did indeed induce the changes in redox status within the cells that were detected by the roGFP constructs. The flow cytometry method was applied was adapted from a study by Sarkar et al. (Sarkar et al., 2013) to conduct proof-of-concept studies to confirm that the intracellular probes were able to detect changes in the redox environment. This is evident from the changes in fluorescence ratios noted after addition of the reducing and oxidising agents seen in **Figure 4-9** and described in detail in 4.3.4. However, because the cells for the flow cytometry experiment were incubated in the redox buffers for 5 and 15 minutes and then passed through the cytometer, any changes that may have occurred within those time points would be undetectable. Also, to establish the highest concentration of DPS/DTT that could be used to induce a change, higher concentrations could be tested in addition to different time points, as

the changes detected, especially for DPS by roGFP-iE seems to increase with 1mM and could still have some range beyond this concentration.

The roGFP-iX constructs and other variants have been used previously in studies to detect changes in the cytosol, ER as well as mitochondria. Hanson *et al.* used the roGFP1 probe to investigate the mitochondrial redox state in HeLa cells by the addition of DTT and H_2O_2 (Hanson et al., 2004). They observed that the mitochondrial redox changes observed were quite similar in a population of cells when compared to the redox state of a single cell, implying that the redox changes observed in the experiments conducted here using flow cytometry may also hold true for real-time measurement of fluorescence in single cells.

Further work will be required to investigate the redox potential of the Golgi. Nonetheless, the data generated using the flow cytometry method as described in section 4.2.6 provide a proof-of-concept that the roGFP probes can be utilized to determine the redox status as also shown in (Sarkar et al., 2013), but in MAb producing cells in the context of this thesis. However, the method could not be used for visualizing real-time, the changing redox status within the individual cells. This would have provided a real-time measurement of the internal redox state in cells during production of the EG2 antibody in the cells at different time points. Changes due to addition of reducing and oxidising agents would also be observed. With the live cell imaging for single cells where changes in redox state can be visualized in each cell, the reduction potential could have been calculated using the following method as has been described previously (van Lith et al., 2011; Lohman and Remington, 2008):

$$R/(1-R) = (F - F_{ox})/(F_{red} - F)(I_{ox}/I_{red}) \quad \textit{Equation 4-1}$$

Where;

R = reduced fraction of the roGFP indicator in the sample

R/(1-R) = ratio of reduced over oxidised roGFP indicator

F = steady state fluorescence ratio of the untreated control sample

F_{ox} = oxidised state fluorescence ratio with addition of the oxidising agent

F_{red} = reduced state fluorescence ratio with addition of the reducing agent

I_{ox} = fluorescence intensity for oxidised state

I_{red} = fluorescence intensity for reduced state

In order to calculate the reduction potential *in vivo,* Nernst equation would then be used with RT/nF at 298 K. R= universal gas constant, T= absolute temperature, n= number of transferred electrons and F= Faraday constant. RT/nF has been calculated to be -29.6mV.

$$E^{\circ\prime} = E^{\circ\prime}_{roGFP} - 29.6\ mV\ log\ (R/1-R) \quad \textit{.....Equation 4-2}$$

where E°' = -229 mV for roGFPiL-KDEL and βGalT4-roGFPiL and – 236 mV for roGFPiE-KDEL and βGalT4-roGFPiE (Lohman and Remington, 2008).

With the real-time intracellular images, and further analysis of the stable pools at different time points during production of the EG2 antibody, the Golgi redox state could have been unravelled, which would have established the redox state required within the glycosylation machinery for the post-translational modifications. Every organelle involved in the pathway would hypothetically require a redox state for the glycosyltransferases to function. However, considering that the ER and Golgi are involved in the glycosylation pathway, it could be hypothesised that the redox homeostasis within both organelles is similar. This has also been supported in reviews by (Meyer and Dick, 2010; Samoylenko et al., 2013).

Redox status of the ER and Golgi during antibody production has not been determined previously. Considering that the protein folding as well as glycosylation pathways take place in the ER and Golgi, it is an important parameter for the formation of disulphide bonds within the antibody as well addition of glycans. It is well known that disulphide bond formation is affected by the redox state of the ER (Bulleid and Ellgaard, 2011; Oka and Bulleid, 2013). Previous studies in the Butler lab have also established that the redox potential and thus, redox state within cell culture is equally important for glycosylation (Dionne et al., 2017b). Thus, an insight into the internal redox potential of each individual organelle and its effect on antibody production would be useful in the manipulation of bioprocess parameters to maintain promote efficient protein folding and consistency of glycan profiles of the antibody. Another interesting approach would be to compare the redox state of plasma cells to CHO cells. Plasma cells secrete large quantities of antibodies naturally, whereas CHO cells have been derived and developed over the years to produce recombinant proteins. Differences between these cells can be utilized to further enhance the capability of CHO cells to increase titer as well as quality of protein produced.

5

Conclusion

Product quality attributes (PQA) including glycosylation have a major impact on the quality and efficacy of a biotherapeutic molecule. Glycosylation is known to affect protein folding, stability, immunogenicity to list a few. In particular, the efficacy which includes ADCC as well as CDC activity of a therapeutic antibody is affected by the fucosylation levels. Similarly, the quality of a biotherapeutic is affected by aberrant glycosylation patterns which could be brought about by differences in bioprocess parameters. Process optimization is required to be able to manufacture consistent products and thus, continuous improvements will be required in this field to be able to adhere to the PQA requirements established by regulatory agencies. In this thesis, efforts towards improving both efficacy and quality of a monoclonal antibody have been described.

Chapter 1 of the thesis gives an extensive introduction to the concepts that have been applied throughout course of the PhD. This also includes an introduction to each of the projects that have been further described in the following chapters. In Chapter 2, experiments that were carried out to improve the efficacy of CHO EG2-hFc have been detailed. The use of the fucosyltransferase inhibitor 2-fluoro peracetylated fucose (2FF) and the prokaryotic RMD gene results in CHO EG2-hFc cells results in defucosylated antibodies. Although neither of the methods led to completely afucosylated antibodies, a combination of both methods resulted in a decrease of fucosylation level to 3% of the glycan. Fucose addition to the cell culture media allowed for the fucosylation level to be reverted to the original level. For the 2FF experiments, the decrease in fucosylation was 17.5% whereas expression of RMD in the CHO EG2-hFc system reduced fucosylation to 16.1%. Both methods were efficient at reducing fucosylation

to comparable levels, and it may not be a requirement for fucosylation levels to reach 0% for high efficacy. In fact, some studies have shown polymorphonuclear cells exhibiting high ADCC activity with heavily fucosylated antibodies (Peipp et al., 2008).

There are other methods to decrease fucosylation. A recent study has used a mannosidase inhibitor Deoxymannojirimycin (DMJ) to generate defucosylated IgG1 in a CHO-DXB11 cell line, although the decrease was from 92% down to 73% (Shalel Levanon et al., 2018). Yet another study, used arabinosylation to replace fucose, which resulted nearly 100% defucosylated antibodies (Hossler et al., 2017b). Other methods include using gene editing technologies such as Zinc Finger Nuclease (Malphettes et al., 2010b) and CRISPR-Cas9 (Ronda et al., 2014) to knock-out the FUT8 gene and thus, generate non-fucosylated products. The advantage of using such technologies is that it would result in targeted biallelic knockouts and could be established as cell lines that can be used for generating multiple MAbs. These could be further used to design MAbs according to therapeutic requirements of various diseases (Schulz et al., 2018). However, currently, due to patent restrictions gene editing can be used only for research and development. Thus, a viable option could still be to use an inhibitor such as 2FF or DMJ for production of defucosylated MAbs for therapeutic applications.

Chapter 3 describes a non-radioactive method to detect ADCC rather than using the conventional radioactive Chromium-51 assay. Although the optimization assays with LDH and NK-92 variants worked, there were issues with measuring cytotoxicity levels with the different variations of EG2-hFc antibody. This could be attributed to factors including batch-to-batch variation of the LDH assay itself or the potency of the antibody variants being tested. However, scope still remains for the assay to be optimized further. The LDH assay could be tested with PBMCs rather than the NK-92 engineered cells as a change in the type of effector cells used

may be the core issue. Some previous studies have shown that with PBMCs, highly fucosylated antibodies may exhibit high ADCC activity (Peipp et al., 2008) and that the choice of effector cells has to be carefully considered. Conventionally, PBMCs have always been used for cytotoxicity assays since they consist of a population of different lymphocytes and monocytes. A high cytotoxicity level could be due to a combination effect of both the PBMCs and type of antibody used. However, the assay requires more optimization to be able to establish it as a standard for measuring the ADCC of an antibody. For future work, it would be ideal to test different combinations of assays, effector as well as target cells along with variants of an antibody. To further assess the sensitivity of the LDH-based assay, PBMCs derived from donors could be used and the result compared to ^{51}Cr release assay. More controls such as a different IgG1 anti-EGFR antibody like Panitumumab (García-Foncillas et al., 2019) could be used to investigate whether the cytotoxicity induced is specific to Cetuximab or if it could be applied to other IgG1 antibodies

Apart from the efficacy of a therapeutic antibody, the consistent glycan profile and thus, the quality of a MAb during the manufacturing process is also critical. In Chapter 4, attempts were made to elucidate the redox status of the intracellular machinery involved in glycosylation to identify changes occurring in the homeostasis of the cells during antibody production. This could help identify the importance of redox status and lead to improvements in process development. The idea behind this work was to visualize the changes within cells occurring within the cells while production of the said antibody takes place. It is now known that the redox status of Golgi as well as pH levels are important for glycosyltransferases (Kellokumpu, 2019) to function as well as for general maintenance of the Golgi. A recent study has highlighted that a change in the levels of oxygen, namely hypoxia, leads to decreased terminal sialylation of glycans (Hassinen et al., 2019). Terminal sialylation is important for protein

secretion and function and this particular study has also shown that the sialyltransferase ST6Gal is sensitive to hypoxia and is non-functional in these conditions whereas the galactosyltransferase ßGALT4-I which is responsible for addition of terminal galactose residues is not affected. The N-glycosylation pathway is a complex network of multiple enzymes working simultaneously and a change in a particular enzyme activity may potentially affect another step in the pathway. Although a first step towards investigating the redox state of the CHO EG2-hFc cells was successful by testing the roGFP probes in changing redox states by flow cytometry, the real-time visualization of cells was not done due to the unavailability of equipment. Redox status of the ER and Golgi during antibody production has not been determined previously. Considering that the protein folding as well as glycosylation pathways take place in the ER and Golgi, it is an important parameter for the formation of disulphide bonds within the antibody as well addition of glycans. It is well known that disulphide bond formation is affected by the redox state of the ER (Bulleid and Ellgaard, 2011; Oka and Bulleid, 2013). Previous studies in the Butler lab have also established that the redox potential and thus, redox state within cell culture is equally important for glycosylation (Dionne et al., 2017b). Thus, an insight into the internal redox potential of each individual organelle and its effect on antibody production would be useful in the manipulation of bioprocess parameters to maintain promote efficient protein folding and consistency of glycan profiles of the antibody.

Glycosylation is a vast area of focus and improvements to control/improve glycosylation in MAb manufacturing are manifold. Apart from fucosylation, which has an effect on ADCC and CDC, controlling levels of sialylation has a major impact on half-lives of MAbs, on safety and immunogenicity and is a much sought after option (Z. Wang et al., 2020). There is potential to improve the glycosylation pathway of CHO cells to make better therapeutics by making use of next-generation genome editing tools such as CRISPR-Cas9 (Ronda et al., 2014). However,

it remains to be seen whether these tools could be accepted by the regulatory agencies to manufacture biotherapeutics. A different approach would be to apply modelling of glycosylation pathways by including bioprocess parameters to predict the conditions that would result in a desired glycan profile (Majewska et al., 2020). Mathematical modelling has been used previously to define cell metabolic processes ((Nolan and K. Lee, 2011)) as well as N-linked glycosylation ((Spahn et al., 2015)). This may potentially avoid undesirable off-target effects such as effects on cell health and quality. (Kotidis et al., 2019) have advanced the strategy further by combining experimental data and computational methods to improve feeding strategies, specifically that of galactose and uridine. They introduced experimental data to the computational method and designed an experiment which was then confirmed by performing the experiment to get the desired results. This lays the foundation for applying machine learning/in silico methods for glycosylation modelling to improve bioprocesses.

The work described in this thesis is an attempt at uncovering some aspects of N-linked glycosylation in CHO cells in the context of MAbs and contribute to the development of this field.

6

References

Aebi, M., 2013. Biochimica et Biophysica Acta. BBA - Molecular Cell Research 1833, 2430–2437. doi:10.1016/j.bbamcr.2013.04.001

Agrawal, V., Slivac, I., Perret, S., Bisson, L., St-Laurent, G., Murad, Y., Zhang, J., Durocher, Y., 2012. Stable expression of chimeric heavy chain antibodies in cho cells, in: single domain antibodies. Humana Press, Totowa, NJ, pp. 287–303. doi:10.1007/978-1-61779-968-6_18

Ayyar, B.V., Arora, S., O'Kennedy, R., 2016. Coming-of-age of antibodies in cancer therapeutics. Trends in Pharmacological Sciences 37, 1009–1028. doi:10.1016/j.tips.2016.09.005

Baker, K.M., Chakravarthi, S., Langton, K.P., Sheppard, A.M., Lu, H., Bulleid, N.J., 2008. Low reduction potential of Ero1alpha regulatory disulphides ensures tight control of substrate oxidation. The EMBO Journal 27, 2988–2997. doi:10.1038/emboj.2008.230

Bas, M., Terrier, A., Jacque, E., Dehenne, A., Pochet-Béghin, V., Beghin, C., Dezetter, A.-S., Dupont, G., Engrand, A., Beaufils, B., Mondon, P., Fournier, N., de Romeuf, C., Jorieux, S., Fontayne, A., Mars, L.T., Monnet, C., 2019. Fc sialylation prolongs serum half-life of therapeutic antibodies. The Journal of Immunology 202, 1582–1594. doi:10.4049/jimmunol.1800896

Becker, D.J., Lowe, J.B., 2003. Fucose: biosynthesis and biological function in mammals. Glycobiology 13, 41R–53R. doi:10.1093/glycob/cwg054

Bell, A., Wang, Z.J., Arbabi-Ghahroudi, M., Chang, T.A., Durocher, Y., Trojahn, U., Baardsnes, J., Jaramillo, M.L., Li, S., Baral, T.N., O'Connor-McCourt, M., MacKenzie, R., Zhang, J., 2010. Cancer Letters. Cancer Letters 289, 81–90. doi:10.1016/j.canlet.2009.08.003

Binyamin, L., Alpaugh, R.K., Hughes, T.L., Lutz, C.T., Campbell, K.S., Weiner, L.M., 2008. Blocking NK cell inhibitory self-recognition promotes antibody-dependent cellular cytotoxicity in a model of anti-lymphoma therapy. J. Immunol. 180, 6392–6401.

Braakman, I., Bulleid, N.J., 2011. Protein folding and modification in the mammalian endoplasmic reticulum. Annu. Rev. Biochem. 80, 71–99. doi:10.1146/annurev-biochem-062209-093836

Broussas, M., Broyer, L., Goetsch, L., 2013. Evaluation of antibody-dependent cell cytotoxicity using lactate dehydrogenase (LDH) measurement. Methods Mol. Biol. 988, 305–317. doi:10.1007/978-1-62703-327-5_19

Bryan, G.J., Kong, N.S., 2018. Impact of host cell line choice on glycan profile. Critical Reviews in Biotechnology 38, 851–867. doi:10.1080/07388551.2017.1416577

Bulleid, N.J., Ellgaard, L., 2011. Multiple ways to make disulfides. Trends in Biochemical Sciences 36, 485–492. doi:10.1016/j.tibs.2011.05.004

Butler, M., 2005. Animal cell cultures: recent achievements and perspectives in the production of biopharmaceuticals. Appl Microbiol Biotechnol 68, 283–291. doi:10.1007/s00253-005-1980-8

Butler, M., Reichl, U., 2017. Animal cell expression systems. Adv. Biochem. Eng. Biotechnol. 3, 568–36. doi:10.1007/10_2017_31

Butler, M., Spearman, M., 2014. ScienceDirect The choice of mammalian cell host and possibilities for glycosylation engineering. Curr. Opin. Biotechnol. 30, 107–112. doi:10.1016/j.copbio.2014.06.010

Cannon, M.B., James Remington, S., 2008. Redox-sensitive green fluorescent protein: probes for dynamic intracellular redox responses. A Review, in: Voynov, V., Caravella, J.A. (Eds.), Therapeutic Proteins, Methods in Molecular Biology™. Humana Press, Totowa, NJ, pp. 50–64. doi:10.1007/978-1-59745-129-1_4

Chakravarthi, S., Bulleid, N.J., 2004. Glutathione is required to regulate the formation of native disulfide bonds within proteins entering the secretory pathway. Journal of Biological Chemistry 279, 39872–39879. doi:10.1074/jbc.M406912200

Chakravarthi, S., Jessop, C.E., Bulleid, N.J., 2006. The role of glutathione in disulphide bond formation and endoplasmic-reticulum-generated oxidative stress. EMBO Rep 7, 271–275. doi:10.1038/sj.embor.7400645

Chames, P., Van Regenmortel, M., Weiss, E., Baty, D., 2009. Therapeutic antibodies: successes, limitations and hopes for the future. British Journal of Pharmacology 157, 220–233. doi:10.1111/j.1476-5381.2009.00190.x

Cheng, Z.J., Garvin, D., Paguio, A., Moravec, R., Engel, L., Fan, F., Surowy, T., 2014. Development of a robust reporter-based ADCC assay with frozen, thaw-and-use cells to measure Fc effector function of therapeutic antibodies. J. Immunol. Methods 414, 69–81. doi:10.1016/j.jim.2014.07.010

Chung, J., 2017. Special issue on therapeutic antibodies and biopharmaceuticals. Exp. Mol. Med. 49, e304–e304. doi:10.1038/emm.2017.46

Cuesta, Ã.N.M., Sainz-Pastor, N., Bonet, J., Oliva, B., lvarez-Vallina, L.Ã., 2010. Multivalent antibodies: when design surpasses evolution. Trends in Biotechnology 28, 355–362. doi:10.1016/j.tibtech.2010.03.007

Cymer, F., Beck, H., Rohde, A., Reusch, D., 2018. Therapeutic monoclonal antibody N-glycosylation - Structure, function and therapeutic potential. Biologicals 52, 1–11. doi:10.1016/j.biologicals.2017.11.001

D'Eall, C., Pon, R.A., Rossotti, M.A., Krahn, N., Spearman, M., Callaghan, D., van Faassen, H., Hussack, G., Stetefeld, J., Butler, M., Durocher, Y., Zhang, J., Henry, K.A., Tanha, J., 2019. Modulating antibody-dependent cellular cytotoxicity of epidermal growth factor receptor-specific heavy-chain antibodies through hinge engineering. Immunol Cell Biol 97, 526–537. doi:10.1111/imcb.12238

da Cunha Santos, G., Shepherd, F.A., Tsao, M.S., 2011. EGFR mutations and lung cancer. Annu Rev Pathol 6, 49–69. doi:10.1146/annurev-pathol-011110-130206

Davies, J., Jiang, L., Pan, L.Z., LaBarre, M.J., Anderson, D., Reff, M., 2001. Expression of GnTIII in a recombinant anti-CD20 CHO production cell line: Expression of antibodies with altered glycoforms leads to an increase in ADCC through higher affinity for FC gamma RIII. Biotechnol. Bioeng. 74, 288–294.

Dekkers, G., Plomp, R., Koeleman, C.A.M., Visser, R., Horsten, von, H.H., Sandig, V., Rispens, T., Wuhrer, M., Vidarsson, G., 2016. Multi-level glyco-engineering techniques to generate IgG with defined Fc-glycans. Sci. Rep. 1–12. doi:10.1038/srep36964

Delic, M., Mattanovich, D., Gasser, B., 2010. Monitoring intracellular redox conditions in the endoplasmic reticulum of living yeasts. FEMS Microbiology Letters 306, 61–66. doi:10.1111/j.1574-6968.2010.01935.x

Dionne, B., Mishra, N., Butler, M., 2017a. A low redox potential affects monoclonal antibody assembly and glycosylation in cell culture. Journal of Biotechnology 246, 71–80. doi:10.1016/j.jbiotec.2017.01.016

Donald, L., Duckworth, H., Standing, K., Gevaert, K., 2006. Mass spectrometry in noncovalent protein interactions and protein assemblies, Cell Biology. Elsevier. doi:10.1016/b978-012164730-8/50243-4

Dooley, C.T., Dore, T.M., Hanson, G.T., Jackson, W.C., Remington, S.J., Tsien, R.Y., 2004. Imaging dynamic redox changes in mammalian cells with green fluorescent protein

indicators. Journal of Biological Chemistry 279, 22284–22293. doi:10.1074/jbc.M312847200

Ecker, D.M., Jones, S.D., Levine, H.L., 2015. The therapeutic monoclonal antibody market. mabs 7, 9–14. doi:10.4161/19420862.2015.989042

Elgundi, Z., Reslan, M., Cruz, E., Sifniotis, V., Kayser, V., 2017. The state-of-play and future of antibody therapeutics. Advanced Drug Delivery Reviews 122, 2–19. doi:10.1016/j.addr.2016.11.004

Ellgaard, L., Sevier, C.S., Bulleid, N.J., 2018. How are proteins reduced in the endoplasmic reticulum? Trends in Biochemical Sciences 43, 32–43. doi:10.1016/j.tibs.2017.10.006

Freeze, H.H., 2002. Sweet solution: sugars to the rescue. J Cell Biol 158, 615–616. doi:10.1083/jcb.200207155

García-Foncillas, J., Sunakawa, Y., Aderka, D., Wainberg, Z., Ronga, P., Witzler, P., Stintzing, S., 2019. Distinguishing features of cetuximab and panitumumab in colorectal cancer and other solid tumors. Front. Oncol. 9, 539–16. doi:10.3389/fonc.2019.00849

Gawlitzek, M., Ryll, T., Lofgren, J., Sliwkowski, M.B., 2000. Ammonium alters N-glycan structures of recombinant TNFR-IgG: degradative versus biosynthetic mechanisms. Biotechnol. Bioeng. 68, 637–646.

Gessner, J.E., Heiken, H., Tamm, A., Schmidt, R.E., 1998. The IgG Fc receptor family. Ann Hematol 76, 231–248.

Goh, J.B., Ng, S.K., 2017. Impact of host cell line choice on glycan profile. Critical Reviews in Biotechnology 38, 851–867. doi:10.1080/07388551.2017.1416577

González-González, E., Camacho-Sandoval, R., Jiménez-Uribe, A., Montes-Luna, A., Cortés-Paniagua, I., Sánchez-Morales, J., Muñoz-García, L., Tenorio-Calvo, A.V., López-Morales, C.A., Velasco-Velázquez, M.A., Pavón, L., Pérez-Tapia, S.M., Medina-Rivero, E., 2019. Validation of an ADCC assay using human primary natural killer cells to evaluate

biotherapeutic products bearing an Fc region. J. Immunol. Methods 464, 87–94. doi:10.1016/j.jim.2018.11.002

Ha, T.K., Kim, Y.-G., Lee, G.M., 2015. Understanding of altered N-glycosylation-related gene expression in recombinant Chinese hamster ovary cells subjected to elevated ammonium concentration by digital mRNA counting. Biotechnol. Bioeng. n/a–n/a. doi:10.1002/bit.25568

Hassinen, A., Khoder-Agha, F., Khosrowabadi, E., Mennerich, D., Harrus, D., Noel, M., Dimova, E.Y., Glumoff, T., Harduin-Lepers, A., Kietzmann, T., Kellokumpu, S., 2019. A Golgi-associated redox switch regulates catalytic activation and cooperative functioning of ST6Gal-I with B4GalT-I. Redox Biology 24, 101182–13. doi:10.1016/j.redox.2019.101182

Hink, M.A., Griep, R.A., Borst, J.W., van Hoek, A., Eppink, M.H.M., Schots, A., Visser, A.J.W.G., 2000. Structural dynamics of green fluorescent protein alone and fused with a single chain Fv protein. Journal of Biological Chemistry 275, 17556–17560. doi:10.1074/jbc.M001348200

Hmiel, L.K., Brorson, K.A., Boyne, M.T., 2014. Post-translational structural modifications of immunoglobulin G and their effect on biological activity. Anal Bioanal Chem 407, 79–94. doi:10.1007/s00216-014-8108-x

Horsten, von, H.H., Ogorek, C., Blanchard, V., Demmler, C., Giese, C., Winkler, K., Kaup, M., Berger, M., Jordan, I., Sandig, V., 2010. Production of non-fucosylated antibodies by co-expression of heterologous GDP-6-deoxy-D-lyxo-4-hexulose reductase. Glycobiology 20, 1607–1618. doi:10.1093/glycob/cwq109

Hossler, P., Chumsae, C., Racicot, C., Ouellette, D., Ibraghimov, A., Serna, D., Mora, A., McDermott, S., Labkovsky, B., Scesney, S., Grinnell, C., Preston, G., Bose, S., Carrillo,

R., 2017a. Arabinosylation of recombinant human immunoglobulin-based protein therapeutics. mAbs 0, 1–20. doi:10.1080/19420862.2017.1294295

Jayapal, K.P., Wlaschin, K.F., Hu, W., Yap, M.G., 2007. Recombinant protein therapeutics from CHO cells-20 years and counting. Chemical Engineering Progress 103, 40.

Jefferis, R., 2009a. Glycosylation as a strategy to improve antibody-based therapeutics. Nat Rev Drug Discov 8, 226–234. doi:10.1038/nrd2804

Jefferis, R., 2009b. Glycosylation as a strategy to improve antibody-based therapeutics. Nat Rev Drug Discov 8, 226–234. doi:10.1038/nrd2804

Jefferis, R., 2009c. Glycosylation as a strategy to improve antibody-based therapeutics. Nat Rev Drug Discov 8, 226–234. doi:10.1038/nrd2804

Jefferis, R., 2007. Antibody therapeutics:Expert Opinion on Biological Therapy 7, 1401–1413. doi:10.1517/14712598.7.9.1401

Jefferis, R., 2005. Glycosylation of natural and recombinant antibody molecules. Adv. Exp. Med. Biol. 564, 143–148. doi:10.1007/0-387-25515-X_26

Jungbauer, A., Graumann, K., 2012. Biopharmaceuticals -- discovery, development and manufacturing. Biotechnol J 7, 1422–1423. doi:10.1002/biot.201200360

Kain, S.R., Adams, M., Kondepudi, A., Yang, T.T., Ward, W.W., Kitts, P., 1995. Green fluorescent protein as a reporter of gene expression and protein localization. Biotech. 19, 650–655.

Kang, S., Zhang, Z., Richardson, J., Shah, B., Gupta, S., Huang, C.-J., Qiu, J., Le, N., Lin, H., Bondarenko, P.V., 2015. Journal of Biotechnology 203, 1–10. doi:10.1016/j.jbiotec.2015.03.002

Kaplon, H., Reichert, J.M., 2018. Antibodies to watch in 2018. mabs 10, 183–203. doi:10.1080/19420862.2018.1415671

Kapur, R., Einarsdottir, H.K., Vidarsson, G., 2014. IgG-effector functions: “The Good, The Bad and The Ugly.” Immunology Letters 160, 139–144. doi:10.1016/j.imlet.2014.01.015

Kellokumpu, S., 2019. Golgi pH, ion and redox homeostasis: how much do they really matter? fcell-07-00093.tex 1–15. doi:10.3389/fcell.2019.00093

Kim, J.Y., Kim, Y.-G., Lee, G.M., 2011. CHO cells in biotechnology for production of recombinant proteins: current state and further potential. Appl Microbiol Biotechnol 93, 917–930. doi:10.1007/s00253-011-3758-5

Kotidis, P., Jedrzejewski, P., Sou, S.N., Sellick, C., Polizzi, K., del Val, I.J., Kontoravdi, C., 2019. Model-based optimization of antibody galactosylation in CHO cell culture. Biotechnol. Bioeng. 116, 1612–1626. doi:10.1002/bit.26960

Kozlovski, V.I., Donald, L.J., Collado, V.M., Spicer, V., Loboda, A.V., Chernushevich, I.V., Ens, W., Standing, K.G., 2011. A TOF mass spectrometer for the study of noncovalent complexes. International Journal of Mass Spectrometry 308, 118–125. doi:https://doi.org/10.1016/j.ijms.2011.08.009

Köhler, G., Milstein, C., 1975. Continuous cultures of fused cells secreting antibody of predefined specificity. Nature 256, 495–497. doi:10.1038/256495a0

Krapp, S., Mimura, Y., Jefferis, R., Huber, R., Sondermann, P., 2003. Structural analysis of human IgG-Fc glycoforms reveals a correlation between glycosylation and structural integrity. Journal of Molecular Biology 325, 979–989. doi:10.1016/S0022-2836(02)01250-0

Kremers, G.J., Gilbert, S.G., Cranfill, P.J., Davidson, M.W., Piston, D.W., 2011. Fluorescent proteins at a glance. Journal of Cell Science 124, 2676–2676. doi:10.1242/jcs.095059

Kunkel, J.P., Jan, D.C., Jamieson, J.C., Butler, M., 1998. Dissolved oxygen concentration in serum-free continuous culture affects N-linked glycosylation of a monoclonal antibody. Journal of Biotechnology 62, 55–71.

Lalonde, M.-E., Durocher, Y., 2017. Therapeutic glycoprotein production in mammalian cells. Journal of Biotechnology 251, 128–140. doi:10.1016/j.jbiotec.2017.04.028

Leatherbarrow, R.J., Rademacher, T.W., Dwek, R.A., Woof, J.M., Clark, A., Burton, D.R., Richardson, N., Feinstein, A., 1985. Effector functions of a monoclonal aglycosylated mouse IgG2a: binding and activation of complement component C1 and interaction with human monocyte Fc receptor. Molecular Immunology 22, 407–415.

Leavy, O., 2010. Therapeutic antibodies: past, presentand future. Nature Publishing Group 10, 297–297. doi:10.1038/nri2763

Lee, Y.-K., Brewer, J.W., Hellman, R., Hendershot, L.M., 1999. BiP and immunoglobulin light chain cooperate to control the folding of heavy chain and ensure the fidelity of immunoglobulin assembly. Molecular Biology of the Cell 10, 2209–2219. doi:10.1091/mbc.10.7.2209

Lewis, N.E., Liu, X., Li, Y., Nagarajan, H., Yerganian, G., O'Brien, E., Bordbar, A., Roth, A.M., Rosenbloom, J., Bian, C., Xie, M., Chen, W., Li, N., Baycin-Hizal, D., Latif, H., Forster, J., Betenbaugh, M.J., Famili, I., Xu, X., Wang, J., Palsson, B.O., 2013. Genomic landscapes of Chinese hamster ovary cell lines as revealed by the Cricetulus griseus draft genome. Nat. Biotechnol. 31, 759–765. doi:10.1038/nbt.2624

Li, F., Vijayasankaran, N., Shen, A.Y., Kiss, R., Amanullah, A., 2010. Cell culture processes for monoclonal antibody production. mabs 2, 466–479. doi:10.4161/mabs.2.5.12720

Li, W., Zhu, Z., Chen, W., Feng, Y., Dimitrov, D.S., 2017. Crystallizable fragment glycoengineering for therapeutic antibodies development. Front. Immunol. 8, 83–15. doi:10.3389/fimmu.2017.01554

Llopis, J., McCaffery, J.M., Miyawaki, A., Farquhar, M.G., Tsien, R.Y., n.d. Measurement of cytosolic, mitochondrial, and Golgi pH in single living cells with green fluorescent proteins.

Lohman, J.R., Remington, S.J., 2008. Development of a family of redox-sensitive green fluorescent protein indicators for use in relatively oxidizing subcellular environments †‡. Biochemistry 47, 8678–8688. doi:10.1021/bi800498g

Majewska, N.I., Tejada, M.L., Betenbaugh, M.J., Agarwal, N., 2020. N-glycosylation of IgG and IgG-like recombinant therapeutic proteins: why is it important and how can we control it? Annu. Rev. Chem. Biomol. Eng. 11, 311–338. doi:10.1146/annurev-chembioeng-102419-010001

Malphettes, L., Freyvert, Y., Chang, J., Liu, P.-Q., Chan, E., Miller, J.C., Zhou, Z., Nguyen, T., Tsai, C., Snowden, A.W., Collingwood, T.N., Gregory, P.D., Cost, G.J., 2010a. Highly efficient deletion of FUT8 in CHO cell lines using zinc-finger nucleases yields cells that produce completely nonfucosylated antibodies. Biotechnol. Bioeng. 106, 774–783. doi:10.1002/bit.22751

Martinelli, E., De Palma, R., Orditura, M., De Vita, F., Ciardiello, F., 2009. Anti-epidermal growth factor receptor monoclonal antibodies in cancer therapy. Clinical & Experimental Immunology 158, 1–9.

Mastrangeli, R., Palinsky, W., Bierau, H., 2018. Glycoengineered antibodies: towards the next-generation of immunotherapeutics. Glycobiology 105, 15005–12. doi:10.1093/glycob/cwy092

Meneses-Acosta, A., Gómez, A., Ramírez, O.T., 2012a. Control of redox potential in hybridoma cultures: effects on MAb production, metabolism, and apoptosis. J Ind Microbiol Biotechnol 39, 1189–1198. doi:10.1007/s10295-012-1125-x

Meneses-Acosta, A., Gómez, A., Ramírez, O.T., 2012b. Control of redox potential in hybridoma cultures: effects on MAb production, metabolism, and apoptosis. J Ind Microbiol Biotechnol 39, 1189–1198. doi:10.1007/s10295-012-1125-x

Mimura, Y., Sondermann, P., Ghirlando, R., Lund, J., Young, S.P., Goodall, M., Jefferis, R., 2001. Role of oligosaccharide residues of IgG1-Fc in Fc RIIb binding. Journal of Biological Chemistry 276, 45539–45547. doi:10.1074/jbc.M107478200

Mishra, N., Spearman, M., Donald, L., Perreault, H., Butler, M., 2020. Comparison of two glycoengineering strategies to control the fucosylation of a monoclonal antibody. Journal of Biotechnology: X 5, 100015. doi:10.1016/j.btecx.2020.100015

Morell, A.G., Gregoriadis, G., Scheinberg, I.H., Hickman, J., Ashwell, G., 1971. The role of sialic acid in determining the survival of glycoproteins in the circulation. Journal of Biological Chemistry 246, 1461–1467.

Muthing, J., Kemminer, S.E., Conradt, H.S., Sagi, D., Nimtz, M., Karst, U., Peter-Katalinic, J., 2003. Effects of buffering conditions and culture pH on production rates and glycosylation of clinical phase I anti-melanoma mouse IgG3 monoclonal antibody R24. Biotechnol. Bioeng. 83, 321–334. doi:10.1002/bit.10673

Neves, H., Kwok, H.F., 2015. Recent advances in the field of anti-cancer immunotherapy. BBA Clin 3, 280–288. doi:10.1016/j.bbacli.2015.04.001

Ng, B.G., Xu, G., Chandy, N., Steyermark, J., Shinde, D.N., Radtke, K., Raymond, K., Lebrilla, C.B., AlAsmari, A., Suchy, S.F., Powis, Z., Faqeih, E.A., Berry, S.A., Kronn, D.F., Freeze, H.H., 2018. Biallelic mutations in FUT8 cause a congenital disorder of glycosylation with defective fucosylation. The American Journal of Human Genetics 102, 188–195.

Nolan, R.P., Lee, K., 2011. Dynamic model of CHO cell metabolism. Metabolic Engineering 13, 108–124. doi:10.1016/j.ymben.2010.09.003

Oka, O.B.V., Bulleid, N.J., 2013. Forming disulfides in the endoplasmic reticulum. Biochimica et Biophysica Acta (BBA) - Molecular Cell Research 1833, 2425–2429. doi:10.1016/j.bbamcr.2013.02.007

Onitsuka, M., Kim, W.-D., Ozaki, H., Kawaguchi, A., Honda, K., Kajiura, H., Fujiyama, K., Asano, R., Kumagai, I., Ohtake, H., Omasa, T., 2011. Enhancement of sialylation on humanized IgG-like bispecific antibody by overexpression of α2,6-sialyltransferase derived from Chinese hamster ovary cells. Appl Microbiol Biotechnol 94, 69–80. doi:10.1007/s00253-011-3814-1

Owen, J.A., Stranford, J.P.A.S.A., 2013. Kuby Immunology 1–832.

Peipp, M., Lammerts van Bueren, J.J., Schneider-Merck, T., Bleeker, W.W.K., Dechant, M., Beyer, T., Repp, R., van Berkel, P.H.C., Vink, T., van de Winkel, J.G.J., Parren, P.W.H.I., Valerius, T., 2008. Antibody fucosylation differentially impacts cytotoxicity mediated by NK and PMN effector cells. Blood 112, 2390–2399. doi:10.1182/blood-2008-03-144600

Puck, T.T., 1958. Genetics of somatic mammalian cells: iii. long-term cultivation of euploid cells from human and animal subjects. Journal of Experimental Medicine 108, 945–956. doi:10.1084/jem.108.6.945

Raju, S., 2003. Glycosylation variations with expression systems. BioProcess International 44–53.

Raju, T.S., Briggs, J.B., Borge, S.M., Jones, A.J., 2000. Species-specific variation in glycosylation of IgG: evidence for the species-specific sialylation and branch-specific galactosylation and importance for engineering recombinant glycoprotein therapeutics. Glycobiology 10, 477–486.

Ravetch, J.V., Bolland, S., 2001. IgG fc receptors. Annu. Rev. Immunol. 19, 275–290.

Raymond, C., Robotham, A., Spearman, M., Butler, M., Kelly, J., Durocher, Y., 2015. Production of α2,6-sialylated IgG1 in CHO cells. mabs 7, 0–583. doi:10.1080/19420862.2015.1029215

Rillahan, C.D., Antonopoulos, A., Lefort, C.T., Sonon, R., Azadi, P., Ley, K., Dell, A., Haslam, S.M., Paulson, J.C., 2012. Global metabolic inhibitors of sialyl- and fucosyltransferases remodel the glycome. Nature Chemical Biology 8, 662–669. doi:10.1038/nchembio.999

Román, V., Murray, J.C., Weiner, L.M., 2013. Antibody Fc: Chapter 1. Antibody-Dependent Cellular Cytotoxicity (ADCC).

Ronda, C., Pedersen, L.E., Hansen, H.G., Kallehauge, T.B., Betenbaugh, M.J., Nielsen, A.T., Kildegaard, H.F., 2014. Accelerating genome editing in CHO cells using CRISPR Cas9 and CRISPy, a web-based target finding tool. Biotechnol. Bioeng. 111, 1604–1616. doi:10.1002/bit.25233

Rueden, C.T., Schindelin, J., Hiner, M.C., DeZonia, B.E., Walter, A.E., Arena, E.T., Eliceiri, K.W., 2017. ImageJ2: ImageJ for the next generation of scientific image data. BMC Bioinformatics 18, 529–26. doi:10.1186/s12859-017-1934-z

Sarkar, D.D., Edwards, S.K., Mauser, J.A., Suarez, A.M., Serowoky, M.A., Hudok, N.L., Hudok, P.L., Nuñez, M., Weber, C.S., Lynch, R.M., Miyashita, O., Tsao, T.-S., 2013. Increased redox-sensitive green fluorescent protein reduction potential in the endoplasmic reticulum following glutathione-mediated dimerization. Biochemistry 52, 3332–3345. doi:10.1021/bi400052u

Sburlati, A.R., Umaña, P., Prati, E.G., Bailey, J.E., 1998. Synthesis of bisected glycoforms of recombinant IFN-beta by overexpression of beta-1,4-N-acetylglucosaminyltransferase III in Chinese hamster ovary cells. Biotechnol Progress 14, 189–192. doi:10.1021/bp970118s

Scallon, B.J., Tam, S.H., McCarthy, S.G., Cai, A.N., Raju, T.S., 2007. Higher levels of sialylated Fc glycans in immunoglobulin G molecules can adversely impact functionality. Molecular Immunology 44, 1524–1534. doi:10.1016/j.molimm.2006.09.005

Schroeder, H.W., Cavacini, L., 2010. Structure and function of immunoglobulins. J. Allergy Clin. Immunol. 125, S41–52. doi:10.1016/j.jaci.2009.09.046

Schulz, M.A., Tian, W., Mao, Y., Van Coillie, J., Sun, L., Larsen, J.S., Chen, Y.-H., Kristensen, C., Vakhrushev, S.Y., Clausen, H., Yang, Z., 2018. Glycoengineering design options for IgG1 in CHO cells using precise gene editing. Glycobiology. doi:10.1093/glycob/cwy022

Shalel Levanon, S., Aharonovitz, O., Maor-Shoshani, A., Abraham, G., Kenett, D., Aloni, Y., 2018. An efficient method to control high mannose and core fucose levels in glycosylated antibody production using deoxymannojirimycin. Journal of Biotechnology 276-277, 54–62. doi:10.1016/j.jbiotec.2018.04.006

Shields, R.L., Lai, J., Keck, R., O'Connell, L.Y., Hong, K., Meng, Y.G., Weikert, S.H.A., Presta, L.G., 2002. Lack of fucose on human IgG1 N-linked oligosaccharide improves binding to human Fcgamma RIII and antibody-dependent cellular toxicity. Journal of Biological Chemistry 277, 26733–26740. doi:10.1074/jbc.M202069200

Shinkawa, T., Nakamura, K., Yamane, N., Shoji-Hosaka, E., Kanda, Y., Sakurada, M., Uchida, K., Anazawa, H., Satoh, M., Yamasaki, M., Hanai, N., Shitara, K., 2003. The absence of fucose but not the presence of galactose or bisecting n-acetylglucosamine of human igg1 complex-type oligosaccharides shows the critical role of enhancing antibody-dependent cellular cytotoxicity. Journal of Biological Chemistry 278, 3466–3473. doi:10.1074/jbc.M210665200

Singh, S., Kumar, N.K., Dwiwedi, P., Charan, J., Kaur, R., Sidhu, P., Chugh, V.K., 2018. Monoclonal Antibodies: A Review. CCP 13, 85–99. doi:10.2174/1574884712666170809124728

Spahn, P.N., Hansen, A.H., Hansen, H.G., Arnsdorf, J., Kildegaard, H.F., Lewis, N.E., 2015. A Markov chain model for N-linked protein glycosylation – towards a low-parameter tool for model-driven glycoengineering. Metabolic Engineering 33, 1–35. doi:10.1016/j.ymben.2015.10.007

Spearman, M., Dionne, B., Butler, M., 2011. The role of glycosylation in therapeutic antibodies, in: Al-Rubeai, M. (Ed.), Cell Line Development, Cell Engineering. Springer Netherlands, Dordrecht, pp. 251–292. doi:10.1007/978-94-007-1257-7_12

Spiegelberg, H.L., Fishkin, B.G., 1972. The catabolism of human G immunoglobulins of different heavy chain subclasses. 3. The catabolism of heavy chain disease proteins and of Fc fragments of myeloma proteins. Clinical & Experimental Immunology 10, 599–607.

Spiess, C., Zhai, Q., Carter, P.J., 2015. Alternative molecular formats and therapeutic applications for bispecific antibodies. Molecular Immunology 67, 95–106. doi:10.1016/j.molimm.2015.01.003

Stadlmann, J., Pabst, M., Altmann, F., 2010. Analytical and Functional Aspects of Antibody Sialylation. J Clin Immunol 30, 15–19. doi:10.1007/s10875-010-9409-2

Stanley, P., 2011. Golgi Glycosylation. Cold Spring Harbor Perspectives in Biology 3, a005199–a005199. doi:10.1101/cshperspect.a005199

Taniguchi, N., Kizuka, Y., 2015. Glycans and cancer: role of N-glycans in cancer biomarker, progression and metastasis, and therapeutics. Adv Cancer Res 126, 11–51. doi:10.1016/bs.acr.2014.11.001

Tavender, T.J., Springate, J.J., Bulleid, N.J., 2010. Recycling of peroxiredoxin IV provides a novel pathway for disulphide formation in the endoplasmic reticulum. The EMBO Journal 29, 4185–4197. doi:10.1038/emboj.2010.273

Tay, M.Z., Wiehe, K., Pollara, J., 2019. Antibody-dependent cellular phagocytosis in antiviral immune responses. Front. Immunol. 10, 332. doi:10.3389/fimmu.2019.00332

Tayi, V.S., Butler, M., 2015. Isolation and quantification of N-glycans from immunoglobulin G antibodies for quantitative glycosylation analysis. Journal of Biological Methods. doi:10.14440/jbm.2015.52

Thomann, M., Reckermann, K., Reusch, D., Prasser, J., Tejada, M.L., 2016. Fc-galactosylation modulates antibody-dependent cellular cytotoxicity of therapeutic antibodies. Molecular Immunology 73, 69–75. doi:10.1016/j.molimm.2016.03.002

Thomann, M., Schlothauer, T., Dashivets, T., Malik, S., Avenal, C., Bulau, P., Rüger, P., Reusch, D., 2015. In Vitro Glycoengineering of IgG1 and Its Effect on Fc Receptor Binding and ADCC Activity. PLoS ONE 10, e0134949–16. doi:10.1371/journal.pone.0134949

Trapani, J.A., Smyth, M.J., 2002. Functional significance of the perforin/granzyme cell death pathway. Nat Rev Immunol 2, 735–747. doi:10.1038/nri911

Umaña, P., Jean-Mairet, J., Moudry, R., Amstutz, H., Bailey, J.E., 1999. Engineered glycoforms of an antineuroblastoma IgG1 with optimized antibody-dependent cellular cytotoxic activity. Nat Biotechnol 17, 176–180. doi:10.1038/6179

van Lith, M., Tiwari, S., Pediani, J., Milligan, G., Bulleid, N.J., 2011a. Real-time monitoring of redox changes in the mammalian endoplasmic reticulum. Journal of Cell Science 124, 2349–2356. doi:10.1242/jcs.085530

Vcelar, S., Melcher, M., Auer, N., Hrdina, A., Puklowski, A., Leisch, F., Jadhav, V., Wenger, T., Baumann, M., Borth, N., 2018. Changes in chromosome counts and patterns in CHO cell lines upon generation of recombinant cell lines and subcloning. Biotechnol J 13, 1700495–9. doi:10.1002/biot.201700495

Wallace, D., Hildesheim, A., Pinto, L.A., 2004. Comparison of benchtop microplate beta counters with the traditional gamma counting method for measurement of chromium-51 release in cytotoxic assays. Clin. Diagn. Lab. Immunol. 11, 255–260. doi:10.1128/cdli.11.2.255-260.2004

Walsh, G., 2009. Post-translational modification of protein biopharmaceuticals. John Wiley & Sons.

Wang, Q., Yin, B., Chung, C.-Y., Betenbaugh, M.J., 2017. Glycoengineering of CHO cells to improve product quality. Methods Mol. Biol. 1603, 25–44. doi:10.1007/978-1-4939-6972-2_2

Wang, S., Halim, A., Schulz, M.A., Frodin, M., Rahman, S.H., Vester-Christensen, M.B., Behrens, C., Kristensen, C., Vakhrushev, S.Y., Bennett, E.P., Wandall, H.H., Yang, Z., Clausen, H., 2015. Engineered CHO cells for production of diverse, homogeneous glycoproteins. Nat. Biotechnol. 33, 842–844. doi:10.1038/nbt.3280

Wang, W., Erbe, A.K., Hank, J.A., Morris, Z.S., Sondel, P.M., 2015. NK cell-mediated antibody-dependent cellular cytotoxicity in cancer immunotherapy. Front. Immunol. 6, 368. doi:10.3389/fimmu.2015.00368

Wang, Z., Zhu, J., Lu, H., 2020. Antibody glycosylation: impact on antibody drug characteristics and quality control. Appl Microbiol Biotechnol 104, 1905–1914. doi:10.1007/s00253-020-10368-7

Weiner, G.J., 2015. Building better monoclonal antibody-based therapeutics. Nature Publishing Group 15, 361–370. doi:10.1038/nrc3930

Wurm, F.M., 2004. Production of recombinant protein therapeutics in cultivated mammalian cells. Nat Biotechnol 22, 1393–1398. doi:10.1038/nbt1026

Yamaguchi, Y., Nishimura, M., Nagano, M., Yagi, H., Sasakawa, H., Uchida, K., Shitara, K., Kato, K., 2006. Glycoform-dependent conformational alteration of the Fc region of human immunoglobulin G1 as revealed by NMR spectroscopy. Biochimica et Biophysica Acta (BBA) - General Subjects 1760, 693–700. doi:10.1016/j.bbagen.2005.10.002

Yamane-Ohnuki, N., Kinoshita, S., Inoue-Urakubo, M., Kusunoki, M., Iida, S., Nakano, R., Wakitani, M., Niwa, R., Sakurada, M., Uchida, K., Shitara, K., Satoh, M., 2004. Establishment of FUT8 knockout Chinese hamster ovary cells: An ideal host cell line for

producing completely defucosylated antibodies with enhanced antibody-dependent cellular cytotoxicity. Biotechnol. Bioeng. 87, 614–622. doi:10.1002/bit.20151

Yamane-Ohnuki, N., Satoh, M., 2009. Production of therapeutic antibodies with controlled fucosylation. mabs 1, 230–236.

Yang, M., Butler, M., 2002a. Effects of ammonia and glucosamine on the heterogeneity of erythropoietin glycoforms. Biotechnol Progress 18, 129–138. doi:10.1021/bp0101334

Yang, M., Butler, M., 2002b. Effects of ammonia and glucosamine on the heterogeneity of erythropoietin glycoforms. Biotechnol Progress 18, 129–138. doi:10.1021/bp0101334

Yang, M., Butler, M., 2000. Effect of ammonia on the glycosylation of human recombinant erythropoietin in culture. Biotechnol Progress 16, 751–759. doi:10.1021/bp000090b

Yu, X., Marshall, M.J.E., Cragg, M.S., Crispin, M., 2017. Improving antibody-based cancer therapeutics through glycan engineering. BioDrugs 1–16. doi:10.1007/s40259-017-0223-8

Zahavi, D., AlDeghaither, D., O'Connell, A., Weiner, L.M., 2018. Enhancing antibody-dependent cell-mediated cytotoxicity: a strategy for improving antibody-based immunotherapy. Antibody Therapeutics 1, 7–12. doi:10.1093/abt/tby002

Zanatta, A., Viegas, C.M., Tonin, A.M., Busanello, E.N.B., Grings, M., Moura, A.P., Leipnitz, G., Wajner, M., 2013. Disturbance of redox homeostasis by ornithine and homocitrulline in rat cerebellum: a possible mechanism of cerebellar dysfunction in HHH syndrome. Life Sci 93, 161–168. doi:10.1016/j.lfs.2013.06.013

Zhang, Jianbing, Liu, X., Bell, A., To, R., Baral, T.N., Azizi, A., Li, J., Cass, B., Durocher, Y., 2009. Transient expression and purification of chimeric heavy chain antibodies. Protein Expression and Purification 65, 77–82. doi:10.1016/j.pep.2008.10.011

Zhang, Jin, Campbell, R.E., Ting, A.Y., Tsien, R.Y., 2002. Creating new fluorescent probes for cell biology. Nat Rev Mol Cell Biol 3, 906–918. doi:10.1038/nrm976

7

Appendix

In order to determine the efficiency of the roGFP-iL and iE probes to measure redox states within the intracellular organelles, a flow cytometry method was applied. This method to measure fluorescence in single cells was adapted from a previous study that was conducted with 3T3-L1 fibroblasts, wherein flow cytometry was used to validate the system (Sarkar et al., 2013). Analysis of the changes in redox conditions in cytosolic, ER and Golgi probes were done using DTT and DPS as reducing and oxidising buffers. The concentrations of DPS and DTT selected were based on concentrations used in (Sarkar et al., 2013) as well as previous work in Butler lab on culture redox potential of antibody producing CHO cells (Dionne et al., 2017) where a range of concentrations were used (0-0.75 mM).

The supplementary table shows the mean intensity values derived from the flow cytometry experiment, analysed using FlowJo™. The ratio of fluorescence intensity (d) for each sample was calculated by dividing the mean intensity at 405nm (b) by the mean intensity at 488nm. These values were normalised by dividing each of the treated sample ratios by the control sample to give the normalised ratio (e). Finally, the log2 values (f) were derived from the normalised ratios.

For example: for the sample EiL 25nM DPS-

Ratio of fluorescence intensity = Mean intensity at 405nm/Mean intensity at 488nm

→3105/3917= 0.7927.

Normalised ratio = Ratio/control ratio = 0.7927/1.4501 = 0.5467

Log2 normalized to baseline = log2 (0.5467) = -0.8713

Supplementary table: Calculation of the redox fluorescence intensity ratios from mean intensity values

(a) Sample name	(b) Mean Intensity at 405nm (Cyan)	(c) Mean Intensity at 488nm (GFP)	(d) Ratio	(e) normalised ratio (divided by control)	(f) log2 Normalized to baseline
EiL 0mM	2542	1753	1.4501	1.0000	0.0000
EiL 0.25mM DPS	3105	3917	0.7927	0.5467	-0.8713
EiL 0.5mM DPS	3293	4161	0.7914	0.5458	-0.8737
EiL 0.75mM DPS	3292	4264	0.7720	0.5324	-0.9094
EiL 1mM DPS	3331	4323	0.7705	0.5314	-0.9122
EiL 0.25mM DTT	2518	1848	1.3626	0.9396	-0.0898
EiL 0.5mM DTT	2525	1868	1.3517	0.9322	-0.1014
EiL 0.75mM DTT	2506	1896	1.3217	0.9115	-0.1337
EiL 1mM DTT	2562	1882	1.3613	0.9388	-0.0911

The fluorescence intensity ratios when plotted against the control sample, show that for the DPS-treated samples show a decrease in values whereas for the DTT-treated samples the ratios do not change significantly from the control (Supplementary figure 1). It was expected that with this experimental set-up, results obtained would be similar to previous studies. However, it is important to note the key differences between the experiment conducted in this thesis and previously published data (Dooley et al., 2004, van Lith et al., 2011 and Sarkar et al., 2013). In all the previous studies, it has been shown that the addition of an oxidising reagent leads to a shift towards a positive ratio whereas addition of a reducing reagent leads to a more negative ratio. However, there are differences in how the experiment described in this thesis has been conducted. The previous studies have performed redox titration experiments wherein varying concentrations of the reagents have been analysed at a range of excitation wavelengths.

From these redox titration experiments which were conducted using fluorescence spectroscopy, the precise excitation wavelengths were chosen (In Dooley et. al- 400nm/480nm; in Sarkar et. al-380nm/450nm and in van Lith et. al- 405nm/465nm). The probes that are used in the papers maybe different and thus, it may be the reason for not detecting the redox changes that were expected in the experiment in this thesis (wavelength used- 405nm/488nm). Sarkar et.al have also discussed that with epifluorescence microscopy, a wider range of excitation wavelengths are available which makes it possible to increase sensitivity at minor redox changes. However, with flow cytometry the detection range is limited to the commonly available wavelength of 405nm. It is possible that in the experiment conducted in this thesis, especially with DTT, the changes were very small and thus not detected by the flow cytometry method.

Nevertheless, it can be seen from supplementary figure 2 that there is a shift in the peaks from DPS-treated samples, when compared to the control peaks. The DTT-treated sample

peaks do not exhibit a shift but from the ratios the changes are minute which may be the reason for not detecting the shift. However, it can still be confirmed from this figure there is a change being observed and with some more optimization, it may be possible to use the flow cytometry method to detect the redox changes.

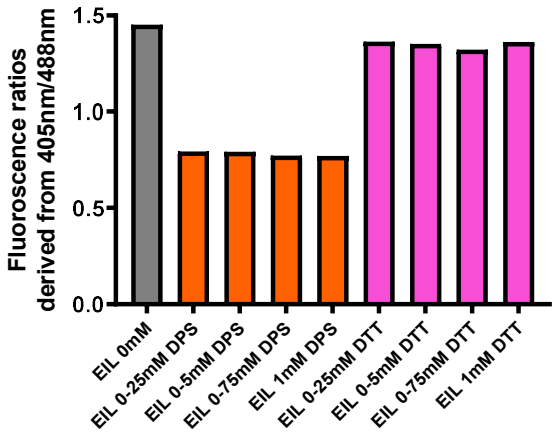

Supplementary figure 1: Fluorescence ratios plotted against roGFP-EiL expressing cells which were treated with varying concentrations of DTT and DTT. Compared to the control (in grey), the DPS-treated samples exhibit lower fluorescence intensity ratios whereas, as can also be observed in supplementary figure 1, there is minimum change in the ratios of fluorescence intensity in samples treated with DTT.

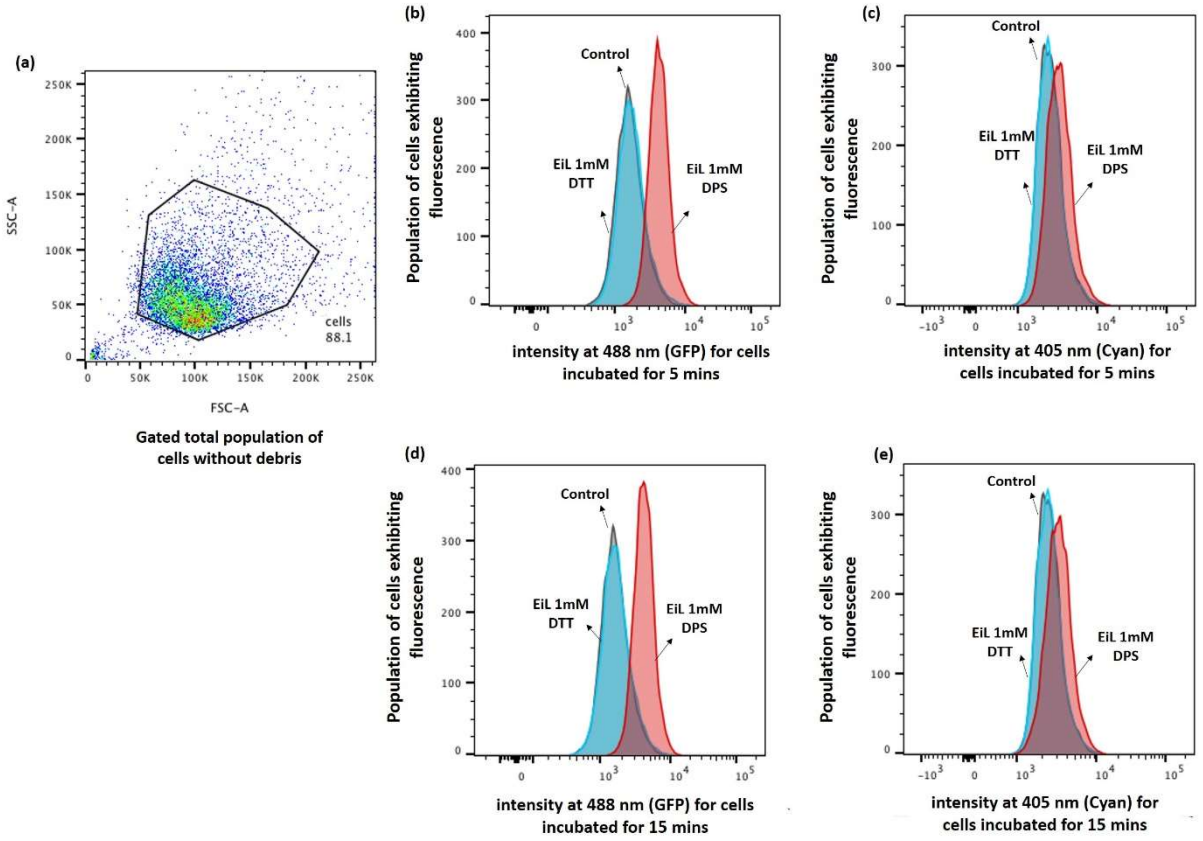

Supplementary figure 2: Histograms of fluorescence intensities against the population of cells exhibiting fluorescence due to addition of oxidising and reducing reagents at 1mM concentration. (a) shows the population of cells that are expressing the roGFP constructs and thus exhibiting fluorescence. (b, c, d & e) shows a population of cells that are responding to the reagents added which is shown by the shift in peaks after 5 and 15 mins.